Molchanov Alexander M.

NUMERICAL METHODS FOR SOLVING THE NAVIER-STOKES EQUATIONS

Moscow, 2018

Annotation

This book is intended for beginners in the field of Computational Fluid Dynamics (CFD), studying in English. If you have never studied CFD before, if you have never worked in the area, and if you have no real idea as to what the discipline is all about, then this book is for you. Although the material has been developed from first principles wherever possible, the book will be of greatest benefit to those who are familiar with the ideas of calculus, elementary vector and matrix algebra and basic numerical methods. The main purpose in writing this book is to provide a simple, satisfying, and motivational approach toward presenting the subject to the reader who is learning about CFD for the first time. In the workplace, CFD is today a mathematically sophisticated discipline.

The book is focused on the problems related to aviation and aerospace topics. However, the proposed methods can be easily applied to a wider sphere of science.

Preface

Navier-Stokes Equations

The Navier-Stokes Equations are the basic governing equations for a viscous, heat conducting fluid. It is a vector equation obtained by applying Second Newton's Law of Motion to a fluid element and is also called the *momentum equation*. It is supplemented by the mass conservation equation, also called *continuity equation* and the *energy equation*. Usually, the term Navier-Stokes equations is used to refer to all of these equations.

Navier-Stokes Equations are the governing equations of Computational Fluid Dynamics (CFD). Computational Fluid Dynamics is the simulation of fluids engineering systems using modeling (mathematical physical problem formulation) and numerical methods (discretization methods, solvers, numerical parameters, and grid generations, etc.). The process is as figure 0.1.

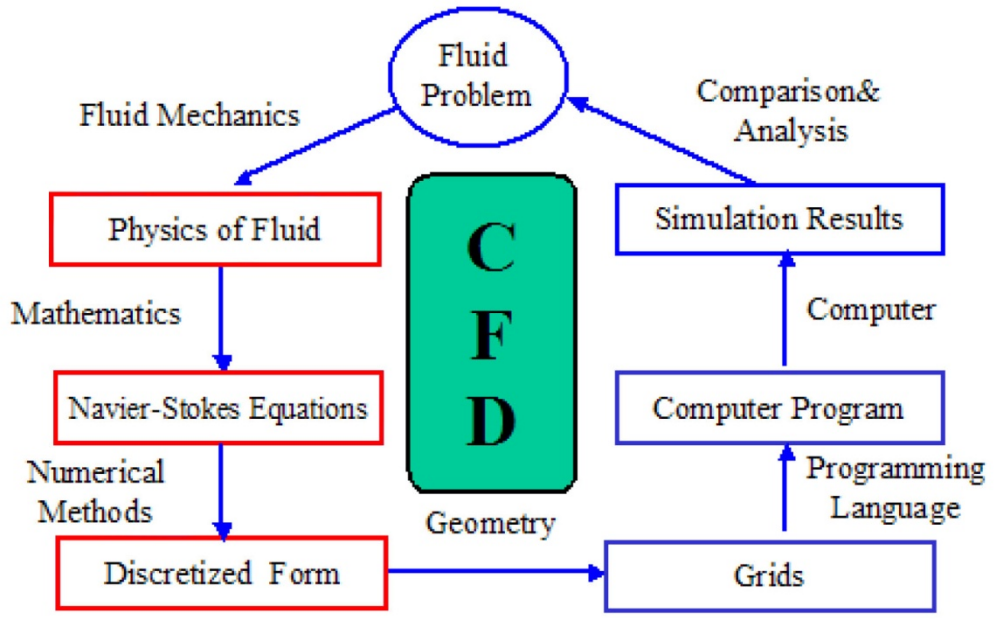

Figure 0.1. Process of Computational Fluid Dynamics

Firstly, we have a fluid problem. To solve this problem, we should know the physical properties of fluid by using Fluid Mechanics. Then we can use mathematical equations to describe these physical properties. This is Navier-Stokes Equations. As the Navier-Stokes Equations are analytical, human can understand it and solve them on a piece of paper. But if we want to solve these equations with computer, we have to translate it to the *discretized form*. The translators are numerical *discretization methods*, such as Finite Difference, Finite Element, Finite Volume methods. Consequently, we also need to divide our whole problem domain into many small parts because our discretization is based on them. Then, we can write programs to solve them. The typical languages are Fortran and C. Normally the programs are run on workstations or supercomputers. In the end, we can get our simulation results. We can compare and analyze the simulation results with experiments and the real problem. If the results are not sufficient to solve the problem, we have to repeat the process until find satisfied solution. This is the process of CFD.

Main objective of this book is to train readers the main methods of the solution of the Navier-Stokes equations so that they *without any assistance* will

be able to create algorithmic programs for the solution of the main problems of aerodynamics and thermophysics as well as other problems of Computational Fluid Dynamics.

Besides, this book intends to provide the theoretical background required for the effective use of commercial codes (ANSYS CFX, FLUENT, FlowVision, etc.) based on the *finite volume method*.

The author did not intend to provide a brief review of all existing methods of the solution of the Navier-Stokes equations, since he does not consider it effective from a practical point of view. However, here are some most effective methods (from the *author's point of view*) described in detail.

The covers the following subject areas:

- Governing equations of viscous fluid flows
- Boundary conditions
- Finite volume discretisation for the key transport phenomena in fluid flows: diffusion, convection and sources
- Discretisation procedures for unsteady phenomena
- Solution algorithms for systems of discretised equations
- Implementation of boundary conditions

Application of Computational Fluid Dynamics

Computational Fluid Dynamics (CFD) is the analysis of systems involving fluid flow, heat transfer and associated phenomena such as chemical reactions by means of computer-based simulation. The technique is very powerful and spans a wide range of industrial and non-industrial application areas. Some examples are:

• aerodynamics of aircraft and vehicles: lift and drag

• hydrodynamics of ships

• power plant: combustion in IC engines and gas turbines

• turbomachinery: flows inside rotating passages, diffusers etc.

• electrical and electronic engineering: cooling of equipment including micro-circuits

• chemical process engineering: mixing and separation, polymer moulding

• external and internal environment of buildings: wind loading and heating/ ventilation

• marine engineering: loads on off-shore structures

• environmental engineering: distribution of pollutants and effluents

• hydrology and oceanography: flows in rivers, estuaries, oceans

• meteorology: weather prediction

• biomedical engineering: blood flows through arteries and veins

Advantages of a Theoretical Calculation

There are three methods in study of Fluid: theory analysis, experiment and simulation (CFD). As a new method, CFD has many advantages compared to experiments. Please refer table 1.

Table 1. Comparison of Simulation and Experiment

	Simulation (CFD)	Experiment
Cost	Cheap	Expensive
Time	Short	Long
Scale	Any	Small/Middle
Information	All	Measured Point

Repeatable	Yes	Some
Safety	Yes	Some Dangerous

Disadvantages of a Theoretical Calculation

A computer analysis works out the implications of a *mathematical model*. The experimental investigation, by contrast, observes the *reality itself*. A perfectly satisfactory numerical technique can produce worthless results if an inadequate mathematical model is employed.

For the purpose of discussing the disadvantages of a theoretical calculation, it is, therefore, useful to divide all practical problems into two groups:

Group A: Problems for which an adequate mathematical description can be written. (Examples: heat conduction, laminar flows, simple turbulent boundary layers.)

Group B: Problems for which an adequate mathematical description has not yet been worked out. (Examples: complex turbulent flows, certain non-Newtonian flows, formation of nitric oxides in turbulent combustion, some two-phase flows.)

Of course, the group into which a given problem falls will be determined by what we are prepared to consider as an "adequate" description.

Disadvantages for Group A. It may be stated that, for most problems of Group A, the theoretical calculation suffers from no disadvantages. The computer solution then represents an alternative that is highly superior to an experimental study. Occasionally, however, one encounters some disadvantages. If the prediction has a very limited objective (such as finding the overall pressure drop for a complicated apparatus), the computation may not be less expensive than an experiment. For difficult problems involving complex geometry, strong

nonlinearities, sensitive fluid-property variations, etc., a numerical solution may be hard to obtain and would be excessively expensive if at all possible.

Extremely fast and small-scale phenomena such as turbulence, if they are to be computed in all their time-dependent detail by solving the unsteady Navier-Stokes equations, are still beyond the practical reach of computational methods. Finally, when the mathematical problem occasionally admits more than one solution, it is not easy to determine whether the computed solution corresponds to reality.

Research in computational methods is aimed at making them more reliable, accurate, and efficient. The disadvantages mentioned here will diminish as this research progresses.

Disadvantages for Group B. The problems of Group B share all the disadvantages of Group A; in addition, there is the uncertainty about the extent to which the computed results would agree with reality. In such cases, some experimental backup is highly desirable.

Research in mathematical models causes a transfer of problems from Group B into Group A. This research consists of proposing a model, working out its implications by computer analysis, and comparing the results with experimental data. Thus, computational methods play a key role in this research. A striking example of this role can be found in the recent development of turbulence models.

1. FLUID DYNAMICS

1.1. Some useful formulas.

Nabla or del operator

Nabla (∇) is the differential operator given in Cartesian coordinates { x, y, z } on three-dimensional Euclidean space by

$$\nabla = \frac{\partial}{\partial x}\mathbf{i} + \frac{\partial}{\partial y}\mathbf{j} + \frac{\partial}{\partial z}\mathbf{k}, \tag{1.1}$$

where { $\mathbf{i}, \mathbf{j}, \mathbf{k}$ } are unit basis vectors.

Examples of using nabla operator in Cartesian coordinates.

1) Divergence

$$\nabla \cdot \mathbf{a} = \operatorname{div} \mathbf{a} = \frac{\partial a_x}{\partial x} + \frac{\partial a_y}{\partial y} + \frac{\partial a_z}{\partial z}, \tag{1.2}$$

Divergence operation decreases the order of the entity operated upon. The divergence of a vector field **a** is a scalar. The divergence of a tensor is a vector. The divergence operation with a scalar is impossible.

2) Gradient

$$\nabla \varphi = \operatorname{grad} \varphi = \frac{\partial \varphi}{\partial x}\mathbf{i} + \frac{\partial \varphi}{\partial y}\mathbf{j} + \frac{\partial \varphi}{\partial z}\mathbf{k}. \tag{1.3}$$

Gradient operation increases the order of the entity operated upon. The gradient of the vector is a tensor. For example, $\nabla\mathbf{V}$ - gradient of the velocity, is a tensor. Here

$\mathbf{VW} \equiv \mathbf{V} \otimes \mathbf{W}$ - tensor product of two vectors.

Gradient of the velocity is given by the following formula

$$\nabla\mathbf{V} = \begin{pmatrix} \frac{\partial V_x}{\partial x} & \frac{\partial V_x}{\partial y} & \frac{\partial V_x}{\partial z} \\ \frac{\partial V_y}{\partial x} & \frac{\partial V_y}{\partial y} & \frac{\partial V_y}{\partial z} \\ \frac{\partial V_z}{\partial x} & \frac{\partial V_z}{\partial y} & \frac{\partial V_z}{\partial z} \end{pmatrix} = \begin{pmatrix} \frac{\partial u}{\partial x} & \frac{\partial u}{\partial y} & \frac{\partial u}{\partial z} \\ \frac{\partial v}{\partial x} & \frac{\partial v}{\partial y} & \frac{\partial v}{\partial z} \\ \frac{\partial w}{\partial x} & \frac{\partial w}{\partial y} & \frac{\partial w}{\partial z} \end{pmatrix} \tag{1.4}$$

since the velocity components in the coordinate system (x,y,z) are denoted by (u,v,w)

3) Laplacian

$$\Delta\varphi = \nabla\cdot\nabla\varphi = \nabla^2\varphi = \mathrm{div}\left(\mathrm{grad}\,\varphi\right), \tag{1.5}$$

where φ is a scalar.

The laplacian of a vector is also a vector:

$$\Delta\mathbf{a} = \nabla^2\mathbf{a} = \begin{pmatrix} \dfrac{\partial^2 a_x}{\partial x^2} + \dfrac{\partial^2 a_x}{\partial y^2} + \dfrac{\partial^2 a_x}{\partial z^2} \\ \dfrac{\partial^2 a_y}{\partial x^2} + \dfrac{\partial^2 a_y}{\partial y^2} + \dfrac{\partial^2 a_y}{\partial z^2} \\ \dfrac{\partial^2 a_z}{\partial x^2} + \dfrac{\partial^2 a_z}{\partial y^2} + \dfrac{\partial^2 a_z}{\partial z^2} \end{pmatrix} \tag{1.6}$$

Laplacian operation does not change the order of the entity operated upon.

<u>*Einstein notation*</u>

Operations on Cartesian components of vectors and tensors may be expressed very efficiently and clearly using index notation. Let **x** be a (three dimensional) vector. Let $\{\mathbf{e}_1,\mathbf{e}_2,\mathbf{e}_3\}$ be a Cartesian basis. Denote the components of **x** in this basis by (x_1,x_2,x_3). Lower case Latin subscripts (i, j, k…) have the range (1,2,3). The symbol x_i denotes three components of a vector x_1,x_2,x_3. The components of the velocity vector are denoted by $u_1, u_2, u_3 \quad \Leftrightarrow \quad u, v, w$.

Summation convention (Einstein convention or Einstein notation): If an index is repeated in a product of vectors or tensors, summation is implied over the repeated index. Thus the following formulas are valid

$$\lambda = a_i b_i \quad \Leftrightarrow \quad \lambda = \sum_{i=1}^{3} a_i b_i \quad \Leftrightarrow \quad \lambda = a_1 b_1 + a_2 b_2 + a_3 b_3 \tag{1.7}$$

$$\frac{\partial u_i}{\partial x_i} \equiv \frac{\partial u_1}{\partial x_1} + \frac{\partial u_2}{\partial x_2} + \frac{\partial u_3}{\partial x_3} \equiv \frac{\partial u}{\partial x} + \frac{\partial v}{\partial y} + \frac{\partial w}{\partial z} \tag{1.8}$$

<u>*Gauss' divergence theorem*</u>. For a vector **a** this theorem states

$$\iiint_V \nabla \cdot \mathbf{a} dV = \oiint_A \mathbf{n} \cdot \mathbf{a} dA \tag{1.9}$$

The physical interpretation of $\mathbf{n} \cdot \mathbf{a}$ is the component of vector **a** in the direction of the vector **n** normal to surface element *dA*. Thus the integral of the divergence of a vector **a** over a volume is equal to the component of **a** in the direction normal to the surface which bounds the volume summed (integrated) over the entire bounding surface *A*.

1.2. Fundamental Equations

The fundamental equations of fluid dynamics are based on the following universal laws of conservation:

Conservation of Mass,

Conservation of momentum,

Conservation of energy.

The equation that results from applying the Conservation of Mass law to a fluid flow is called the *continuity equation*. The Conservation of Momentum law is nothing more than Newton's Second Law. When this law is applied to a fluid flow, it yields a vector equation known as the *momentum equation*.

The Conservation of Energy law is identical to the First Law of Thermodynamics, and the resulting fluid dynamic equation is named the *energy equation*. In addition to the equations developed from these universal laws, it is necessary to establish relationships between fluid properties in order to close the system of equations. An example of such a relationship is the equation of state, which relates the thermodynamic variables pressure p, density ρ, and temperature T.

Historically, there have been two different approaches taken to derive the equations of fluid dynamics: the phenomenological approach and the kinetic theory approach. In the phenomenological approach, certain relations between

stress and rate of strain and heat flux and temperature gradient are postulated, and the fluid dynamic equations are then developed from the conservation laws. The required constants of proportionality between stress and rate of strain and heat flux and temperature gradient (which are called transport coefficients) must be determined experimentally in this approach. In the kinetic theory approach (also called the mathematical theory of nonuniform gases), the fluid dynamic equations are obtained with the transport coefficients defined in terms of certain integral relations, which involve the dynamics of colliding particles. The drawback of this approach is that the interparticle forces must be specified in order to evaluate the collision integrals. Thus a mathematical uncertainty takes the place of the experimental uncertainty of the phenomenological approach. These two approaches will yield the same fluid dynamic equations if equivalent assumptions are made during their derivations.

The derivation of the fundamental equations of fluid dynamics will not be presented here. The fundamental equations given initially in this chapter were derived for a uniform, homogeneous fluid without mass diffusion or finite-rate chemical reactions. In order to include these later effects it is necessary to consider extra relations, called the species continuity equations, and to add terms to the energy equation to account for diffusion.

1.3. Continuity Equation

The Conservation of Mass law applied to a fluid passing through an infinitesimal, fixed control volume (see Fig. 1.1) yields the following equation of continuity:

$$\frac{\partial \rho}{\partial t} + \nabla \cdot (\rho \mathbf{V}) = 0 \tag{1.10}$$

where ρ is the fluid density, $\mathbf{V}$ is the fluid velocity

The first term in Eq. (1.10) represents the rate of increase of the density in the control volume, and the second term represents the rate of mass flux passing out of the control surface (which surrounds the control volume) per unit volume.

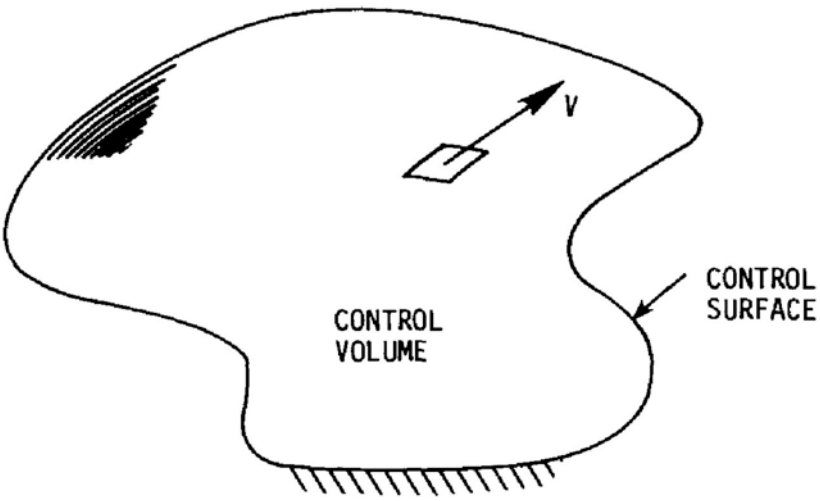

Figure 1.1. Control volume for Eulerian approach

It is convenient to use the substantial derivative

$$\frac{D\rho}{Dt} \equiv \frac{\partial \rho}{\partial t} + \mathbf{V} \cdot \nabla(\rho) \tag{1.11}$$

to change Eq. (1.10) into the form

$$\frac{D\rho}{Dt} + \rho(\nabla \cdot \mathbf{V}) = 0 \tag{1.12}$$

Equation (1.10) was derived using the Eulerian approach. In this approach, a fixed control volume is utilized, and the changes to the fluid are recorded as the fluid passes through the control volume. In the alternative Lagrangian approach, the changes to the properties of a fluid element are recorded by an observer moving with the fluid element. The Eulerian viewpoint is commonly used in fluid mechanics.

We may use another form of Eq. (1.10):

$$\frac{\partial \rho}{\partial t} + div(\rho \mathbf{V}) = 0 \tag{1.13}$$

For a Cartesian coordinate system, where u,v,w represent the x, y, z components of the velocity vector, Eq. (1.10) becomes

$$\frac{\partial \rho}{\partial t}+\frac{\partial}{\partial x}(\rho u)+\frac{\partial}{\partial y}(\rho v)+\frac{\partial}{\partial z}(\rho w)=0 \tag{1.14}$$

Note that this equation is in conservation-law (divergence) form.

Using Einstein notation, we obtain the following form of Eq. (1.14)

$$\frac{\partial \rho}{\partial t}+\frac{\partial}{\partial x_i}(\rho u_i)=0 \tag{1.15}$$

which is much simpler than the initial one.

A flow in which the density of each fluid element remains constant is called incompressible. Mathematically, this implies that

$$\frac{D\rho}{Dt}=0 \tag{1.16}$$

which reduces Eq. (1.12) to

$$\nabla \cdot \mathbf{V}=0 \tag{1.17}$$

or

$$\frac{\partial u_i}{\partial x_i}=0 \tag{1.18}$$

for the Cartesian coordinate system. For steady air flows with speed V < 100m/s or M < 0.3 the assumption of incompressibility is a good approximation.

1.4. Momentum Equation

Newton's Second Law applied to a fluid passing through an arbitrary, fixed control volume yields the following momentum equation:

$$\frac{\partial}{\partial t}(\rho \mathbf{V})+\nabla \cdot (\rho \mathbf{V}\mathbf{V})=\rho \mathbf{f}+\nabla \cdot \mathbf{\Pi} \tag{1.19}$$

The first term in this equation represents the rate of increase of momentum per unit volume in the control volume. The second term represents the rate of momentum lost by convection (per unit volume) through the control surface. Note that $\rho\mathbf{VV}$ is a tensor, so that $\nabla\cdot(\rho\mathbf{VV})$ is not a simple divergence. This term can be expanded, however, as

$$\nabla\cdot(\rho\mathbf{VV}) = \rho\mathbf{V}\cdot\nabla\mathbf{V} + \mathbf{V}\left(\nabla\cdot(\rho\mathbf{V})\right) \tag{1.20}$$

When this expression for $\nabla\cdot(\rho\mathbf{VV})$ is substituted into Eq. (1.19), and the resulting equation is simplified using the continuity equation (1.10), the momentum equation reduces to

$$\rho\frac{D\mathbf{V}}{Dt} \equiv \rho\frac{\partial\mathbf{V}}{\partial t} + \rho\mathbf{V}\cdot\nabla\mathbf{V} = \rho\mathbf{f} + \nabla\cdot\mathbf{\Pi} \tag{1.21}$$

The first term on the right-hand side of Eq. (1.21) is the body force per unit volume. Body forces act at a distance and apply to the entire mass of the fluid. The most common body force is the gravitational force. In this case, the force per unit mass (**f**) equals the acceleration of gravity vector **g**:

$$\rho\mathbf{f} = \rho\mathbf{g} \tag{1.22}$$

The second term on the right-hand side of Eq. (1.21) represents the surface forces per unit volume. These forces are applied by the external stresses on the fluid element. The stresses consist of normal stresses and shearing stresses and are represented by the components of the stress tensor **Π**.

The momentum equation given above is quite general and is applicable to both continuum and noncontinuum flows. It is only when approximate expressions are inserted for the shear-stress tensor that Eq. (1.19) loses its generality. For all gases that can be treated as a continuum, and most liquids, it has been observed that the stress at a point is linearly dependent on the rates of strain (deformation) of the fluid. A fluid that behaves in this manner is called a *Newtonian fluid*. With this assumption, it is possible to derive a general

deformation law that relates the stress tensor to the pressure and velocity components. In compact tensor notation, this relation becomes

$$\Pi_{ij} = -p\delta_{ij} + \mu\left(\frac{\partial u_i}{\partial x_j} + \frac{\partial u_j}{\partial x_i}\right) + \delta_{ij}\mu'\frac{\partial u_k}{\partial x_k}, \quad i,j,k = 1,2,3 \tag{1.23}$$

where δ_{ij} is the Kronecker delta function ($\delta_{ij} = 1 \; if \;\; i = j$ and $\delta_{ij} = 0 \; if \;\; i \neq j$); u_1, u_2, u_3 represent the three components of the velocity vector **V**; x_1,x_2,x_3 represent the three components of the position vector; μ is the coefficient of viscosity (dynamic viscosity), and μ' is the second coefficient of viscosity. The two coefficients of viscosity are related to the coefficient of bulk viscosity κ by the expression

$$\kappa = \frac{2}{3}\mu + \mu' \tag{1.24}$$

In general, it is believed that κ is negligible except in the study of the structure of shock waves and in the absorption and attenuation of acoustic waves. For this reason, we will ignore bulk viscosity for the remainder of the text. With κ = 0, the second coefficient of viscosity becomes

$$\mu' = -\frac{2}{3}\mu \tag{1.25}$$

and the stress tensor may be written as

$$\Pi_{ij} = -p\delta_{ij} + \mu\left[\left(\frac{\partial u_i}{\partial x_j} + \frac{\partial u_j}{\partial x_i}\right) - \frac{2}{3}\delta_{ij}\frac{\partial u_k}{\partial x_k}\right], \quad i,j,k = 1,2,3 \tag{1.26}$$

The stress tensor is frequently separated in the following manner:

$$\Pi_{ij} = -p\delta_{ij} + \tau_{ij} \tag{1.27}$$

where τ_{ij} represents the viscous stress tensor given by

$$\tau_{ij} = \mu\left[\left(\frac{\partial u_i}{\partial x_j} + \frac{\partial u_j}{\partial x_i}\right) - \frac{2}{3}\delta_{ij}\frac{\partial u_k}{\partial x_k}\right], \quad i,j,k = 1,2,3 \tag{1.28}$$

In vector form Eq. (1.28) is written as

$$\boldsymbol{\tau} = \mu\left[\nabla\mathbf{V} + (\nabla\mathbf{V})^T - \frac{2}{3}(\nabla\cdot\mathbf{V})\mathbf{I}\right] \tag{1.29}$$

where **I** is the identity tensor, upper index *T* means tensor transposition.

Upon substituting Eq. (1.26) into Eq. (1.21), the famous *Navier-Stokes equation* is obtained:

$$\rho\frac{D\mathbf{V}}{Dt} = \rho\mathbf{f} - \nabla p + \nabla\cdot\boldsymbol{\tau} \tag{1.30}$$

Using Einstein notation and Eq. (1.27), we can obtain the following form of Eq. (1.19) for a Cartesian coordinate system

$$\frac{\partial}{\partial t}(\rho u_i) + \frac{\partial}{\partial x_j}\left(\rho u_i u_j + p\delta_{ij} - \tau_{ij}\right) = \rho f_i, \quad i = 1,2,3 \tag{1.31}$$

or

$$\begin{aligned}
&\frac{\partial}{\partial t}(\rho u) + \frac{\partial}{\partial x}(\rho uu + p - \tau_{xx}) + \frac{\partial}{\partial y}\left(\rho uv - \tau_{xy}\right) + \frac{\partial}{\partial z}(\rho uw - \tau_{xz}) = \rho f_x,\\
&\frac{\partial}{\partial t}(\rho v) + \frac{\partial}{\partial x}\left(\rho vu - \tau_{yx}\right) + \frac{\partial}{\partial y}\left(\rho vv + p - \tau_{yy}\right) + \frac{\partial}{\partial z}\left(\rho vz - \tau_{yz}\right) = \rho f_y,\\
&\frac{\partial}{\partial t}(\rho w) + \frac{\partial}{\partial x}(\rho wu - \tau_{zx}) + \frac{\partial}{\partial y}\left(\rho wv - \tau_{zy}\right) + \frac{\partial}{\partial z}(\rho ww + p - \tau_{zz}) = \rho f_z
\end{aligned} \tag{1.32}$$

This is the conservation-law form of the Navier-Stokes equations. Utilizing Eq. (1.21), these equations can be rewritten in non-conservation form as

$$\rho\frac{\partial u_i}{\partial t} + \rho u_j\frac{\partial u_i}{\partial x_j} = \rho f_i - \frac{\partial p}{\partial x_i} + \frac{\partial \tau_{ij}}{\partial x_j}, \quad i = 1,2,3 \tag{1.33}$$

or

$$\begin{aligned}
&\rho\frac{\partial u}{\partial t} + \rho u\frac{\partial u}{\partial x} + \rho v\frac{\partial u}{\partial y} + \rho w\frac{\partial u}{\partial z} = \rho f_x - \frac{\partial p}{\partial x} + \frac{\partial \tau_{xx}}{\partial x} + \frac{\partial \tau_{xy}}{\partial y} + \frac{\partial \tau_{xz}}{\partial z}\\
&\rho\frac{\partial v}{\partial t} + \rho u\frac{\partial v}{\partial x} + \rho v\frac{\partial v}{\partial y} + \rho w\frac{\partial v}{\partial z} = \rho f_y - \frac{\partial p}{\partial y} + \frac{\partial \tau_{yx}}{\partial x} + \frac{\partial \tau_{yy}}{\partial y} + \frac{\partial \tau_{yz}}{\partial z}\\
&\rho\frac{\partial w}{\partial t} + \rho u\frac{\partial w}{\partial x} + \rho v\frac{\partial w}{\partial y} + \rho w\frac{\partial w}{\partial z} = \rho f_z - \frac{\partial p}{\partial z} + \frac{\partial \tau_{zx}}{\partial x} + \frac{\partial \tau_{zy}}{\partial y} + \frac{\partial \tau_{zz}}{\partial z}
\end{aligned} \tag{1.34}$$

In equations (1.32) and (1.34) the components of the viscous stress tensor τ_{ij} are given by

$$\tau_{xx} = \frac{2}{3}\mu\left(2\frac{\partial u}{\partial x} - \frac{\partial v}{\partial y} - \frac{\partial w}{\partial z}\right), \quad \tau_{yy} = \frac{2}{3}\mu\left(2\frac{\partial v}{\partial y} - \frac{\partial u}{\partial x} - \frac{\partial w}{\partial z}\right), \quad \tau_{zz} = \frac{2}{3}\mu\left(2\frac{\partial w}{\partial z} - \frac{\partial u}{\partial x} - \frac{\partial v}{\partial y}\right),$$
$$\tau_{xy} = \tau_{yx} = \mu\left(\frac{\partial u}{\partial y} + \frac{\partial v}{\partial x}\right), \quad \tau_{xz} = \tau_{zx} = \mu\left(\frac{\partial u}{\partial z} + \frac{\partial w}{\partial x}\right), \quad \tau_{yz} = \tau_{zy} = \mu\left(\frac{\partial v}{\partial z} + \frac{\partial w}{\partial y}\right) \tag{1.35}$$

The Navier-Stokes equations form the basis upon which the entire science of viscous flow theory has been developed. Strictly speaking, the term Navier-Stokes equations refers to the components of the viscous momentum equation [Eq. (1.33)]. However, it is common practice to include the continuity equation and the energy equation in the set of equations referred to as the Navier-Stokes equations.

If the flow is incompressible and the coefficient of viscosity (μ) is assumed constant, Eq. (1.30) will reduce to the much simpler form

$$\rho\frac{D\mathbf{V}}{Dt} = \rho\mathbf{f} - \nabla p + \mu\nabla^2\mathbf{V} \tag{1.36}$$

It should be remembered that Eq. (1.36) is derived by assuming a constant viscosity, which may be a poor approximation for the nonisothermal flow of a liquid whose viscosity is highly temperature dependent. On the other hand, the viscosity of gases is only moderately temperature dependent, and Eq. (1.36) is a good approximation for the incompressible flow of a gas.

The term

$$\mathrm{e}_{ij} = \frac{1}{2}\left(\frac{\partial u_i}{\partial x_j} + \frac{\partial u_j}{\partial x_i}\right) \tag{1.37}$$

is called the rate of strain. It is a symmetric tensor. In continuum mechanics, the strain rate tensor is a physical quantity that describes the rate of change of the deformation of a material in the neighborhood of a certain point, at a certain moment of time.

So we can rewrite Eq. (1.28) using (1.37)

$$\tau_{ij} = \mu\left(2\mathrm{e}_{ij} - \frac{2}{3}\delta_{ij}\frac{\partial u_k}{\partial x_k}\right), \quad i,j,k = 1,2,3 \tag{1.38}$$

1.5. Energy Equation

The First Law of Thermodynamics applied to a fluid passing through an infinitesimal, fixed control volume yields the following energy equation:

$$\frac{\partial}{\partial t}(\rho E) + \nabla\cdot(\rho E\,\mathbf{V}) = \frac{\partial Q}{\partial t} - \nabla\cdot\boldsymbol{q} + \rho\mathbf{f}\cdot\mathbf{V} + \nabla\cdot(\boldsymbol{\Pi}\cdot\mathbf{V}) \tag{1.39}$$

where E is the total energy per unit mass given by

$$E = e + \frac{V^2}{2} + \textit{potential energy} + \ldots \tag{1.40}$$

and e is the internal energy per unit mass. The first term on the left-hand side of Eq. (1.39) represents the rate of increase of E in the control volume, while the second term represents the rate of total energy lost by convection through the control surface. The first term on the right-hand side of Eq. (1.39) is the rate of heat produced per unit volume by external agencies, while the second term ($\nabla\cdot\boldsymbol{q}$) is the rate of heat lost by conduction (per unit volume) through the control surface. Fourier's law for heat transfer by conduction will be assumed, so that the heat transfer $\boldsymbol{q}$ can be expressed as

$$\boldsymbol{q} = -\lambda\nabla T \tag{1.41}$$

where λ is the coefficient of thermal conductivity and T is the temperature. The third term on the right-hand side of Eq. (1.39) represents the work done on the control volume (per unit volume) by the body forces, while the fourth term represents the work done on the control volume (per unit volume) by the surface forces. It should be obvious that Eq. (1.39) is simply the First Law of Thermodynamics applied to the control volume. That is, the increase of energy in the system is equal to heat added to the system plus the work done on the system.

For a Cartesian coordinate system, Eq. (1.39) becomes

$$\frac{\partial}{\partial t}(\rho E)-\frac{\partial Q}{\partial t}+\frac{\partial}{\partial x_i}\left(\rho E\, u_i+pu_i+q_i-\tau_{ij}u_j\right)=\rho f_i u_i \tag{1.42}$$

which is in conservation-law form. We can write this equation in more detail without using Einstein notation:

$$\begin{aligned}&\frac{\partial}{\partial t}(\rho E)-\frac{\partial Q}{\partial t}+\frac{\partial}{\partial x}\left(\rho E\, u+pu+q_x-\tau_{xx}u-\tau_{xy}v-\tau_{xz}w\right)\\&+\frac{\partial}{\partial y}\left(\rho E\, v+pv+q_y-\tau_{yx}u-\tau_{yy}v-\tau_{yz}w\right)\\&+\frac{\partial}{\partial z}\left(\rho E\, w+pw+q_z-\tau_{zx}u-\tau_{zy}v-\tau_{zz}w\right)=\rho f_x u+\rho f_y v+\rho f_z w\end{aligned} \tag{1.43}$$

Using the continuity equation, the left-hand side of Eq. (1.39) can be replaced by the following expression:

$$\rho\frac{D}{Dt}E=\frac{\partial}{\partial t}(\rho E)+\nabla\cdot(\rho E\,\mathbf{V}) \tag{1.44}$$

which is equivalent to

$$\rho\frac{D}{Dt}E=\rho\frac{De}{Dt}+\rho\frac{D}{Dt}\left(\frac{V^2}{2}\right) \tag{1.45}$$

if only internal energy and kinetic energy are considered significant in Eq. (1.40). Forming the scalar dot product of Eq. (1.30) with the velocity vector **V** allows one to obtain

$$\rho\frac{D\mathbf{V}}{Dt}\cdot\mathbf{V}=\rho\mathbf{f}\cdot\mathbf{V}-\nabla p\cdot\mathbf{V}+(\nabla\cdot\boldsymbol{\tau})\cdot\mathbf{V} \tag{1.46}$$

Now if Eqs. (1.44), (1.45) and (1.46) are combined and substituted into Eq. (1.39), a useful variation of the original energy equation is obtained:

$$\rho\frac{De}{Dt}+p\nabla\cdot\mathbf{V}=\frac{\partial Q}{\partial t}-\nabla\cdot\boldsymbol{q}+\nabla\cdot(\boldsymbol{\tau}\cdot\mathbf{V})-(\nabla\cdot\boldsymbol{\tau})\cdot\mathbf{V} \tag{1.47}$$

Development of formula:

$$\frac{\partial}{\partial t}(\rho E)+\nabla\cdot(\rho E\,\mathbf{V})=\frac{\partial Q}{\partial t}-\nabla\cdot\boldsymbol{q}+\rho\mathbf{f}\cdot\mathbf{V}-\nabla\cdot(p\mathbf{V})+\nabla\cdot(\boldsymbol{\tau}\cdot\mathbf{V})$$

$$\rho\frac{De}{Dt}+\rho\mathbf{V}\cdot\frac{D\mathbf{V}}{Dt}=\frac{\partial Q}{\partial t}-\nabla\cdot\boldsymbol{q}+\rho\mathbf{f}\cdot\mathbf{V}-\nabla\cdot(p\mathbf{V})+\nabla\cdot(\boldsymbol{\tau}\cdot\mathbf{V})$$

$$\rho\frac{De}{Dt}+\rho\mathbf{f}\cdot\mathbf{V}-\nabla p\cdot\mathbf{V}+(\nabla\cdot\boldsymbol{\tau})\cdot\mathbf{V}$$

$$=\frac{\partial Q}{\partial t}-\nabla\cdot\boldsymbol{q}+\rho\mathbf{f}\cdot\mathbf{V}-\nabla\cdot(p\mathbf{V})+\nabla\cdot(\boldsymbol{\tau}\cdot\mathbf{V})$$

$$\rho\frac{De}{Dt}+p\nabla\cdot\mathbf{V}=\frac{\partial Q}{\partial t}-\nabla\cdot\boldsymbol{q}+\nabla\cdot(\boldsymbol{\tau}\cdot\mathbf{V})-(\nabla\cdot\boldsymbol{\tau})\cdot\mathbf{V}$$

The last two terms in Eq. (1.47) can be combined into a single term, since

$$\nabla\cdot(\boldsymbol{\tau}\cdot\mathbf{V})-(\nabla\cdot\boldsymbol{\tau})\cdot\mathbf{V}=\boldsymbol{\tau}:\nabla\mathbf{V}\equiv\Phi\ , \tag{1.48}$$

where $\boldsymbol{\tau}:\nabla\mathbf{V}$ is the double dot product of two tensors. This term is customarily called the dissipation function Φ and represents the rate at which mechanical energy is expended in the process of deformation of the fluid due to viscosity. After inserting the dissipation function, Eq. (1.47) becomes

$$\rho\frac{De}{Dt}+p\nabla\cdot\mathbf{V}=\frac{\partial Q}{\partial t}-\nabla\cdot\boldsymbol{q}+\Phi \tag{1.49}$$

Using the definition of enthalpy

$$h=e+\frac{p}{\rho} \tag{1.50}$$

and the continuity equation, Eq. (1.49) can be rewritten as

$$\rho\frac{Dh}{Dt}=\frac{Dp}{Dt}+\frac{\partial Q}{\partial t}-\nabla\cdot\boldsymbol{q}+\Phi \tag{1.51}$$

For a Cartesian coordinate system, the dissipation function, which is always positive if $\mu'=-\frac{2}{3}\mu$, becomes

$$\begin{aligned}\Phi&=\tau_{ij}\frac{\partial u_i}{\partial x_j}\\&=\mu\left[2\left(\frac{\partial u}{\partial x}\right)^2+2\left(\frac{\partial v}{\partial y}\right)^2+2\left(\frac{\partial w}{\partial z}\right)^2+\left(\frac{\partial v}{\partial x}+\frac{\partial u}{\partial y}\right)^2+\left(\frac{\partial w}{\partial y}+\frac{\partial v}{\partial z}\right)^2\right.\\&\left.+\left(\frac{\partial u}{\partial z}+\frac{\partial w}{\partial x}\right)^2-\frac{2}{3}\left(\frac{\partial u}{\partial x}+\frac{\partial v}{\partial y}+\frac{\partial w}{\partial z}\right)^2\right]\end{aligned} \tag{1.52}$$

If the flow is incompressible, and if the coefficient of thermal conductivity is assumed constant, Eq. (1.49) reduces to

$$\rho \frac{De}{Dt} = \frac{\partial Q}{\partial t} - \lambda \nabla^2 T + \Phi \tag{1.53}$$

1.6. Equation of State

In order to close the system of fluid dynamic equations it is necessary to establish relations between the thermodynamic variables (p, ρ, T, e, h) as well as to relate the transport properties (μ, λ) to the thermodynamic variables. For example, consider a compressible flow without external heat addition or body forces and use Eq. (1.14) for the continuity equation, Eqs. (1.34) for the three momentum equations, and Eq. (1.43) for the energy equation. These five scalar equations contain seven unknowns p, ρ, T, e, u, v, w, provided that the transport coefficients μ, λ can be related to the thermodynamic properties in the list of unknowns. It is obvious that two additional equations are required to close the system. These two additional equations can be obtained by determining relations that exist between the thermodynamic variables. Relations of this type are known as equations of state. According to the state principle of thermodynamics, the local thermodynamic state is fixed by any two independent thermodynamic variables, provided that the chemical composition of the fluid is not changing owing to diffusion or finite-rate chemical reactions. Thus for the present example, if we choose e and p as the two independent variables, then equations of state of the form

$$p = p(e, \rho), \quad T = T(e, \rho) \tag{1.54}$$

are required.

For most problems in gas dynamics, it is possible to assume a *perfect gas*. A perfect gas is defined as a gas whose intermolecular forces are negligible. A perfect gas obeys the perfect gas equation of state,

$$p = \rho R T \tag{1.55}$$

where R is the gas constant. The intermolecular forces become important under conditions of high pressure and relatively low temperature. For these conditions, the gas no longer obeys the perfect gas equation of state, and an alternative equation of state must be used. An example is the Van der Waals equation of state,

$$\left(p + a\rho^2\right)\left(\frac{1}{\rho} - b\right) = RT \tag{1.56}$$

where a and b are constants for each type of gas.

For problems involving a perfect gas at relatively low temperatures, it is possible to also assume a *calorically perfect gas*. A calorically perfect gas is defined as a perfect gas with constant specific heats. In a calorically perfect gas, the specific heat at constant volume c_v, the specific heat at constant pressure c_p, and the ratio of specific heats γ all remain constant, and the following relations exist:

$$e = c_v T, \quad h = c_p T, \quad \gamma = \frac{c_p}{c_v}, \quad c_v = \frac{R}{\gamma - 1}, \quad c_p = \frac{\gamma R}{\gamma - 1} \tag{1.57}$$

For air at standard conditions, R = 287 $m^2/(s^2\ K)$ and γ = 1.4. If we assume that the fluid in our example is a calorically perfect gas, then Eqs. (1.54) become

$$p = \left(\gamma - 1\right)\rho e, \quad T = \frac{\left(\gamma - 1\right)e}{R} \tag{1.58}$$

For fluids that cannot be considered calorically perfect, the required state relations can be found in the form of tables, charts, or curve fits.

The coefficients of viscosity and thermal conductivity can be related to the thermodynamic variables using kinetic theory. For example, Sutherland's formulas for viscosity and thermal conductivity are given by

$$\mu = C_1 \frac{T^{3/2}}{T + C_2}, \quad \lambda = C_3 \frac{T^{3/2}}{T + C_4} \tag{1.59}$$

where C_1-C_4 are constants for a given gas. For air at moderate temperatures, C_1 = 1.458×10^{-6} kg/(m s K$^{1/2}$), C_2 = 110.4 K, C_3 = 2.495 ×10^{-3} (kg m)/(s^{3}K$^{3/2}$), and C_4 = 194 K. The Prandtl number

$$\mathrm{Pr} = \frac{\mu c_p}{\lambda} \tag{1.60}$$

is often used to determine the coefficient of thermal conductivity к once ц. is known. This is possible because the ratio (c_p/Pr), which appears in the expression

$$\lambda = \frac{c_p}{\mathrm{Pr}}\mu \tag{1.61}$$

is approximately constant for most gases. For air at standard conditions, Pr = 0.72.

1.7. Vector Form of Equations

Before applying a numerical algorithm to the governing fluid dynamic equations, it is often convenient to combine the equations into a compact vector form. For example, the compressible Navier-Stokes equations in Cartesian coordinates without body forces, mass diffusion, finite-rate chemical reactions, or external heat addition can be written as

$$\frac{\partial \mathbf{U}}{\partial t} + \frac{\partial \mathbf{E}}{\partial x} + \frac{\partial \mathbf{F}}{\partial y} + \frac{\partial \mathbf{G}}{\partial z} = 0 \tag{1.62}$$

where **U**, **E**, **F**, and **G** are vectors given by

$$\mathbf{U} = \begin{bmatrix} \rho \\ \rho u \\ \rho v \\ \rho w \\ \rho E \end{bmatrix} \tag{1.63}$$

$$\mathbf{E} = \begin{bmatrix} \rho u \\ \rho u^2 + p - \tau_{xx} \\ \rho v u - \tau_{yx} \\ \rho w u - \tau_{zx} \\ \rho u\left(E + p/\rho\right) - u\tau_{xx} - v\tau_{yx} - w\tau_{zx} + q_x \end{bmatrix} \tag{1.64}$$

$$\mathbf{F} = \begin{bmatrix} \rho v \\ \rho u v - \tau_{xy} \\ \rho v^2 + p - \tau_{yy} \\ \rho w v - \tau_{zy} \\ \rho v\left(E + p/\rho\right) - u\tau_{xy} - v\tau_{yy} - w\tau_{zy} + q_y \end{bmatrix} \tag{1.65}$$

$$\mathbf{G} = \begin{bmatrix} \rho w \\ \rho u w - \tau_{xz} \\ \rho v w - \tau_{yz} \\ \rho w^2 + p - \tau_{zz} \\ \rho w\left(E + p/\rho\right) - u\tau_{xz} - v\tau_{yz} - w\tau_{zz} + q_z \end{bmatrix} \tag{1.66}$$

The first row of the vector Eq. (1.62) corresponds to the continuity equation as given by Eq. (1.14). Likewise, the second, third, and fourth rows are the momentum equations, Eqs. (1.34), while the fifth row is the energy equation, Eq. (1.43). With the Navier-Stokes equations written in this form, it is often easier to code the desired numerical algorithm. Other fluid dynamic equations that are written in conservation-law form can be placed in a similar vector form.

Vectors **E**, **F** and **G** are contains two parts: inviscid and viscous. And the inviscid flux consists of two physically distinct parts, i.e., convective and pressure fluxes. The former is associated with the flow (advection) speed, while the latter with the acoustic speed; or respectively classified as the linear and nonlinear fields.

1.8. Orthogonal Curvilinear Coordinates

The basic equations of fluid dynamics are valid for any coordinate system. We have previously expressed these equations in terms of a Cartesian coordinate system. For many applications it is more convenient to use a different

orthogonal coordinate system. Let us define $\{\zeta^1, \zeta^2, \zeta^3\}$ to be a set of generalized orthogonal curvilinear coordinates whose origin is at point P and let $\mathbf{g}_1, \mathbf{g}_2, \mathbf{g}_3$ be the corresponding unit vectors (see Fig. 1.2). The rectangular Cartesian coordinates are related to the generalized curvilinear coordinates by

$$\begin{aligned} x &= x\left(\zeta^1, \zeta^2, \zeta^3\right), \\ y &= y\left(\zeta^1, \zeta^2, \zeta^3\right), \\ z &= z\left(\zeta^1, \zeta^2, \zeta^3\right) \end{aligned} \tag{1.67}$$

or using Einstein notation

$$x_i = x_i\left(\zeta^1, \zeta^2, \zeta^3\right), \quad i = 1,2,3 \tag{1.68}$$

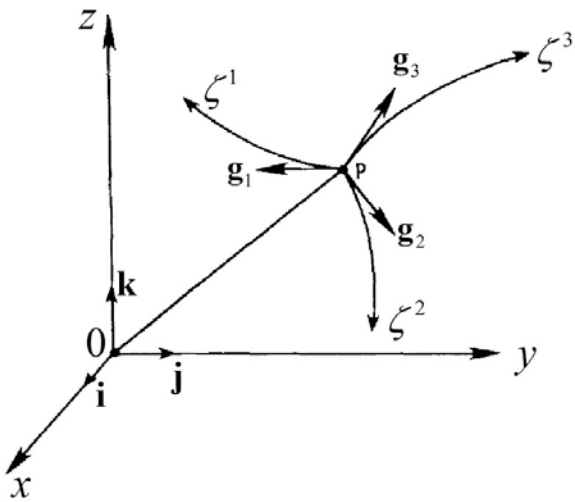

Figure 1.2. Orthogonal curvilinear coordinate system.

so if the Jacobian

$$\frac{\partial(x, y, z,)}{\partial\left(\zeta^1, \zeta^2, \zeta^3\right)}$$

is nonzero, then

$$\zeta^j = \zeta^j\left(x_1, x_2, x_3\right), \quad j = 1,2,3 \tag{1.69}$$

The elemental arc length *ds* in Cartesian coordinates is obtained from

$$(ds)^2 = (dx)^2 + (dy)^2 + (dz)^2 \equiv (dx_i)^2 \tag{1.70}$$

If Eq. (1.68) is differentiated, the following result is obtained:

$$dx_i = \frac{\partial x_i}{\partial \zeta^j} d\zeta^j, \quad i = 1,2,3 \tag{1.71}$$

where

$$(g_j)_i = \frac{\partial x_i}{\partial \zeta^j}, \quad i = 1,2,3, \quad j = 1,2,3$$

is *i*-th component of the vector $\mathbf{g}_j$ in Cartesian coordinates (x_1, x_2, x_3). So that

$$\mathbf{g}_j = \frac{\partial x_i}{\partial \zeta^j} \mathbf{i}_i, \quad j = 1,2,3 \tag{1.72}$$

Scalar product of basis vectors equals

$$\mathbf{g}_j \cdot \mathbf{g}_k = \left(\frac{\partial x_i}{\partial \zeta^j} \mathbf{i}_i \right) \cdot \left(\frac{\partial x_m}{\partial \zeta^k} \mathbf{i}_m \right) = \left(\frac{\partial x_i}{\partial \zeta^j} \right) \left(\frac{\partial x_m}{\partial \zeta^k} \right) \mathbf{i}_i \cdot \mathbf{i}_m = \left(\frac{\partial x_i}{\partial \zeta^j} \right) \left(\frac{\partial x_i}{\partial \zeta^k} \right) \tag{1.73}$$

For an orthogonal curvilinear coordinates we have the following:

$$\mathbf{g}_j \cdot \mathbf{g}_k = 0 \quad if \quad j \neq k \tag{1.74}$$

So

$$\left(\frac{\partial x_i}{\partial \zeta^j} \right) \left(\frac{\partial x_i}{\partial \zeta^k} \right) = \begin{cases} \left(\frac{\partial x_i}{\partial \zeta^j} \right)^2, \; if \;\; j = k \\ 0, \quad if \;\; j \neq k \end{cases} \tag{1.75}$$

If Eq. (1.71) is substituted into Eq. (1.70), the following result is obtained:

$$\begin{aligned} (ds)^2 &= dx_i \, dx_i = \frac{\partial x_i}{\partial \zeta^j} \frac{\partial x_i}{\partial \zeta^k} d\zeta^j d\zeta^k \\ &= \frac{\partial x}{\partial \zeta^j} \frac{\partial x}{\partial \zeta^k} d\zeta^j d\zeta^k + \frac{\partial y}{\partial \zeta^j} \frac{\partial y}{\partial \zeta^k} d\zeta^j d\zeta^k + \frac{\partial z}{\partial \zeta^j} \frac{\partial z}{\partial \zeta^k} d\zeta^j d\zeta^k \\ &= (h_1)^2 \left(d\zeta^1 \right)^2 + (h_2)^2 \left(d\zeta^2 \right)^2 + (h_3)^2 \left(d\zeta^3 \right)^2 \end{aligned} \tag{1.76}$$

where

$$
\begin{aligned}
(h_1)^2 &= \left(\frac{\partial x}{\partial \zeta^1}\right)^2 + \left(\frac{\partial y}{\partial \zeta^1}\right)^2 + \left(\frac{\partial z}{\partial \zeta^1}\right)^2 \\
(h_2)^2 &= \left(\frac{\partial x}{\partial \zeta^2}\right)^2 + \left(\frac{\partial y}{\partial \zeta^2}\right)^2 + \left(\frac{\partial z}{\partial \zeta^2}\right)^2 \\
(h_3)^2 &= \left(\frac{\partial x}{\partial \zeta^3}\right)^2 + \left(\frac{\partial y}{\partial \zeta^3}\right)^2 + \left(\frac{\partial z}{\partial \zeta^3}\right)^2
\end{aligned}
\tag{1.77}
$$

The above formulas can now be used to derive the fluid dynamic equations in any orthogonal curvilinear coordinate system. Examples include

Cartesian coordinates

$$
\begin{aligned}
\zeta_1 &= x, \quad h_1 = 1, \quad u_1 = u \\
\zeta_2 &= y, \quad h_2 = 1, \quad u_2 = v \\
\zeta_3 &= z, \quad h_3 = 1, \quad u_3 = w
\end{aligned}
$$

Cylindrical coordinates

$$
\begin{aligned}
\zeta_1 &= r, \quad h_1 = 1, \quad u_1 = u_r \\
\zeta_2 &= \theta, \quad h_2 = r, \quad u_2 = u_\theta \\
\zeta_3 &= z, \quad h_3 = 1, \quad u_3 = u_z
\end{aligned}
$$

Spherical coordinates

$$
\begin{aligned}
\zeta_1 &= r, \quad h_1 = 1, \quad u_1 = yu_r \\
\zeta_2 &= \theta, \quad h_2 = r, \quad u_2 = u_\theta \\
\zeta_3 &= \phi, \quad h_3 = r\sin\theta, \quad u_3 = u_\phi
\end{aligned}
$$

Two-dimensional (2-D) or axisymmetric body intrinsic coordinates

$$
\begin{aligned}
\zeta_1 &= \xi, \quad h_1 = 1 + K(\xi)\eta, \quad u_1 = u \\
\zeta_2 &= \eta, \quad h_2 = 1, \qquad\qquad\quad u_2 = v \\
\zeta_3 &= \phi, \quad h_3 = \left[r(\xi) + \eta\cos\alpha(\xi)\right]^m, \quad u_3 = mw
\end{aligned}
$$

where $K(\xi)$ is the local body curvature, $r(\xi)$ is the cylindrical radius, and

$$
m = \begin{cases} 0, & \text{for 2-D flow} \\ 1, & \text{for axisymmetric flow} \end{cases}
$$

These coordinate systems are illustrated in Fig. 1.3.

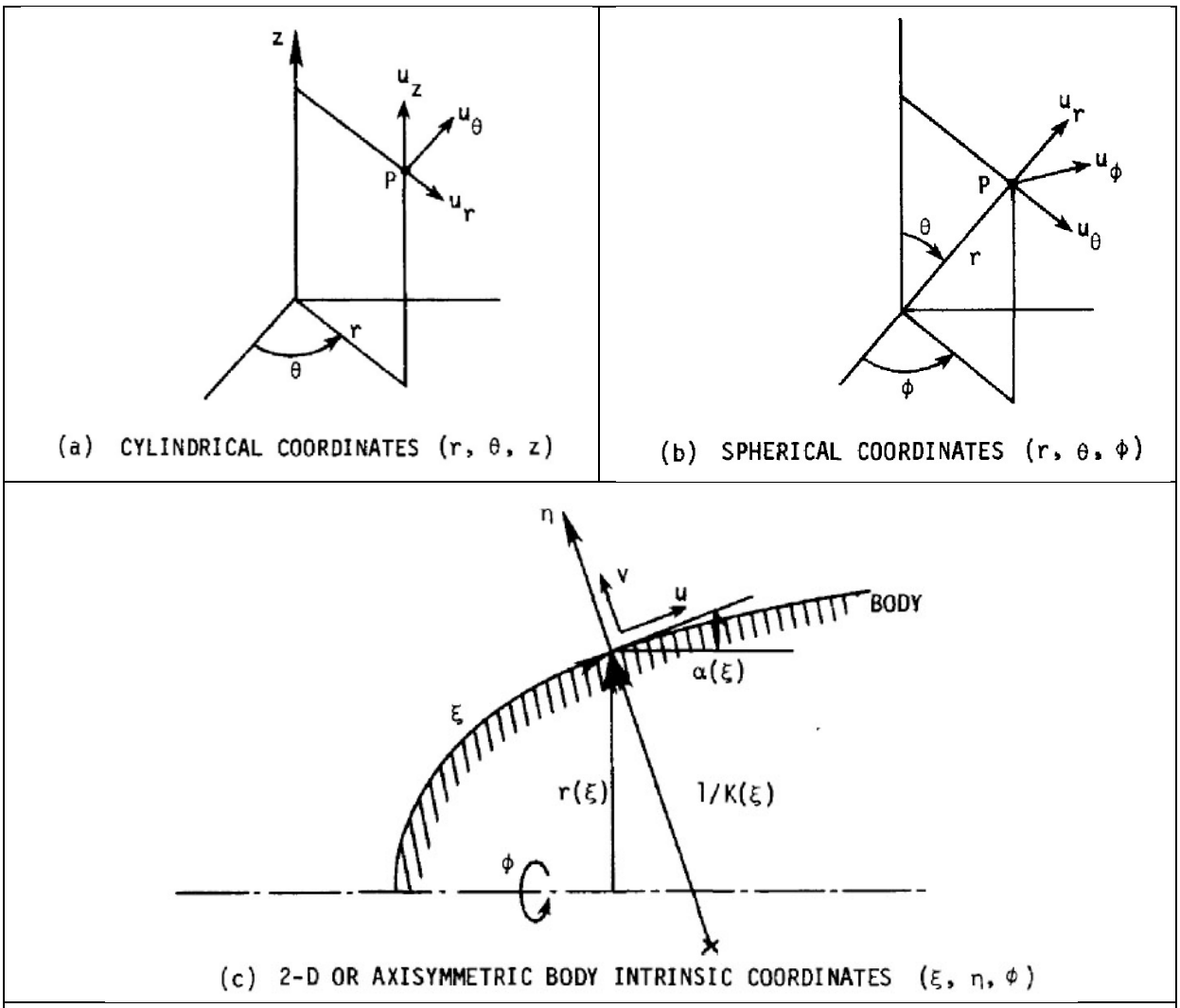

Figure 1.3. Curvilinear coordinate systems, (a) Cylindrical coordinates; (b) spherical coordinates; (c) 2-D or axisymmetric body intrinsic coordinates.

We will give the main equations in a cylindrical system of coordinates as an example:

$$\frac{\partial \rho}{\partial t}+\frac{\partial}{\partial r}(\rho u_r)+\frac{1}{r}\frac{\partial}{\partial \theta}(\rho u_\theta)+\frac{\partial}{\partial z}(\rho u_z)+\frac{\rho u_r}{r}=0, \tag{1.78}$$

$$\begin{aligned}&\frac{\partial}{\partial t}(\rho u_r)+\frac{\partial}{\partial r}(\rho u_r u_r+p-\tau_{rr})+\frac{1}{r}\frac{\partial}{\partial \theta}(\rho u_\theta u_r-\tau_{r\theta})+\frac{\partial}{\partial z}(\rho u_z u_r-\tau_{zr})\\&+\frac{1}{r}(\rho u_r u_r-\rho u_\theta u_\theta-\tau_{rr}+\tau_{\theta\theta})=\rho F_r\end{aligned}, \tag{1.79}$$

$$\begin{aligned}&\frac{\partial}{\partial t}(\rho u_\theta)+\frac{\partial}{\partial r}(\rho u_r u_\theta-\tau_{r\theta})+\frac{1}{r}\frac{\partial}{\partial \theta}(\rho u_\theta u_\theta+p-\tau_{\theta\theta})+\frac{\partial}{\partial z}(\rho u_z u_\theta-\tau_{z\theta})\\&+\frac{2}{r}(\rho u_r u_\theta-\tau_{r\theta})=\rho F_\theta\end{aligned}, \tag{1.80}$$

$$\frac{\partial}{\partial t}(\rho u_z)+\frac{\partial}{\partial r}(\rho u_r u_z-\tau_{rz})+\frac{1}{r}\frac{\partial}{\partial\theta}(\rho u_\theta u_z-\tau_{\theta z})+\frac{\partial}{\partial z}(\rho u_z u_z+p-\tau_{zz})$$
$$+\frac{1}{r}(\rho u_r u_z-\tau_{rz})=\rho F_z \quad , \qquad (1.81)$$

$$\frac{\partial(\rho E)}{\partial t}+\frac{\partial f_r}{\partial r}+\frac{1}{r}\frac{\partial f_\theta}{\partial\theta}+\frac{\partial f_z}{\partial z}+\frac{f_r}{r}=\rho\left(F_r u_r+F_\theta u_\theta+F_z u_z\right) \qquad (1.82)$$

where

$$\tau_{rr}=\frac{2}{3}\mu\left[2\frac{\partial u_r}{\partial r}-\frac{1}{r}\left(u_r+\frac{\partial u_\theta}{\partial\theta}\right)-\frac{\partial u_z}{\partial z}\right] \qquad (1.83)$$

$$\tau_{\theta\theta}=\frac{2}{3}\mu\left[-\frac{\partial u_r}{\partial r}+\frac{2}{r}\left(\frac{\partial u_\theta}{\partial\eta^2}+u_r\right)-\frac{\partial u_z}{\partial z}\right] \qquad (1.84)$$

$$\tau_{zz}=\frac{2}{3}\mu\left[-\frac{\partial u_r}{\partial r}-\frac{1}{r}\left(u_r+\frac{\partial u_\theta}{\partial\theta}\right)+2\frac{\partial u_z}{\partial z}\right] \qquad (1.85)$$

$$\tau_{r\theta}=\mu\left[\frac{\partial u_\theta}{\partial r}+\frac{1}{r}\left(\frac{\partial u_r}{\partial\theta}-u_\theta\right)\right] \qquad (1.86)$$

$$\tau_{rz}=\mu\left(\frac{\partial u_z}{\partial r}+\frac{\partial u_r}{\partial z}\right) \qquad (1.87)$$

$$\tau_{\theta z}=\mu\left(\frac{1}{r}\frac{\partial u_z}{\partial\theta}+\frac{\partial u_\theta}{\partial z}\right) \qquad (1.88)$$

$$q_r=-\lambda\frac{\partial T}{\partial r},\quad q_\theta=-\lambda\frac{1}{r}\frac{\partial T}{\partial\theta},\quad q_z=-\lambda\frac{\partial T}{\partial z} \qquad (1.89)$$

$$\begin{aligned} f_r&=\rho u_r H+q_r-u_r\tau_{rr}-u_\theta\tau_{r\theta}-u_z\tau_{zr},\\ f_\theta&=\rho u_\theta H+q_\theta-u_r\tau_{r\theta}-u_\theta\tau_{\theta\theta}-u_z\tau_{z\theta},\\ f_z&=\rho u_z H+q_z-u_r\tau_{rz}-u_\theta\tau_{\theta z}-u_z\tau_{zz} \end{aligned} \qquad (1.90)$$

1.9. General transport equation

All the main equations, which governs the time-dependent three-dimensional fluid flow and heat transfer of a compressible Newtonian fluid, can be presented in a single form.

For example, let's consider the equation of momentum in a projection to an axis x (1.32).

Eq. (1.32) it can be written as

$$\begin{aligned}&\frac{\partial}{\partial t}(\rho u)+\frac{\partial}{\partial x}(\rho uu)+\frac{\partial}{\partial y}(\rho uv)+\frac{\partial}{\partial z}(\rho uw)\\&=-\frac{\partial p}{\partial x}+\frac{\partial}{\partial x}(\tau_{xx})+\frac{\partial}{\partial y}(\tau_{xy})+\frac{\partial}{\partial z}(\tau_{xz})+\rho f_x,\end{aligned} \tag{1.91}$$

Using Eqs. (1.35) we obtain from Eq. (1.91)

$$\begin{aligned}&\frac{\partial}{\partial t}(\rho u)+\frac{\partial}{\partial x}(\rho uu)+\frac{\partial}{\partial y}(\rho uv)+\frac{\partial}{\partial z}(\rho uw)=-\frac{\partial p}{\partial x}+\frac{\partial}{\partial x}\left(\mu\frac{\partial u}{\partial x}\right)+\frac{\partial}{\partial y}\left(\mu\frac{\partial u}{\partial y}\right)+\frac{\partial}{\partial z}\left(\mu\frac{\partial u}{\partial z}\right)\\&+\frac{\partial}{\partial x}\left(\mu\frac{\partial u}{\partial x}\right)+\frac{\partial}{\partial y}\left(\mu\frac{\partial v}{\partial x}\right)+\frac{\partial}{\partial z}\left(\mu\frac{\partial w}{\partial x}\right)-\frac{2}{3}\frac{\partial}{\partial x}\left(\mu\frac{\partial u}{\partial x}+\mu\frac{\partial v}{\partial y}+\mu\frac{\partial w}{\partial z}\right)+\rho f_x\end{aligned} \tag{1.92}$$

or

$$\begin{aligned}&\frac{\partial}{\partial t}(\rho u)+div(\rho u\mathbf{V})=-\frac{\partial p}{\partial x}+div(\mu\ grad\ u)\\&+\frac{\partial}{\partial x}\left(\mu\frac{\partial u}{\partial x}\right)+\frac{\partial}{\partial y}\left(\mu\frac{\partial v}{\partial x}\right)+\frac{\partial}{\partial z}\left(\mu\frac{\partial w}{\partial x}\right)-\frac{2}{3}\frac{\partial}{\partial x}(div\mathbf{V})+\rho f_x\end{aligned} \tag{1.93}$$

We quote in Table 1.1. the conservative or divergence form of the system of equations.

Table 1.1.

Equation	
Continuity	$\frac{\partial\rho}{\partial t}+div(\rho\mathbf{V})=0$
x- Momentum	$\frac{\partial}{\partial t}(\rho u)+div(\rho u\mathbf{V})=-\frac{\partial p}{\partial x}+div(\mu\ grad\ u)+S_{Mx}$
y- Momentum	$\frac{\partial}{\partial t}(\rho v)+div(\rho v\mathbf{V})=-\frac{\partial p}{\partial y}+div(\mu\ grad\ v)+S_{My}$
z- Momentum	$\frac{\partial}{\partial t}(\rho w)+div(\rho w\mathbf{V})=-\frac{\partial p}{\partial z}+div(\mu\ grad\ w)+S_{Mz}$
Energy	$\frac{\partial}{\partial t}(\rho e)+div(\rho e\mathbf{V})=-p\ div\mathbf{V}+div(\lambda\ grad\ T)+\frac{\partial Q}{\partial t}+\Phi$

where, for example

$$S_{Mx} = \frac{\partial}{\partial x}\left(\mu \frac{\partial u}{\partial x}\right) + \frac{\partial}{\partial y}\left(\mu \frac{\partial v}{\partial x}\right) + \frac{\partial}{\partial z}\left(\mu \frac{\partial w}{\partial x}\right) - \frac{2}{3}\frac{\partial}{\partial x}\left(div\mathbf{V}\right) + \rho f_x$$

There are significant commonalities between the various equations. If we introduce a general variable ϕ the conservative form of all fluid flow equations, including equations for scalar quantities such as temperature, can usefully be written in the following form:

$$\frac{\partial}{\partial t}\left(\rho\phi\right) + \nabla \cdot \left(\rho \mathbf{V} \phi\right) = \nabla \cdot \left(\Gamma \nabla \phi\right) + S_\phi \tag{1.94}$$

In words

Rate of increase of ϕ of fluid element	+	Net rate of flow of ϕ out of fluid element	=	Rate of increase of ϕ due to diffusion	+	Rate of ϕ increase of due to sources

Here

Table 1.2

Equation	ϕ	Γ	S_ϕ
Continuity	1	0	0
x- Momentum	u	μ	$-\frac{\partial p}{\partial x} + S_{Mx}$
y- Momentum	v	μ	$-\frac{\partial p}{\partial y} + S_{My}$
z- Momentum	w	μ	$-\frac{\partial p}{\partial z} + S_{Mz}$
Energy	e	$\frac{\lambda}{c_v}$	$-p\, div\mathbf{V} + \frac{\partial Q}{\partial t} + \Phi$

The equation (1.94) is the so-called transport equation for property ϕ. It clearly highlights the various transport processes: the **rate of change** term and the **convective** term on the left hand side and the **diffusive** term (Γ=diffusion

coefficient) and the **source** term respectively on the right hand side. In order to bring out the common features we have, of course, had to hide the terms that are not shared between the equations in the source terms. Note that equations (1.94) can be made to work for the internal energy equation by changing e into T by means of an equation of state.

The equation (1.94) is used as the starting point for computational procedures in the finite volume method. By setting ϕ equal to 1, u, v, w and e (or T or E) and selecting appropriate values for the diffusion coefficient Γ and source terms we obtain special forms of Table 2.1 for each of the five partial differential equations for mass, momentum and energy conservation. The key step of the finite volume method, which is to be developed in the next Chapter, is the integration of (1.94) over a three-dimensional control volume V yielding

$$\iiint_V \frac{\partial}{\partial t}(\rho\phi)\,dV + \iiint_V \nabla\cdot(\rho\boldsymbol{V}\phi)\,dV = \iiint_V \nabla\cdot(\Gamma\,\nabla\,\phi)\,dV + \iiint_V S_\phi\,dV \quad (1.95)$$

The volume integrals in the second term on the left hand side, the convective term, and in the first term on the right hand side, the diffusive term, are re-written as integrals over the entire bounding surface of the control volume by using Gauss' divergence theorem. For a vector **a** this theorem states

$$\iiint_V \nabla\cdot\mathbf{a}\,dV = \oiint_A \mathbf{n}\cdot\mathbf{a}\,dA \quad (1.96)$$

The physical interpretation of $\mathbf{n}\cdot\mathbf{a}$ is the component of vector **a** in the direction of the vector **n** normal to surface element dA. Thus the integral of the divergence of a vector **a** over a volume is equal to the component of **a** in the direction normal to the surface which bounds the volume summed (integrated) over the entire bounding surface A. Applying Gauss' divergence theorem, equation (1.95) can be written as follows:

$$\iiint_V \frac{\partial}{\partial t}(\rho\phi)\,dV + \oiint_A \mathbf{n}\cdot(\rho\boldsymbol{V}\phi)\,dA = \oiint_A \mathbf{n}\cdot(\Gamma\,\nabla\,\phi)\,dA + \iiint_V S_\phi\,dV \quad (1.97)$$

The order of integration and differentiation has been changed in the first term on the left hand side of (1.97) to illustrate its physical meaning. This term signifies the **rate of change of the total amount of fluid property ϕ in the control volume**. The product $\mathbf{n}\cdot(\rho \boldsymbol{V}\phi)$ expresses the flux component of property ϕ due to fluid flow along the outward normal vector **n**, so the second term on the left hand side of (1.97), the convective term, is therefore the **net rate of decrease of fluid property ϕ of the fluid element due to convection**.

A diffusive flux is positive in the direction of a negative gradient of the fluid property ϕ, i.e. along direction -*grad* ϕ. For instance, heat is conducted in the direction of negative temperature gradients. Thus, the product $\mathbf{n}\cdot(-\Gamma\nabla\phi)$ is the component of diffusion flux along the outward normal vector, and so out of the fluid element. Similarly, the product $\mathbf{n}\cdot(\Gamma\nabla\phi)$, which is also equal to $\Gamma(-\mathbf{n}\cdot(-\nabla\phi))$, can be interpreted as a positive diffusion flux in the direction of the inward normal vector **-n**, i.e. into the fluid element. The first term on the right hand side of (1.97), the diffusive term, is thus associated with a flux into the element and represents the **net rate of increase of fluid property ϕ of the fluid element due to diffusion**. The final term on the right hand side of this equation gives the rate of increase of property ϕ **as a result of sources** inside the fluid element.

In words, relationship (1.97) for the fluid in the control volume can be expressed as follows:

Rate of increase of ϕ	+	Net rate of decrease of ϕ due to convection across the boundaries	=	Rate of increase of ϕ due to diffusion across the boundaries	+	Net rate of creation of ϕ

This discussion clarifies that integration of the partial differential equation generates a statement of the conservation of a fluid property for a finite size (macroscopic) control volume.

Multiplying the continuity equation by ϕ and subtracting the obtained result from equation (1.94), we can rewrite it in non-conservation form as

$$\rho \frac{\partial \phi}{\partial t} + \rho \mathbf{V} \cdot \nabla(\phi) = \nabla \cdot (\Gamma \nabla \phi) + S_\phi \tag{1.98}$$

Analyzing the Eq. (1.98), we can receive several special cases.

1) If convective and diffusive terms are equal to zero, we have an ordinary differential equation

$$\frac{d\phi}{dt} = \frac{S_\phi}{\rho} \tag{1.99}$$

2) If convective and source terms are equal to zero, we have an equation of parabolic type

$$\rho \frac{\partial \phi}{\partial t} = \frac{\partial}{\partial x}\left(\Gamma \frac{\partial \phi}{\partial x}\right) + \frac{\partial}{\partial y}\left(\Gamma \frac{\partial \phi}{\partial y}\right) + \frac{\partial}{\partial z}\left(\Gamma \frac{\partial \phi}{\partial z}\right) \tag{1.100}$$

3) If diffusive and source terms are equal to zero, we have an equation of hyperbolic type

$$\frac{\partial \phi}{\partial t} + u \frac{\partial \phi}{\partial x} + v \frac{\partial \phi}{\partial y} + w \frac{\partial \phi}{\partial z} = 0 \tag{1.101}$$

4) In a case of steady-state flow, with the absence of convective and source terms, a generalized equation is an elliptic one

$$\frac{\partial}{\partial x}\left(\Gamma \frac{\partial \phi}{\partial x}\right) + \frac{\partial}{\partial y}\left(\Gamma \frac{\partial \phi}{\partial y}\right) + \frac{\partial}{\partial z}\left(\Gamma \frac{\partial \phi}{\partial z}\right) = 0 \tag{1.102}$$

5) For steady state 2D boundary layer approximation the equation (1.98) is as follows

$$\rho u \frac{\partial \Phi}{\partial x} + \rho v \frac{\partial \Phi}{\partial y} = \frac{\partial}{\partial y}\left(\Gamma \frac{\partial \Phi}{\partial y}\right) \tag{1.103}$$

In such form this equation is also brought to parabolic type from the point of view of longitudinal coordinate.

In each of these five cases different numerical methods are applied. The boundary conditions differ as well.

Different terms of the equation (1.94) can play a defining role in different areas of real flows at different timepoints.

Therefore, it is preferable to choose a method of numerical interpretation not for all equation in general, but for its different parts.

From this point of view, it is convenient to use the interpretation of properties of coordinates offered by S. Patankar [3], both spatial and temporary.

1.10. One-Way and Two-Way Coordinates

We shall now consider new concepts about the properties of coordinates and then establish a connection between these and the standard mathematical terminology.

Definitions. A *two-way* coordinate is such that the conditions at a given location in that coordinate are influenced by changes in conditions on *either* side of that location. A *one-way* coordinate is such that the conditions at a given location in that coordinate are influenced by changes in conditions on *only* one side of that location.

Examples. One-dimensional steady heat conduction in a rod provides an example of a two-way coordinate. The temperature of any given point in the rod can be influenced by changing the temperature of either end. Normally, space coordinates are two-way coordinates. Time, on the other hand, is *always* a one-way coordinate. During the unsteady cooling of a solid, the temperature at a given instant can be influenced by changing only those conditions that prevailed *before* that instant. It is a matter of common experience that yesterday's events

affect today's happenings, but tomorrow's conditions have no influence on what happens today.

Space as a one-way coordinate. What is more interesting is that even a space coordinate can very nearly become one-way under the action of fluid flow. If there is a strong unidirectional flow in the coordinate direction, then significant influences travel only from upstream to downstream. The conditions at a point are then affected largely by the upstream conditions, and very little by the downstream ones. The one-way nature of a space coordinate is an approximation. It is true that convection is a one-way process, but diffusion (which is always present) has two-way influences. However, when the flow rate is large, convection overpowers diffusion and thus makes the space coordinate nearly one-way.

Parabolic, elliptic, hyperbolic. It appears that the mathematical terms parabolic and elliptic, which are used for the classification of differential equations, correspond to our computational concepts of one-way and two-way coordinates. The term parabolic indicates a one-way behavior, while elliptic signifies the two-way concept.

It would be more meaningful if situations were described as being parabolic or elliptic in a given coordinate. Thus, the unsteady heat conduction problem, which is normally called parabolic, is actually parabolic in time and elliptic in the space coordinates. The steady heat conduction problem is elliptic in all coordinates. A two-dimensional boundary layer is parabolic in the streamwise coordinate and elliptic in the cross-stream coordinate.

Since such descriptions are unconventional, a connection with established practice can perhaps be achieved by the following rule:

A situation is parabolic if there exists at least one one-way coordinate;

otherwise, it is elliptic.

A flow with one one-way space coordinate is sometimes called a boundary-layer-type flow, while a flow with all two-way coordinates is referred to as a recirculating flow.

What about the third category, namely, hyperbolic? It so happens that a hyperbolic situation does not neatly fit into the computational classification. A hyperbolic problem has a kind of one-way behavior, which is, however, not along coordinate directions but along special lines called *characteristics*. There are numerical methods that make use of the characteristic lines, but they are restricted to hyperbolic problems.

Computational implications. The motivation for the foregoing discussion about one-way and two-way coordinates is that, if a one-way coordinate can be identified in a given situation, substantial economy of computer storage and computer time is possible. Let us consider an unsteady two-dimensional heat conduction problem. We shall construct a two-dimensional array of grid points in the calculation domain. At any instant of time, there will be a corresponding two-dimensional temperature field. Such a field will have to be handled in the computer for each of the successive instants of time. However, since time is a one-way coordinate, the temperature field at a given time is not affected by the future temperature fields. Indeed, the entire unsteady problem can be reduced to the required repetitions of one basic step, namely this: Given the temperature field at time t, find the temperature field at time $t + \Delta t$. Thus, computer storage will be needed only for these two temperature fields; the same storage space can be used, over and over again, for all the time steps.

In this manner, starting with a given initial temperature field, we are able to "march" forward to successive instants of time. During any time step, only one two-dimensional array of temperatures forms the unknowns to be treated simultaneously. They are decoupled from all future values of temperature, and

the previous values that influence them are known. Thus, we need to solve a much simpler set of equations, with a consequent saving of computer time.

Problems

1. In conjunction with the spatially marching solutions of Eq. (1.62) for an inviscid flow, the elements of the solution vector **E** are given as:

$$E_1 = \rho u, \quad E_2 = \rho u^2 + p, \quad E_3 = \rho v u, \quad E_4 = \rho w u, \quad E_5 = \rho u\left(E + p/\rho\right) \quad (1.104)$$

Derive expressions for the primitive variables ρ, u, v, w and p in terms of E_1, $E2$, $E3$, $E4$ and $E5$. Assume a *calorically perfect gas* (with constant γ).

2. Derive the momentum and energy equations for a viscous flow in integral form. Show that all three conservation equations continuity momentum, and energy can be put in a single generic integral form.

2. DISCRETIZATION METHODS

2.1.The Task

A numerical solution of a differential equation consists of a set of numbers from which the distribution of the dependent variable ϕ can be constructed. In this sense, a numerical method is akin to a laboratory experiment, in which a set of instrument readings enables us to establish the distribution of the measured quantity in the domain under investigation. The numerical analyst and the laboratory experimenter both must remain content with only a finite number of numerical values as the outcome, although this number can, at least in principle, be made large enough for practical purposes.

Let us suppose that we decide to represent the variation of ϕ by a polynomial in x,

$$\phi = a_0 + a_1 x + a_2 x^2 + ... + a_m x^m \tag{2.1}$$

and employ a numerical method to find the finite number of coefficients $a_0, a_1, a_2, ..., a_m$. This will enable us to evaluate ϕ at any location x by substituting the value of x and the values of the a's into Eq. (2.1). This procedure is, however, somewhat inconvenient if our ultimate interest is to obtain the values of ϕ at various locations. The values of the a's are, by themselves, not particularly meaningful, and the substitution operation must be carried out to arrive at the required values of ϕ. This leads us to the following thought: Why not construct a method that employs the values of ϕ at a number of given points as the primary unknowns? Indeed, most numerical methods for solving differential equations do belong in this category, and therefore we shall limit our attention to such methods.

Thus, a numerical method treats as its basic unknowns the values of the dependent variable at a finite number of locations (called the *grid points*) in the calculation domain. The method includes the tasks of providing a set of algebraic equations for these unknowns and of prescribing an algorithm for solving the equations.

In focusing attention on the values at the grid points, we have replaced the continuous information contained in the exact solution of the differential equation with discrete values. We have thus discretized the distribution of ϕ, and it is appropriate to refer to this class of numerical methods as *discretization methods*.

The algebraic equations involving the unknown values of ϕ at chosen grid points, which we shall now name the *discretization equations*, are derived from the differential equation governing ϕ. In this derivation, we must employ some assumption about how ϕ varies *between* the grid points. Although this "profile" of ϕ could be chosen such that a single algebraic expression suffices for the whole calculation domain, it is often more practical to use *piecewise* profiles

such that a given segment describes the variation of ϕ over only a small region in terms of the ϕ values at the grid points within and around that region. Thus, it is common to subdivide the calculation domain into a number of subdomains or elements such that a separate profile assumption can be associated with each subdomain.

In this manner, we encounter the discretization concept in another context. The continuum calculation domain has been discretized. It is this systematic discretization of space and of the dependent variables that makes it possible to replace the governing differential equations with simple *algebraic equations*, which can be solved with relative ease.

For simplicity, in this section it is assumed that the variable ϕ is a function of the only independent variable x. However, the ideas developed here will also be applicable in the case of the dependence of more than one independent variable.

Suppose that a differential boundary-value problem is given on some interval, D on the x-axis. This means that one is given a differential equation (or system of equations) which the solution must satisfy in the interval, D, and auxiliary conditions on ϕ at one or both ends of this interval. The differential boundary-value problem will be written in the symbolic form

$$L\phi = f \tag{2.2}$$

Where L is a given differential operator, and f is a given right-hand side. Thus, for example, to write the problem

$$\begin{cases} \dfrac{d\phi}{dx} + \dfrac{x}{1+\phi^2} = \cos(x), \quad 0 \le x \le 1, \\ \phi(0) = 3 \end{cases} \tag{2.3}$$

in form (2.2) we need only take

$$L\phi \equiv \begin{cases} \dfrac{d\phi}{dx} + \dfrac{x}{1+\phi^2}, & 0 \le x \le 1, \\ \phi(0) \end{cases}$$
$$f \equiv \begin{cases} \cos(x), & 0 \le x \le 1, \\ 3 \end{cases} \tag{2.4}$$

We will assume that the solution $\phi(x)$ of problem (2.2) on the interval *D*, exists. In order to calculate this solution by the numerical method, we must first of all choose, on the interval *D*, a finite set of points which, in totality, we will call a "*net*" and designate by the symbol D_h; then we set out to find, not the solution, $\phi(x)$, of problem (2.2), but a table, $[\phi]_h$ of values of the solution at the points of the net D_h. It is assumed that the net depends on a parameter $h = \Delta x > 0$, which can take on positive values as small as desired. As the "step-size" *h* goes to zero the net becomes steadily "*finer*". For example, if the interval *D* is [0,1] and the number of grid nodes is equal to *N*, then we can assume that the step is equal to $h = 1/N$, and take, as the net D_h, the totality of points $x_0 = 0, x_1 = h, x_2 = 2h, \ldots, x_N = Nh = 1$. The desired net $[\phi]_h$, in this case takes on, at the points $x_n = nh$ of the net D_h.

For the approximate computation of the table $[\phi]_h$ of solution- values, in the case of problem (2.3), one could use, for example, the system of equations

$$\begin{cases} \dfrac{\phi_{n+1} - \phi_n}{h} + \dfrac{x_n}{1+\phi_n^{\,2}} = \cos(x_n), & n = 0,1,\ldots,N-1 \\ \phi_0 = 3 \end{cases} \tag{2.5}$$

obtained by substituting for the derivative $\dfrac{d\phi}{dx}$ at the points of the net, the difference approximation

$$\frac{d\phi}{dx} \simeq \frac{\phi(x+h) - \phi(x)}{h}$$

The solution $\phi^{(h)} = (\phi_0, \phi_1, \phi_2, ..., \phi_N)$ of system (2.5) is defined on the same net as the desired net function $[\phi]_h$. It's values $\phi_1, \phi_2, ..., \phi_N$ at the points x_1, x_2, ... , x_N are consecutively calculated from Eq. (2.5) for n = 0, 1,.... N-1.

Suppose that for the approximate computation of the solution of the differential boundary-value problem (2.2), i.e. for the approximation computation of the net function $[\phi]_h$ via Eq. (2.2), we have constructed a system of equations which we will write symbolically, by analogy with Eq. (2.2), in the form

$$L_h \phi^{(h)} = f^{(h)} \tag{2.6}$$

Difference scheme (2.5) for differential boundary-value problem (2.4) may be taken as example of this differencing process.

To write scheme (2.5) in form (2.6) we may set

$$\begin{aligned} L_h \phi^{(h)} &= \begin{cases} \dfrac{\phi_{n+1} - \phi_n}{h} + \dfrac{x_n}{1 + \phi_n^{\,2}}, & n = 0,1,...,N-1 \\ \phi_0 \end{cases} \\ f^{(h)} &= \begin{cases} \cos(nh), & n = 0,1,...,N-1 \\ 3 \end{cases} \end{aligned} \tag{2.7}$$

2.2. Taylor-Series Formulation

The usual procedure for deriving finite-difference equations consists of approximating the derivatives in the differential equation via a truncated Taylor series. Let us consider the grid points shown in Fig. 2.1. For grid point 2, located midway between grid points 1 and 3 such that $\Delta x = x_2 - x_1 = x_3 - x_2$, the Taylor-series expansion around 2 gives

$$\phi_{n-1} = \phi_n - \left(\frac{\partial \phi}{\partial x}\right)_n h + \frac{1}{2}\left(\frac{\partial^2 \phi}{\partial x^2}\right)_n h^2 - \ldots$$
$$\phi_{n+1} = \phi_n + \left(\frac{\partial \phi}{\partial x}\right)_n h + \frac{1}{2}\left(\frac{\partial^2 \phi}{\partial x^2}\right)_n h^2 - \ldots \tag{2.8}$$

where $h = \Delta x$.

Truncating the series just after the third term, and adding and subtracting the two equations, we obtain

$$\left(\frac{\partial \phi}{\partial x}\right)_n \approx \frac{\phi_{n+1} - \phi_{n-1}}{2h} \tag{2.9}$$

and

$$\left(\frac{\partial^2 \phi}{\partial x^2}\right)_n \approx \frac{\phi_{n+1} - 2\phi_n + \phi_{n-1}}{h^2} \tag{2.10}$$

If in the second of the equations (1.108) we truncate the series just after the second term, then we obtain:

$$\left(\frac{\partial \phi}{\partial x}\right)_n \approx \frac{\phi_{n+1} - \phi_n}{h} \tag{2.11}$$

The substitution of such expressions into the differential equation leads to the *finite-difference equation*.

The method includes the assumption that the variation of ϕ is somewhat like a polynomial in *x*, so that the higher derivatives are unimportant. This assumption, however, leads to an undesirable formulation when, for example, exponential variations are encountered. The Taylor-series formulation is relatively straightforward but allows less flexibility and provides little insight into the physical meanings of the terms.

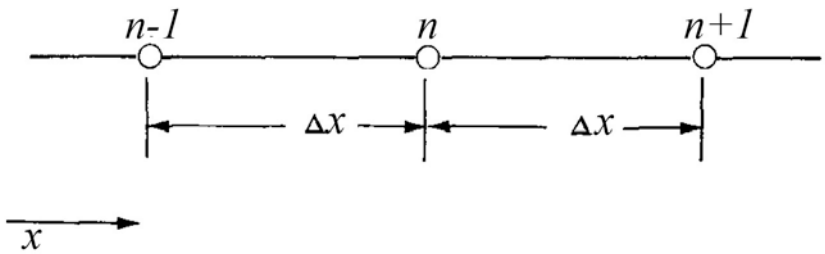

Fig.2.1 Three successive grid points used for the Taylor-series expansion.

An expression given by Eq. (2.11) is called a *forward difference*; an expression

$$\left(\frac{\partial \phi}{\partial x}\right)_n \approx \frac{\phi_n - \phi_{n-1}}{h} \tag{2.12}$$

is called a *backward difference* and finite difference approximation of derivative given by Eq. (2.9) is called *central difference.*

2.3. Control Volume Approach

Often elementary textbooks on heat transfer derive the finite-difference equation via the Taylor-series method and then demonstrate that the resulting equation is consistent with a heat balance over a small region surrounding a grid point. We have also seen that the control-volume formulation can be regarded as a special version of the method of weighted residuals. The basic idea of the control-volume formulation is easy to understand and lends itself to direct physical interpretation. The calculation domain is divided into a number of nonoverlapping control volumes such that there is one control volume surrounding each grid point. The differential equation is integrated over each control volume. Piecewise profiles expressing the variation of ϕ between the grid points are used to evaluate the required integrals. Piecewise profiles expressing the variation of ϕ between the grid points are used to evaluate the required integrals

The discretization equation obtained in this manner expresses the conservation principle for ϕ for the finite control volume, just as the differential equation expresses it for an infinitesimal control volume.

The most attractive feature of the control-volume formulation is that the resulting solution would imply that the integral conservation of quantities such as mass, momentum, and energy is exactly satisfied over any group of control volumes and, of course, over the whole calculation domain. This characteristic exists for any number of grid points - not just in a limiting sense when the number of grid points becomes large. Thus, even the coarse-grid solution exhibits exact integral balances.

When the discretization equations are solved to obtain the grid-point values of the dependent variable, the result can be viewed in two different ways. In the finite-element method and in most weighted-residual methods, the assumed variation of ϕ consisting of the grid-point values and the interpolation functions (or profiles) between the grid points is taken as the approximate solution. In the finite-difference method, however, only the grid-point values of ϕ are considered to constitute the solution, without any explicit reference as to how ϕ varies between the grid points. This is akin to a laboratory experiment where the distribution of a quantity is obtained in terms of the measured values at some discrete locations without any statement about the variation *between* these locations. In our control-volume approach, we shall also adopt this view. We shall seek the solution in the form of the grid-point values only. The interpolation formulas or the profiles will be regarded as auxiliary relations needed to evaluate the required integrals in the formulation. Once the discretization equations are derived, the profile assumptions can be forgotten. This viewpoint permits complete freedom of choice in employing, if we wish, different profile assumptions for integrating different terms in the differential equation.

To make the foregoing discussion more concrete, we shall now derive the control-volume discretization equation for a simple situation.

Let us consider steady one-dimensional heat conduction governed by

$$\frac{d}{dx}\left(\lambda\frac{dT}{dx}\right)+S=0 \tag{2.13}$$

where λ is the thermal conductivity, T is the temperature, and S is the rate of heat generation per unit volume.

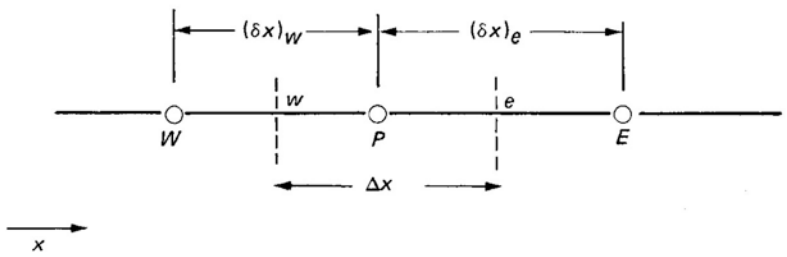

Figure 2.2 Grid-point cluster for the one-dimensional problem.

Preparation. To derive the discretization equation, we shall employ the grid-point cluster shown in Fig. 2.2. We focus attention on the grid point P, which has the grid points E and W as its neighbors. (E denotes the east side, i.e., the positive x direction, while W stands for west or the negative x direction.) The dashed lines show the faces of the control volume; their exact locations are unimportant for the time being. The letters e and w denote these faces. For the one-dimensional problem under consideration, we shall assume a unit thickness in the y and z directions. Thus, the volume of the control volume shown is $\Delta x\times 1\times 1$. If we integrate Eq. (2.13) over the control volume, we get

$$\left(\lambda\frac{dT}{dx}\right)_e-\left(\lambda\frac{dT}{dx}\right)_w+\int_w^e S dx=0 \tag{2.14}$$

Profile assumption. To make further progress, we need a profile assumption or an interpolation formula. Two simple profile assumptions are shown in Fig.

2.3. The simplest possibility is to assume that the value of T at a grid point prevails over the control volume surrounding it. This gives the stepwise profile sketched in Fig. 2.3a. For this profile, the slope dT/dx is not defined at the control-volume faces (i.e., at w or e). A profile that does not suffer from this difficulty is the piecewise-linear profile (Fig. 2.3b). Here, linear interpolation functions are used between the grid points.

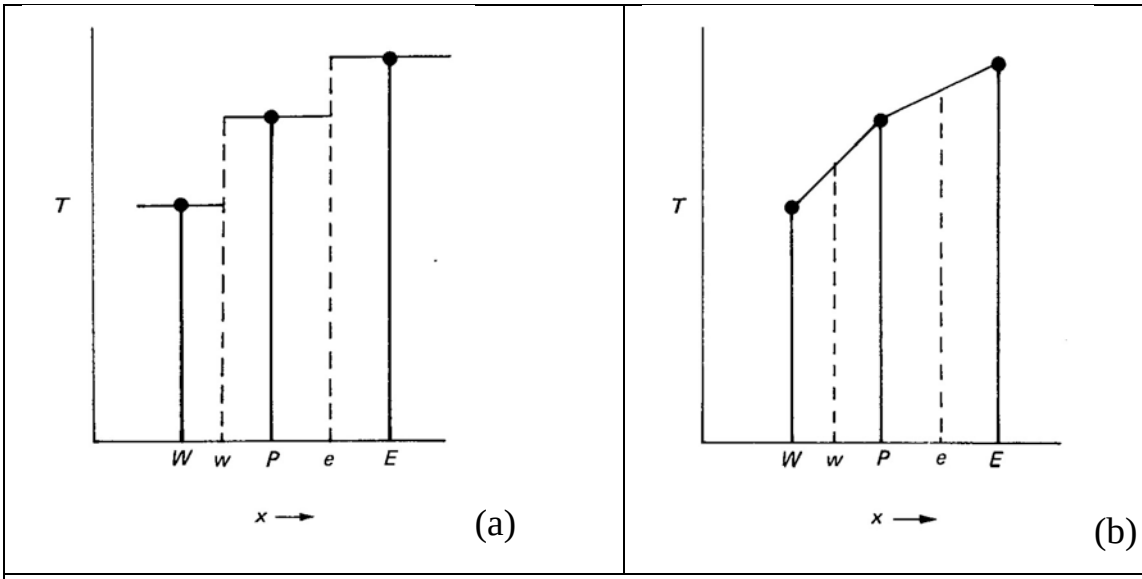

Figure 2.3. Two simple profile assumptions, (a) Stepwise profile; (b) piecewise-linear profile.

The discretization equation. If we evaluate the derivatives dT/dx in Eq. (2.14) from the piecewise-linear profile, the resulting equation will be

$$\lambda_e \frac{T_E - T_P}{(\delta x)_e} - \lambda_w \frac{T_P - T_W}{(\delta x)_w} + \bar{S}\Delta x = 0 \tag{2.15}$$

where $\bar{S}$ is the average value of S over the control volume.

Treatment of the source term. Let's give some attention to the source term S in Eq. (2.13). Often, the source term is a function of the dependent variable T itself, and it is then desirable to acknowledge this dependence in constructing the discretization equation. We can, however, formally account for only a linear dependence because, as we shall see later, the discretization equations will be solved by the techniques for linear algebraic equations. The procedure for

"linearizing" a given $S \sim T$ relationship will be discussed in the next chapter. Here, it is sufficient to express the average value S as

$$\bar{S} = S_C + S_P T_P \tag{2.16}$$

where S_C stands for the constant part of S, while S_P is the coefficient of T_P. (Obviously, S_P does *not* stand for S evaluated at point P.)

The appearance of T_P in Eq. (2.16) reveals that, in expressing the average value S, we have presumed that the value T_P prevails over the control volume; in other words, the stepwise profile shown in Fig. 3.3a has been used. (It should be noted that we are free to use the stepwise profile for the source term while using the piecewise-linear profile for the *dT/dx* term.)

With the linearized source expression, the discretization equation (2.15) will be the following:

$$a_P T_P = a_E T_E + a_W T_W + b \tag{2.17}$$

where

$$\begin{aligned} &a_P = a_E + a_W - S_P h, \\ &a_E = \frac{\lambda_e}{(\delta x)_e}, \quad a_W = \frac{\lambda_w}{(\delta x)_w}, \quad b = S_C \Delta x \end{aligned} \tag{2.18}$$

In general, it is convenient to think of Eq. (2.17) as having the form

$$a_P T_P = \sum a_{nb} T_{nb} + b \ , \tag{2.19}$$

where the subscript *nb* denotes a neighbor, and the summation is to be taken over all the neighbors.

2.4. The basic rules derived from a physical sense of control volume method

The formulas from previous chapter provide sufficient background to allow the formulation of the basic rules that our discretization equations should obey,

to ensure physical realism and overall balance. These seemingly simple rules have far-reaching implications, and they will guide the development of methods throughout this book.

Rule 1: Consistency at control-volume faces. When a face is common to two adjacent control volumes, the flux across it must be represented by the same expression in the discretization equations for the two control volumes.

Discussion. Obviously, the heat flux that leaves one control volume through a particular face must be identical to the flux that enters the next control volume through the same face. Otherwise, the overall balance would not be satisfied. Although this requirement is easy to understand, subtle violations must be watched for. For the control volume shown in Fig. 2.2, we could have evaluated the interface heat fluxes $\lambda dT/dx$ from a quadratic profile passing through T_W, T_P, and T_E. The use of the same kind of formulation for the next control volume implies that the gradient dT/dx at the common interface is calculated from different profiles, depending on which control volume is being considered. The resulting inconsistency in dT/dx (and hence in the heat flux) is sketched in Fig. 2.4.

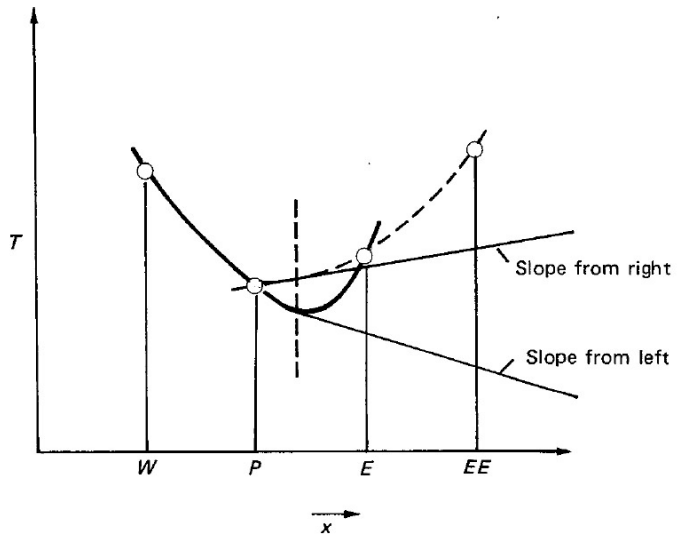

Figure 2.4. Flux inconsistency resulting from quadratic profile.

Another practice that could lead to flux inconsistency is to assume that the fluxes at the faces of a given control volume are all governed by the center-point conductivity λ_P. Then the heat flux at the interface e (shown in Fig. 2.2) will be expressed as $\lambda_P\ (T_P - T_E)/(\delta x)_e$ when the control volume surrounding the point P is considered, and as $\lambda_E\ (T_P - T_E)/(\delta x)_e$ when the equation with E as the center point is constructed. To avoid such inconsistencies, it is useful to remember that an interface flux must be considered in its own right, and not as belonging to a certain control volume.

Rule 2: Positive coefficients. Most situations of interest here will be such that the value of a dependent variable at a grid point is influenced by the values at neighboring grid points only through the processes of convection and diffusion. Then it follows that an increase in the value at one grid point should, with other conditions remaining unchanged, lead to an increase (and not a decrease) in the value at the neighboring grid point. In Eq. (2.17), if an increase in T_E must lead to an increase in T_P, it follows that the coefficients a_E and a_P must have the same sign. In other words, for the general equation (2.19), the neighbor coefficients a_{nb} and the center-point coefficient a_P all must be of the same sign. We can, of course, choose to make them all positive or all negative. Let us decide to write our discretization equations such that the coefficients are positive; then Rule 2 can be stated as follows:

All coefficients (a_P and neighbor coefficients a_{nb}) must always be positive.

Comments. The coefficient definitions given in Eqs. (2.18) show that our illustrative discretization equation [Eq. (2.17)] does obey the positive coefficient rule. However there are numerous formulations that frequently violate this rule. Usually, the consequence is a physically unrealistic solution. The presence of a negative neighbor coefficient can lead to the situation in which an increase in a boundary temperature causes the temperature at the adjacent grid point to

decrease. We shall accept only those formulations that guarantee positive coefficients under all circumstances.

Rule 3: Negative-slope linearization of the source term. If we consider the coefficient definitions in Eqs. (2.18), it appears that, even if the neighbor coefficients are positive, the center-point coefficient a_P can become negative via the S_P term. Of course, the danger can be completely avoided by requiring that S_P will not be positive. Thus, we formulate Rule 3 as follows:

When the source term is linearized as $\bar{S} = S_C + S_P T_P$, the coefficient S_P must always be less than or equal to zero.

Remarks. This rule is not as arbitrary as it sounds. Most physical processes do have a negative-slope relationship between the source term and the dependent variable. Indeed, if S_P were positive, the physical situation could become unstable. A positive S_P implies that, as T_P increases, the source term increases; if an effective heat-removal mechanism is not available, this may, in turn, lead to an increase in T_P, and so on. Computationally, it is vital to keep S_P negative so that instabilities and physically unrealistic solutions do not arise. The source-term linearization is further discussed in the next chapter. It is sufficient to note here that, for computational success, the principle of negative S_P is essential.

2.5. Convergence

We must give a precise meaning to the requirement that $\phi^{(h)} \to [\phi]_h$, the convergence requirement that we will impose on discretization schemes.

We will say that the solution $\phi^{(h)}$ of the difference boundary-value problem (2.6) *converges*, as the net is refined, to the solution of a boundary- value problem (2.2), if

$$\left\| [\phi]_h - \phi^{(h)} \right\| \to 0 \quad \text{as} \quad h \to 0 \tag{2.20}$$

where $\phi^{(h)} = (\phi_0, \phi_1, \phi_2, ..., \phi_N)$ is the solution of system (2.6)

$$L_h\phi^{(h)} = f^{(h)}$$

The norm can be defined in various ways. One can, for example, take as the norm of the maximum value of the module

$$\left\|[\phi]_h - \phi^{(h)}\right\| = \max_n \left|\phi(x_n) - \phi_n\right| \tag{2.21}$$

Another definition of the norm:

$$\left\|[\phi]_h - \phi^{(h)}\right\| = \left(\frac{1}{N}\sum_{n=0}^{N}\left|\phi(x_n) - \phi_n\right|^2\right)^{1/2} \tag{2.22}$$

If in addition the inequality

$$\left\|[\phi]_h - \phi^{(h)}\right\| < ch^k \tag{2.23}$$

is satisfied, where $c > 0$ and $k > 0$ are constants not depending on h, we will say that convergence is of order h^k, or that the numerical scheme has k'th order accuracy.

The requirement that the numerical scheme be convergent is the fundamental requirement which will be imposed on discretization scheme (2.6) for the numerical solution of the differential boundary-value problem (2.2). When this requirement is met then, with the aid of discretization scheme (2.6) , the solution ϕ can be computed to any prescribed accuracy, if h is taken small enough. We have rigorously formulated the concept of convergence and have come up to the central question: i.e., how does one construct a convergent discretization scheme (2.6) for computation of the solution of differential boundary-value problem (2.2)? For one and the same differential boundary-value problem one can get different discretization schemes (2.6), choosing different nets D_h, and replacing the derivatives by various discretization approximations. Some of them may be unsuitable for computation.

2.6.Approximation.

We now give a precise meaning to the concept of approximation of boundary value problem (2.2)

$$L\phi = f \tag{2.24}$$

on the solution ϕ , by discretization scheme (2.6)

$$L_h\phi^{(h)} = f^{(h)} \tag{2.25}$$

For this purpose one must state more precisely what is meant by the residual $\delta f^{(h)}$

$$L_h[\phi]_h = f^{(h)} + \delta f^{(h)} \ , \tag{2.26}$$

which forms when the net function $[\phi]_h$, the table of values of the required solution ϕ, is substituted into Eq. (2.25); and one must make a precise statement as to its magnitude.

Convergence of the magnitude of $\delta f^{(h)}$ to zero, as $h \to 0$, we then take as the definition of approximation.

We start with the consideration of an example of a discretization scheme for the numerical solution of the differential problem

$$\frac{d^2\phi}{dx^2} + a(x)\frac{d\phi}{dx} = 0, \quad 0 \le x \le 1 \tag{2.27}$$

As a discretization scheme for the approximate computation of $[\phi]_h$ we use the equation-set in form (2.25)

$$\begin{aligned} L_h\phi^{(h)} &= \frac{\phi_{n+1} - 2\phi_n + \phi_{n-1}}{h^2} + a(x_n)\frac{\phi_{n+1} - \phi_{n-1}}{2h}, \\ f^{(h)} &= 0 \end{aligned} \tag{2.28}$$

By Taylor's formula we have:

$$
\begin{aligned}
\phi(x_{n-1}) &= \phi(x_n) - \phi'(x_n)h + \frac{1}{2}\phi''(x_n)h^2 - \frac{1}{6}\phi'''(x_n)h^3 + \frac{1}{24}\phi^{(IV)}(\xi_1)h^4 \\
\phi(x_{n+1}) &= \phi(x_n) + \phi'(x_n)h + \frac{1}{2}\phi''(x_n)h^2 + \frac{1}{6}\phi'''(x_n)h^3 + \frac{1}{24}\phi^{(IV)}(\xi_2)h^4 \\
\phi(x_{n-1}) &= \phi(x_n) - \phi'(x_n)h + \frac{1}{2}\phi''(x_n)h^2 - \frac{1}{6}\phi'''(\xi_3)h^3 \\
\phi(x_{n+1}) &= \phi(x_n) + \phi'(x_n)h + \frac{1}{2}\phi''(x_n)h^2 + \frac{1}{6}\phi'''(\xi_4)h^3
\end{aligned}
\tag{2.29}
$$

where $\xi_1, \xi_2, \xi_3, \xi_4$ are certain points in the interval $[x_{n-1}, x_{n+1}]$.

Let us determine $L_h[\phi]_h$ by substituting in the expression (2.28) the function $\phi(x_n)$ instead of the function ϕ_n, $\phi(x_{n-1})$ instead of ϕ_{n-1}, $\phi(x_{n+1})$ instead of ϕ_{n+1}.

Therefore the expression

$$
\begin{aligned}
&L_h[\phi]_h = \frac{\phi(x_{n+1}) - 2\phi(x_n) + \phi(x_{n-1})}{h^2} + a(x_n)\frac{\phi(x_{n+1}) - \phi(x_{n-1})}{2h}, \\
&n = 1, 2, \ldots, N-1
\end{aligned}
\tag{2.30}
$$

can be rewritten thus:

$$
\begin{aligned}
&L_h[\phi]_h = \phi''(x_n) + a(x_n)\phi'(x_n) \\
&+ \left[\frac{\phi^{(IV)}(\xi_1) + \phi^{(IV)}(\xi_2)}{24} + a(x_n)\frac{\phi'''(\xi_3) + \phi'''(\xi_4)}{12} \right] h^2
\end{aligned}
\tag{2.31}
$$

Taking Eq. (2.27) into account, we obtain

$$
L_h[\phi]_h = f^{(h)} + \delta f^{(h)} \tag{2.32}
$$

where

$$
\delta f^{(h)} = h^2 \left[\frac{\phi^{(IV)}(\xi_1) + \phi^{(IV)}(\xi_2)}{24} + a(x_n)\frac{\phi'''(\xi_3) + \phi'''(\xi_4)}{12} \right] \tag{2.33}
$$

If function ϕ has bounded derivatives, then we can write that

$$
\left\| \delta f^{(h)} \right\| \le Ch^2 \tag{2.34}
$$

where C is some constant, depending on ϕ, but not dependent on h.

Now we can define *approximation*. [4, p.98] We will say that the numeric scheme $L_h\phi^{(h)} = f^{(h)}$ approximates the problem $L\phi = f$ on the solution ϕ if $\left\|\delta f^{(h)}\right\| \to 0$ as $h \to 0$. If, moreover, the inequality

$$\left\|\delta f^{(h)}\right\|_{F_h} \le ch^k \tag{2.35}$$

is satisfied, where $c > 0$ and $k > 0$ are constants, then we will say that the approximation is of order h^k, or order k with respect to the magnitude of h.

Thus the numeric scheme (2.28) for the problem (2.27) has the second order of approximation.

2.7. Stability of a discretization scheme.

Suppose that, for the approximate solution of the boundary-value problem

$$L\phi = f \tag{2.36}$$

we have constructed the discretization scheme

$$L_h\phi^{(h)} = f^{(h)}, \tag{2.37}$$

which approximates problem (2.36) on the solution ϕ to some order h^k. This means that the residual $\delta f^{(h)}$

$$L_h[\phi]_h = f^{(h)} + \delta f^{(h)} \tag{2.38}$$

which appears when the table, $[\phi]_h$, of values of the solution ϕ, is substituted into Eq. (2.37), satisfies a bound of the form

$$\left\|\delta f^{(h)}\right\|_{\Phi_h} \le C_1 h^k \tag{2.39}$$

where C_1 is some constant not depending on h.

It can be shown, that approximation is not sufficient for convergence generally. *Stability* is needed in addition.

We will call discretization scheme (2.37) *stable* if there exists numbers, $h_0 > 0$ and $\delta > 0$, such that for any $h < h_0$ and any $\varepsilon^{(h)}$ such as

$$\left\|\varepsilon^{(h)}\right\| < \delta$$

the difference problem

$$L_h z^{(h)} = f^{(h)} + \varepsilon^{(h)} \tag{2.40}$$

obtained from problem (2.37) through the addition to the right-hand side of a perturbation $\varepsilon^{(h)}$, has one and only one solution $z^{(h)}$ and moreover, this solution deviates from the solution, $\phi^{(h)}$, of the unperturbed problem (2.37) by a net function $z^{(h)} - \phi^{(h)}$, satisfying the bound

$$\left\|z^{(h)} - \phi^{(h)}\right\| \le C\left\|\varepsilon^{(h)}\right\| \tag{2.41}$$

where C is some constant not depending on h.

Inequality Eq. (2.41) signifies that a small perturbation $\varepsilon^{(h)}$, of the right-hand side of discretization scheme (2.37) evokes a perturbation, $z^{(h)} - \phi^{(h)}$ in the solution, which is uniformly small with respect to h.

Suppose the operator L_h is linear. We can prove that in this case the above definition of stability is equivalent to the following:

Discretization scheme $L_h \phi^{(h)} = f^{(h)}$ is stable, if for any $f^{(h)}$, it has a unique solution $\phi^{(h)}$ and

$$\left\|\phi^{(h)}\right\| \le C\left\|f^{(h)}\right\| \tag{2.42}$$

where C is some constant not depending on h.

2.8. Convergence as a consequence of approximation and stability

We show, now, that from approximation and stability follows convergence.

We will formulate the following theorem without proof.

Suppose that the discretization scheme $L_h\phi^{(h)} = f^{(h)}$ approximates the problem $L\phi = f$ on the solution ϕ to order h^k, and is stable .

Then the solution, $\phi^{(h)}$, of the difference problem $L_h\phi^{(h)} = f^{(h)}$ converges to $[\phi]_h$, satisfying the bound

$$\left\| [\phi]_h - \phi^{(h)} \right\|_{\Phi_h} \le (CC_1)h^k \tag{2.43}$$

where C and C_1 are the numbers entering into bounds (2.39) and (2.41).

2.9. Spectral analysis of the difference problem

Here we develop the Von Neumann method, useful in a wide range of circumstances for the study of difference problems with initial conditions.

Let us consider the following problem.

In an plane $D = \{t \ge 0, \quad -\infty < x < \infty\}$ we need to find a function $\phi(t,x)$, which satisfies the equation

$$\frac{\partial \phi}{\partial t} + u\frac{\partial \phi}{\partial x} = 0 \tag{2.44}$$

and the boundary conditions

$$\phi(0,x) = g(x), \quad -\infty < x < \infty \tag{2.45}$$

Let u be greater than 0: $u > 0$.

We use the following discretization scheme

$$\begin{cases} \dfrac{\phi_m^{n+1} - \phi_m^n}{\Delta t} + u\dfrac{\phi_m^n - \phi_{m-1}^n}{\Delta x} = 0, \\ \phi_m^0 = g(x_m), \quad n = 0,1,2,...; \quad m = 0, \pm 1, \pm 2,... \end{cases} \tag{2.46}$$

where

$$t^n = n\Delta t, \quad n = 0,1,2,...$$
$$x_m = m\Delta x, \quad m = 0, \pm 1, \pm 2,... \tag{2.47}$$

It is possible to show that a condition of stability *equation reference goes here* (2.42) in this case takes the form

$$\max_m \left|\phi_m^n\right| \le C_1 \left(\max_m \left|g_m\right|\right), \quad n = 0,1,2,... \tag{2.48}$$

i.e. that the solution of the problem (2.46) should satisfy the condition

$$\max_m \left|\phi_m^n\right| \le C_1 \left(\max_m \left|\phi_m^0\right|\right), \quad n = 0,1,2,... \tag{2.49}$$

Necessary spectral condition for stability. For the stability of problem (2.46) with respect to starting data it is necessary that condition (2.49) be fulfilled, in particular, when $\left\{\phi_m^0\right\}$ is any harmonic

$$\phi_m^0 = e^{i\alpha m} \tag{2.50}$$

where i is imaginary unit, α is a real parameter. In this case the solution of problem (2.46) for initial conditions (2.50) has the form

$$\phi_m^n = \lambda^n e^{i\alpha m} \tag{2.51}$$

where $\lambda = \lambda(\alpha)$ is determined by substituting expression (2.51) into the homogeneous difference equation of problem (2.46):

$$\lambda = 1 - \frac{u\Delta t}{\Delta x}\left(1 - e^{-i\alpha}\right) = 1 - r + re^{-i\alpha},$$
$$r = \frac{u\Delta t}{\Delta x} = const \tag{2.52}$$

For the solution (2.51) we may write

$$\max_m \left|\phi_m^n\right| = \left|\lambda(\alpha)\right|^n \max_m \left|\phi_m^0\right| \tag{2.53}$$

Therefore, if condition (2.49) is to be satisfied, it is necessary that, for all real α, we have

$$\left|\lambda(\alpha)\right|^n \le C_1 \tag{2.54}$$

Since this condition must be satisfied for any value of *n*, it is equivalent to the condition

$$\left|\lambda(\alpha)\right| \le 1 \tag{2.55}$$

Precisely this is the *necessary spectral condition of Von Neumann* as applied to the example under consideration.

Let us now use the above-formulated criterion to analyze the stability of problem (2.44). The spectrum (2.52) constitutes a circle, with center at the point (1 - *r*) and radius *r*, in the complex plane. In the case $r < 1$ this region lies inside the unit circle (and is tangent to it at the point λ=1); for $r = 1$ it coincides with the unit circle, and for $r > 1$ lies outside the unit circle (Fig. 2.5). Correspondingly the necessary condition for stability *equation reference goes here* is fulfilled for $r \le 1$, and not fulfilled when $r > 1$.

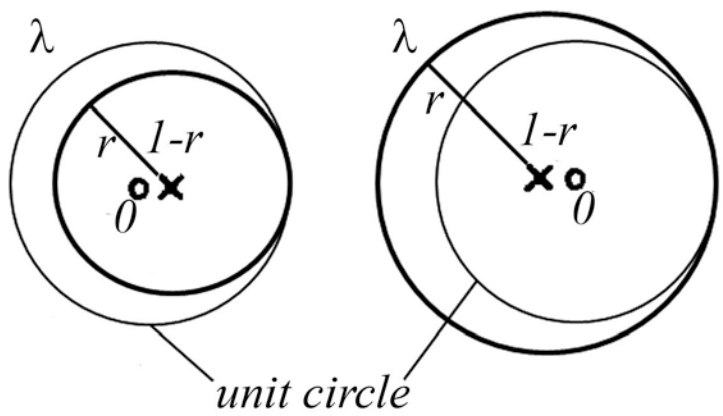

Fig. 2.5. Necessary spectral condition for stability

We can show that the necessary Von Neumann stability condition turns out to be sensitive enough, in this particular case, so as to separate precisely the region of stability from the region of instability.

If the necessary Von Neumann condition (2.55) is not satisfied then one cannot expect stability for <u>any</u> reasonable choice of norms, and if it is satisfied one may hope to achieve stability for <u>some</u> reasonably defined norms.

Parameter $r = \frac{u\Delta t}{\Delta x}$ is called *Courant-Friedrichs-Levy number*

$$CFL = \frac{u\Delta t}{\Delta x} \tag{2.56}$$

and condition

$$CFL \le 1 \tag{2.57}$$

is called *Courant-Friedrichs-Levy condition.*

A similar analysis for case $u < 0$ shows that for the discretization scheme (2.46) the condition (2.55) is not satisfied at any values of parameters, and, therefore, this scheme is always unstable. In this case, for a problem (2.44) the following discretization scheme will be stable

$$\frac{\phi_m^{n+1} - \phi_m^n}{\Delta t} + u\frac{\phi_{m+1}^n - \phi_m^n}{\Delta x} = 0 \tag{2.58}$$

on the following condition

$$CFL = \frac{|u|\Delta t}{\Delta x} \le 1 \tag{2.59}$$

2.10. Explicit, Crank-Nicolson, and Fully Implicit Schemes

We will conduct an analysis of stability of a numerical scheme for a non-stationary one-dimensional thermal conductivity equation

$$\rho C\frac{\partial T}{\partial t} = \frac{\partial}{\partial x}\left(\lambda\frac{\partial T}{\partial x}\right) \tag{2.60}$$

According to the *Principle of frozen coefficients*, the analysis of stability of this nonlinear equation can be replaced with the analysis of the equation

$$\frac{\partial T}{\partial t} = a\frac{\partial^2 T}{\partial x^2} \tag{2.61}$$

where

$$a = \frac{\lambda}{\rho C} = const \tag{2.62}$$

We consider the following discretization scheme, approximating the heat transfer equation (2.61):

$$\frac{T_m^{n+1}-T_m^n}{\Delta t}-a\left[(1-f)\frac{T_{m+1}^n-2T_m^n+T_{m-1}^n}{\Delta x^2}+f\frac{T_{m+1}^{n+1}-2T_m^{n+1}+T_{m-1}^{n+1}}{\Delta x^2}\right]=0 \qquad (2.63)$$

For certain specific values of the weighting factor *f*, the discretization equation reduces to one of different schemes for parabolic differential equations. In particular, *f* = 0 leads to the *explicit scheme*, *f* =0.5 to the *Crank-Nicolson scheme*, and *f* =1 to the *fully implicit scheme*. We shall briefly discuss these schemes and finally indicate the fully implicit scheme as our preference.

Let us consider two special cases.

1) Explicit scheme, *f* = 0

Substitution of the expression $T_m^n=\lambda^n e^{i\alpha m}$ into the corresponding homogeneous difference equation leads to the relation

$$\frac{\lambda-1}{\Delta t}-a\frac{e^{i\alpha}-2+e^{-i\alpha}}{\Delta x^2}=0 \qquad (2.64)$$

Using Euler's formula

$$e^{i\alpha}=\cos\alpha+i\sin\alpha \qquad (2.65)$$

we get from Eq. (2.64)

$$\lambda(\alpha)=1-\frac{2a\Delta t}{\Delta x^2}(1-\cos\alpha)=1-\frac{4a\Delta t}{\Delta x^2}\sin^2\frac{\alpha}{2} \qquad (2.66)$$

Solving the inequality (2.55) $|\lambda(\alpha)|\le 1$, we get the necessary condition of stability:

$$\Delta t\le\frac{\Delta x^2}{2a} \qquad (2.67)$$

2) Fully implicit scheme, *f* =1

Substitution of $T_m^n=\lambda^n e^{i\alpha m}$ into Eq. (2.63) gives

$$\frac{\lambda-1}{\Delta t}-a\frac{\lambda\left(e^{i\alpha}-2+e^{-i\alpha}\right)}{\Delta x^2}=0 \qquad (2.68)$$

It leads to the expression

$$\lambda(\alpha)=\frac{1}{1+\frac{4a\Delta t}{\Delta x^2}\sin^2\frac{\alpha}{2}} \qquad (2.69)$$

It is obvious that $|\lambda(\alpha)| \le 1$ at any positive value a, i.e. the necessary condition of stability is satisfied at any time step.

We can formulate the following rule: implicit schemes more often stable in comparison with explicit ones. But at the same time, the process of solution of a system of linear algebraic equations, which derive from discretization of the initial equations, becomes very complicated.

Eq. (2.63) can be rewritten as

$$\left(1+2f\frac{a\Delta t}{\Delta x^2}\right)\delta T_m^{n+1} - f\frac{a\Delta t}{\Delta x^2}\delta T_{m+1}^{n+1} - f\frac{a\Delta t}{\Delta x^2}\delta T_{m-1}^{n+1} = \Delta T_m^n \tag{2.70}$$

where

$$\Delta T_m^n = \frac{a\Delta t}{\Delta x^2}\left(T_{m+1}^n - 2T_m^n + T_{m-1}^n\right) \text{ -} \tag{2.71}$$

the solution of explicit form of Eq. (2.63).

Then Eq. (2.70) takes the form

$$a_m \delta T_m^{n+1} = b_m \delta T_{m+1}^{n+1} + c_m \delta T_{m-1}^{n+1} + d_m \tag{2.72}$$

where

$$a_m = \left(1+2f\frac{a\Delta t}{\Delta x^2}\right), \quad b_m = c_m = f\frac{a\Delta t}{\Delta x^2}$$
$$d_m = \Delta T_m^n \tag{2.73}$$

2.11. TriDiagonal-Matrix Algorithm

The solution of the discretization equations like (2.72) for the one-dimensional situation can be obtained by the standard Gaussian-elimination method. Because of the particularly simple form of the equations, the elimination process turns into a convenient algorithm. This is sometimes called the Thomas algorithm or the TDMA (TriDiagonal-Matrix Algorithm). The designation TDMA refers to the fact that when the matrix of the coefficients of these equations is written, all the nonzero coefficients align themselves along three diagonals of the matrix.

For convenience in presenting the algorithm, it is necessary to use somewhat different nomenclature. Suppose the grid points were numbered 1,2,3,...,*N*, with points 1 and *N* denoting the boundary points. The discretization equations can be written as

$$a_i\Phi_i = b_i\Phi_{i+1} + c_i\Phi_{i-1} + d_i \tag{2.74}$$

where $i = 1, 2, ..., N-1, N$

Thus, the function Φ_i is related to the neighboring functions Φ_{i+1} and Φ_{i-1}. To account for the special form of the boundary-point equations, let us set

$$c_1 = 0, \quad b_N = 0 \tag{2.75}$$

so that the functions Φ_0 and Φ_{N+1} will not have any meaningful role to play. (When the function boundary values are given, these boundary-point equations take a rather trivial form. For example, if Φ_1 is given, we have $a_1 = 1, b_1 = 0, c_1 = 0, \quad d_1 = \Phi_1$.)

These conditions imply that Φ_1 is known in terms of Φ_2. The equation for *i*=2 is a relation between Φ_1, Φ_2 and Φ_3. But, since Φ_1 can be expressed in terms of Φ_2, this relation reduces to a relation between Φ_2 and Φ_3. In other words, Φ_2 can be expressed in terms of Φ_3. This process of substitution can be continued until Φ_N is formally expressed in terms of Φ_{N+1}. But, because Φ_{N+1} has no meaningful existence, we actually obtain the numerical value of Φ_N at this stage. This enables us to begin the "back-substitution" process in which Φ_{N-1} is obtained from Φ_N, Φ_{N-2} from Φ_{N-1}, Φ_2 from Φ_3, and Φ_1 from Φ_2. This is the essence of the TDMA.

Suppose, in the forward-substitution process, we seek a relation

$$\Phi_i = P_i\Phi_{i+1} + Q_i \tag{2.76}$$

after we have just obtained

$$\Phi_{i-1} = P_{i-1}\Phi_i + Q_{i-1} \tag{2.77}$$

Substitution of Eq. (2.77) into Eq. (2.74) leads to

$$\Phi_i = \frac{b_i}{(a_i - c_i P_{i-1})}\Phi_{i+1} + \frac{c_i Q_{i-1} + d_i}{(a_i - c_i P_{i-1})} \tag{2.78}$$

which can be rearranged to look like Eq. (2.76). In other words, the coefficients P_i, and Q_i then stand for

$$P_i = \frac{b_i}{(a_i - c_i P_{i-1})}, \quad Q_i = \frac{c_i Q_{i-1} + d_i}{(a_i - c_i P_{i-1})} \tag{2.79}$$

These are recurrence relations, since they give P_i and Q_i in terms of P_{i-1} and Q_{i-1}. To start the recurrence process, we note that Eq. (2.74) for *i*=1 is almost of the form (2.76). Thus, the values of P_1 and Q_1 are given by

$$P_1 = \frac{b_1}{a_1}, \quad Q_1 = \frac{d_1}{a_1} \tag{2.80}$$

[It is interesting to note that these expressions do follow from Eq. (2.79) after the substitution $c_1 = 0$.]

At the other end of the P_i, Q_i, sequence, we note that $b_N = 0$. This leads to $P_N = 0$ PN - 0, and hence from Eq. (2.76) we obtain

$$Q_N = \Phi_N \tag{2.81}$$

Now we are in a position to start the back substitution via Eq. (2.76).

Summary of the algorithm.

1. Calculate P_1, Q_1 from Eq. (2.80).
2. Use the recurrence relations (2.79), to obtain P_i, Q_i for $i = 2,3,...,N$
3. Set $Q_N = \Phi_N$
4. Use Eq. (2.76) for $i = N-1, N-2,...,3,2,1$, to obtain $\Phi_{N-1}, \Phi_{N-2},...,\Phi_3, \Phi_2, \Phi_1$.

The tridiagonal-matrix algorithm is a very powerful and convenient equation solver whenever the algebraic equations can be represented in the form of Eq. (2.74). Unlike general matrix methods, the TDMA requires computer storage and computer time proportional only to *N*, rather than to N^2 or N^3.

2.12. Time-development method for steady state problems

To calculate the solutions of many of the stationary problems of mathematical physics, describing various equilibrium states, one considers these equilibria as the results of the approach-to-steady-state of processes developing in time, whose computational treatment is simpler than the direct calculation of the equilibrium state itself.

We illustrate the use of the method of time-development via the example of an algorithm for the computational solution of the Dirichlet problem for heat-transfer equation

$$\frac{\partial}{\partial x}\left(\Gamma\frac{\partial\phi}{\partial x}\right)+\frac{\partial}{\partial y}\left(\Gamma\frac{\partial\phi}{\partial y}\right)+S=0 \tag{2.82}$$

This equation is elliptic. The Dirichlet boundary conditions are given by $\phi_w=\psi(x,y)$

Consider the auxiliary nonstationary heat-flow problem

$$\begin{aligned}&\rho\frac{\partial\phi}{\partial t}=\frac{\partial}{\partial x}\left(\Gamma\frac{\partial\phi}{\partial x}\right)+\frac{\partial}{\partial y}\left(\Gamma\frac{\partial\phi}{\partial y}\right)+S,\\&\phi(0,x,y)=\phi_0(x,y),\\&\phi_w=\psi(x,y)\end{aligned} \tag{2.83}$$

where S and $\psi(x,y)$ are the same as in problem (2.82), and $\phi_0(x,y)$ is arbitrary.

Since the distribution of heat sources S (x,y), and the boundary temperature ϕ_w, are time-independent, it is natural to expect that the solution, $\phi(t,x,y)$ will change more and more slowly with time, and that the temperature distribution $\phi(t,x,y)$, in the limit as $t\to\infty$, will evolve into the equilibrium temperature distribution $\phi(x,y)$ characterized by problem (2.82).

Therefore instead of stationary problem (2.82) one can solve nonstationary problem (2.83) out to the time, t, when the solution stops changing within the accuracy we require. This is the idea behind the solution of stationary problems by the "time-development method ".

Problems

1. Determine the order of approximation of the difference scheme

$$\frac{\phi_i^{n+1}-\phi_i^n}{\Delta t}-u\frac{\phi_{i+1}^n-\phi_{i-1}^n}{2\Delta x}=f\left(t^n,x_i\right),\qquad (2.84)$$
$$n=0,1,2,\ldots;\quad i=0,\pm 1,\pm 2,\ldots$$

for Cauchy problem for equation

$$\frac{\partial\phi}{\partial t}-u\frac{\partial\phi}{\partial x}=f\left(t,x\right)\qquad (2.85)$$

2. Investigate stability of the difference scheme (2.84) for equation (2.85) for two cases: 1) $u>0$; 2) $u<0$

3. NUMERICAL SOLUTION OF THE NAVIER-STOKES EQUATIONS

In chapter 1 the governing fluid dynamic equations were obtained. In a vector form they are written as

$$\frac{\partial\mathbf{U}}{\partial t}+\frac{\partial\mathbf{E}}{\partial x}+\frac{\partial\mathbf{F}}{\partial y}+\frac{\partial\mathbf{G}}{\partial z}=0\qquad (3.1)$$

where **U**, **E**, **F**, and **G** are vectors given by Eqs. (1.63)-(1.66).

3.1. Desirable Numerical Properties

The following is a list of desirable properties for a numerical method for solving the Navier-Stokes equations.

1. Accuracy - second order or higher.
2. Efficiency - unrestricted time step size Δt.
3. No added numerical dissipation - to control numerical instability.

4. No dependence of the steady state solution on the choice of Δt.

5. Using of Upwind Schemes and splitting of inviscid fluxes.

6. Fully conservative to prevent numerical losses in mass, momentum and energy.

A short discussion of each item follows.

1. First order accurate methods tend to be highly dissipative, which often smears flow features that should be crisp and competes with the physically relevant dissipative processes in the flow. Paradoxically, however, the use of first order flux split procedures at isolated discontinuities in the flow can improve numerical precision locally, but their use throughout the flow field calculation will in general artificially increase dissipation and losses in conserved quantities.

2. Navier-Stokes calculations of engineering interest still require thousands of time steps to converge to steady state solutions. This is far too many and too costly for practical use in aerodynamic design. Unrestricted choice of the size of the time step could reduce the number of required iterations to a reasonable twenty or less for steady state converging solutions. Unsteady solutions following a time history of several cycles or more would require correspondingly more iterations depending upon the temporal resolution required.

3. The appearance of some numerical procedures for solving the Navier-Stokes equations is dominated by the presence of explicit and implicit numerical dissipative terms added to suppress the natural tendency of the procedures to be unstable. All numerical procedures must be to some degree dissipative to control numerical instabilities. Some inherently possess the needed dissipation through the type of difference operators used to approximate the terms of the governing differential equations. Others artificially add new viscous-like terms to the approximating difference equations themselves. For the former, dissipation is related to the eigenvalue-eigenvector structure of the governing equations. Dissipation of each eigenvector is proportional to its own eigenvalue, almost

independently of the others. For the latter, the added terms may bear no relation to the mathematical structure of the governing equations and some components of the solution may be destroyed in the attempt to control unwanted growth in another physically unrelated component.

4. The fourth item above is usually raised as a criticism of the predictor-corrector methods. The finite difference operators in the predictor and corrector steps are of different type, usually one-sided forward or backward difference operators. As a steady state solution is approached, if by chance one step satisfies the converged solution requirement of no solution change, the other, using the same solution data differently, will most likely calculate a solution change of the order of the truncation error of the difference equations. Reducing solution change residuals to computer machine zero is therefore impossible and a pseudo unsteady dancing of the numerical solution about the steady state solution is obtained. This has generally been an unwanted nuisance, but it does serve to indicate the margin of error present in the numerical solution. Methods using the same difference approximations, usually central difference approximations, for each step of the calculation have the advantage of being able to converge to machine zero, orders of magnitude below the truncation error present in the solution. This advantage enables these methods to converge to the same steady solution independent of the time step size.

5. Interest in flux splitting procedures has grown rapidly since the pioneering work of Steger and Warming in the late 1970's [Ref. 13]. These procedures take into consideration the direction of information travel to compute fluxes and therefore can approximate the physics of the governing equations more realistically than otherwise. Splitting the flux vectors into subvectors whose associated eigenvalues are of the same sign allows use of one-sided (upwind) operators. These methods are more robust and computationlly efficient than conventional spatially centered schemes. The schemes based on central space discretizations which have a symmetry with respect to a change in sign of the Jacobian eigenvalues does not distinguish upstream from downstream

influences. Hence the physical propagation of perturbations along characteristics, typical of hyperbolic equations, is not considered in the definition of the numerical model. The family of upwind schemes is directed towards an introduction of the physical properties of the flow equations into the discretized formulation and has led to the family of techniques known as upwinding, covering a variety of approaches, such as flux vector splitting, flux difference splitting and various 'flux controlling' methods.

6. Finally, the desirability of the last item, the conservation of mass, momentum and energy by a numerical procedure, is self evident.

3.2. MacCormack Explicit Method

The MacCormack method [2] is a widely used scheme for solving fluid flow equations. The basic algorithm is explicit predictor-corrector method. The options are used when desired to increase the numerical efficiency or precision of the calculation. It can be programmed quickly and all explicit boundary conditions can be tested before the considerably larger efforts required for implementing any of the listed options. Let's consider at first 2D case. Briefly, the algorithm is as follows for advancing the numerical solution of Eq. (3.1) by Δt in time at each mesh point i,j.

(1) predictor step

$$\begin{aligned} \Delta\mathbf{U}_{i,j}^{n} &= -\Delta t\left(\frac{D_{+}\mathbf{E}_{i,j}^{n}}{\Delta x}+\frac{D_{+}\mathbf{F}_{i,j}^{n}}{\Delta y}\right), \\ \mathbf{U}_{i,j}^{\overline{n+1}} &= \mathbf{U}_{i,j}^{n}+\Delta\mathbf{U}_{i,j}^{n} \end{aligned} \tag{3.2}$$

(2) corrector step

$$\begin{aligned} \Delta\mathbf{U}_{i,j}^{\overline{n+1}} &= -\Delta t\left(\frac{D_{-}\mathbf{E}_{i,j}^{\overline{n+1}}}{\Delta x}+\frac{D_{-}\mathbf{F}_{i,j}^{\overline{n+1}}}{\Delta y}\right), \\ \mathbf{U}_{i,j}^{n+1} &= \frac{1}{2}\left(\mathbf{U}_{i,j}^{n}+\mathbf{U}_{i,j}^{\overline{n+1}}+\Delta\mathbf{U}_{i,j}^{\overline{n+1}}\right) \end{aligned} \tag{3.3}$$

In the above, forward difference operators are used in the predictor step and backward difference operators are used in the corrector step. This choice could

have been reversed or one forward and one backward difference could have been used in each. There are four different choices that should be cycled through during the course of a calculation. Though not indicated in the above, the viscous terms should be central differenced whenever possible. Let

$$\mathbf{E} = \underbrace{\mathbf{E}'}_{inviscid\ part} + \underbrace{\mathbf{E}''}_{viscous\ part} \tag{3.4}$$

$$\frac{\partial \mathbf{E}'}{\partial x} \simeq \begin{cases} \dfrac{D_+\mathbf{E}'_{i,j}}{\Delta x} = \dfrac{\mathbf{E}'_{i+1,j} - \mathbf{E}'_{i,j}}{\Delta x} & (\,forward\ difference\ operator\,) \\ \dfrac{D_-\mathbf{E}'_{i,j}}{\Delta x} = \dfrac{\mathbf{E}'_{i,j} - \mathbf{E}'_{i-1,j}}{\Delta x} & (\,backward\ difference\ operator\,) \end{cases} \tag{3.5}$$

However, the terms $\frac{\partial}{\partial x}\left(\mu \frac{\partial u}{\partial x}\right)$ and $\frac{\partial}{\partial x}\left(\mu \frac{\partial v}{\partial y}\right)$ appearing in viscous part $\frac{\partial \mathbf{E}''}{\partial x}$ are differenced as follows. For a forward difference

$$\begin{aligned} \frac{\partial}{\partial x}\left(\mu \frac{\partial u}{\partial x}\right) &\simeq \frac{\mu_{i+1,j}\left(u_{i+1,j} - u_{i,j}\right) - \mu_{i,j}\left(u_{i,j} - u_{i-1,j}\right)}{\Delta x^2} \\ \frac{\partial}{\partial x}\left(\mu \frac{\partial v}{\partial y}\right) &\simeq \frac{\mu_{i+1,j}\left(v_{i+1,j+1} - v_{i+1,j-1}\right) - \mu_{i,j}\left(v_{i,j+1} - v_{i,j-1}\right)}{2\Delta x \Delta y} \end{aligned} \tag{3.6}$$

For a backward difference

$$\begin{aligned} \frac{\partial}{\partial x}\left(\mu \frac{\partial u}{\partial x}\right) &\simeq \frac{\mu_{i,j}\left(u_{i+1,j} - u_{i,j}\right) - \mu_{i-1,j}\left(u_{i,j} - u_{i-1,j}\right)}{\Delta x^2} \\ \frac{\partial}{\partial x}\left(\mu \frac{\partial v}{\partial y}\right) &\simeq \frac{\mu_{i,j}\left(v_{i,j+1} - v_{i,j-1}\right) - \mu_{i-1,j}\left(v_{i-1,j+1} - v_{i-1,j-1}\right)}{2\Delta x \Delta y} \end{aligned} \tag{3.7}$$

McCormack's method is very convenient for practical use, but it has a number of serious shortcomings. From the six above-stated requirements it possesses only 1 and 6. As for other requirements:

(2) the method is explicit, therefore there are restrictions for a step Δt

(3) to obtain a stable solution it is necessary to add artificial numerical dissipation

(4) the convergence on a predictor and correcter can be various (see above)

(5) the scheme does not consider the propagation of influence in inviscid members, therefore some oscillations may appear

The latest work of McCormack [14] proposed an implicit version of this scheme for lifting of restrictions on a step. But it has an inflexibility to set all types of possible boundary conditions within the implicit part of the calculation. Therefore the author abandoned this scheme.

3.3. The finite volume approximation of Navier-Stockes equations

The vector form of Navier-Stockes equations (Eq. (1.62)) is written as

$$\frac{\partial \mathbf{U}}{\partial t}+\frac{\partial \mathbf{E}}{\partial x}+\frac{\partial \mathbf{F}}{\partial y}+\frac{\partial \mathbf{G}}{\partial z}=0 \tag{3.8}$$

or in 2D case as

$$\frac{\partial \mathbf{U}}{\partial t}+\frac{\partial \mathbf{E}}{\partial x}+\frac{\partial \mathbf{F}}{\partial y}=0 \tag{3.9}$$

Parameters **E,F,G** in the Eq. (3.8) can be interpreted as components of a vector $\vec{\boldsymbol{F}}=\left(\boldsymbol{F}_x,\boldsymbol{F}_y,\boldsymbol{F}_z\right)\equiv\left(\mathbf{E},\mathbf{F},\mathbf{G}\right)$ in the coordinate system (*x*,*y*,*z*). So, Eq. (3.8) can be rewritten as

$$\frac{\partial \mathbf{U}}{\partial t}+div\,\vec{\boldsymbol{F}}=0 \tag{3.10}$$

This conservation equation may be written in an integral form for an arbitrary control-volume *V* as follows:

$$\frac{\partial}{\partial t}\iiint_V \mathbf{U}dV+\iiint_V div\,\vec{\boldsymbol{F}}dV=0\ , \tag{3.11}$$

where *V* is the volume of a control volume, $\vec{\boldsymbol{F}}$ represents both the inviscid and viscous flux of the conserved quantities **U** through the control surfaces.

Using Gauss-Ostrogradsky theorem, we obtain from Eq. (3.11):

$$\frac{\partial}{\partial t}\iiint_V \mathbf{U}dV+\oiint_S \vec{\boldsymbol{F}}\bullet\vec{\boldsymbol{n}}dS=0 \tag{3.12}$$

where $\vec{\boldsymbol{n}}dS$ is a vector element of the control surface with outward normal $\vec{\boldsymbol{n}}$.

We consider that a control volume *V* has the form of a parallelepiped with sides parallel to the axes *x*,*y*,*z*, respectively $\left(V=\Delta x\times\Delta y\times\Delta z\right)$. A two-dimensional version of this control on the 0xy plane is shown in Fig. 3.1 (shaded area).

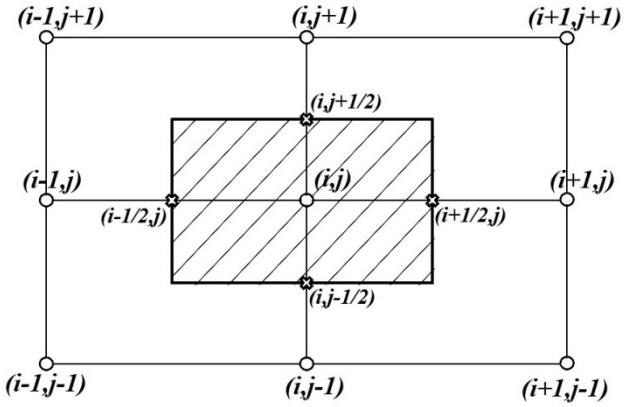

Fig.3.1. Two-dimensional finite-volume cell

For this cell volume, the flux quantity in Eq. (3.12) taking into account that $\vec{F} = (\mathbf{E}, \mathbf{F}, \mathbf{G})$ is rewritten as an integral over each face thereby yielding

$$\frac{\partial}{\partial t}\iiint_V \mathbf{U} dV + \iint_{\Delta y \Delta z} \left(\mathbf{E}_{i+1/2} - \mathbf{E}_{i-1/2}\right) dydz + \iint_{\Delta x \Delta z} \left(\mathbf{F}_{j+1/2} - \mathbf{F}_{j-1/2}\right) dxdz + \iint_{\Delta x \Delta y} \left(\mathbf{G}_{k+1/2} - \mathbf{G}_{k-1/2}\right) dxdy = 0 \tag{3.13}$$

Here the indices *i*,*j*,*k* represent the cell location. The vector **U** contains the conservation variables which are defined at the center of the cell *i*,*j*,*k*. The fluxes are defined at the cell interfaces which are represented by non-whole indices. The vectors **E**,**F** and **G** represent the inviscid flux and viscous stress/transport through the cell interfaces in the *x*,*y*,*z* directions, respectively.

The basic assumption is that each flux is constant over the entire face, i.e. for example, for a flux along the axis *x* we have:

$$\iint_{\Delta y \Delta z} \left(\mathbf{E}_{i+1/2} - \mathbf{E}_{i-1/2}\right) dydz \simeq \left(\mathbf{E}_{i+1/2} - \mathbf{E}_{i-1/2}\right) \Delta y \Delta z \tag{3.14}$$

In addition, we suppose that

$$\iiint_V \mathbf{U} dV \simeq \mathbf{U}_{i,j,k} V = \mathbf{U}_{i,j,k} \Delta x \Delta y \Delta z \tag{3.15}$$

where $\mathbf{U}_{i,j,k}$ is the value of vector $\mathbf{U}$ in the center of the cell.

So that Eq. (3.13) can be rewritten as

$$\left(\frac{\partial \mathbf{U}}{\partial t}\right)_{i,j,k} + \frac{\mathbf{E}_{i+1/2,j,k} - \mathbf{E}_{i-1/2,j,k}}{\Delta x} + \frac{\mathbf{F}_{i,j+1/2,k} - \mathbf{F}_{i,j-1/2,k}}{\Delta y} + \frac{\mathbf{G}_{i,j,k+1/2} - \mathbf{G}_{i,j,k-1/2}}{\Delta z} = 0 \tag{3.16}$$

which is the finite volume approximation of the basic vector equation (3.8).

3.4. Splitting of inviscid fluxes.

As we know, the inviscid flux consist of two physically distinct parts, i.e., convective and pressure fluxes. The former is associated with the flow (advection) speed, while the latter with the acoustic speed; or respectively classified as the linear and nonlinear fields.

In this section we review the restrictions placed on spatial difference approximations by the characteristic speeds (eigenvalues) of a hyperbolic system.

To illustrate the basic notions we consider a one-dimensional system of conservation laws

$$\frac{\partial \mathbf{U}}{\partial t} + \frac{\partial \mathbf{E}}{\partial x} = 0 \tag{3.17}$$

where **U** and **E** are *m*-component column vectors.

This equation is obtained from Eq. (1.62) in the one-dimensional case.

The finite volume approximation (3.16) reduces to

$$\left(\frac{\partial \mathbf{U}}{\partial t}\right)_{i} + \frac{\mathbf{E}_{i+1/2} - \mathbf{E}_{i-1/2}}{\Delta x} = \mathbf{0} \tag{3.18}$$

Viscous terms are not taken into account. The system (3.17) can be rewritten as a quasi-linear system

$$\frac{\partial \mathbf{U}}{\partial t} + \boldsymbol{A}(\mathbf{U})\frac{\partial \mathbf{U}}{\partial x} = 0 \tag{3.19}$$

where $\boldsymbol{A}$ is the Jacobian matrix $\boldsymbol{A}(\mathbf{U}) = \frac{\partial \mathbf{E}}{\partial \mathbf{U}}$. The system (3.19) is hyperbolic at the point (x, t, **U**) if there exists a similarity transformation such that

$$\boldsymbol{SAS}^{-1} = \boldsymbol{\Lambda} = \begin{pmatrix} \lambda_1 & & & 0 \\ & \lambda_2 & & \\ & & \ddots & \\ 0 & & & \lambda_m \end{pmatrix} \tag{3.20}$$

where $\boldsymbol{\Lambda}$ a diagonal matrix, the eigenvalues λ_l of $\boldsymbol{A}$ are real, and the norms of $\boldsymbol{S}$ and $\boldsymbol{S}^{-1}$ are uniformly bounded.

For the purpose of a linear stability analysis, we assume that the coefficient matrix $\boldsymbol{A}$ is "frozen", that is, constant. By virture of Eq. (3.20), Eq. (3.19) can be rewritten as

$$\begin{aligned} &\frac{\partial \mathbf{U}}{\partial t} + \boldsymbol{S}^{-1}\boldsymbol{\Lambda}\boldsymbol{S}\frac{\partial \mathbf{U}}{\partial x} = 0 \rightarrow \\ &\frac{\partial}{\partial t}\left(\boldsymbol{S}\mathbf{U}\right) + {}^{-1}\boldsymbol{\Lambda}\frac{\partial}{\partial x}\left(\boldsymbol{S}\mathbf{U}\right) = 0 \end{aligned} \tag{3.21}$$

So that Eq. (3.19) is transformed to the *uncoupled* system

$$\frac{\partial u_l}{\partial t} + \lambda_l \frac{\partial u_l}{\partial x} = 0, \quad l = 1, 2, 3, ..., m \tag{3.22}$$

by defining a new vector

$$\widetilde{\mathbf{U}} = \left(u_1, u_2, u_3, ..., u_m\right)^T = \boldsymbol{S}\mathbf{U} \tag{3.23}$$

where index T means matrix transposition.

Consequently, when analyzing the stability of numerical algorithms as applied to the linearized version of the system (3.19), we need only examine the scalar Eq. (3.22). For simplicity, the subscript l will be dropped.

So let's examine the model equation

$$\frac{\partial u}{\partial t} + \lambda \frac{\partial u}{\partial x} = 0 \tag{3.24}$$

In Chapter 2 it was shown that for this type of equations only the following difference schemes can be stable:

$$\begin{aligned} &\frac{\delta u_j}{\Delta t} + \lambda \frac{u_j - u_{j-1}}{\Delta x} = 0, \quad if\ \lambda > 0 \\ &\frac{\delta u_j}{\Delta t} + \lambda \frac{u_{j+1} - u_j}{\Delta x} = 0, \quad if\ \lambda < 0 \end{aligned} \tag{3.25}$$

In summary, for one-sided spatial difference approximations we have the following result: If $\frac{\partial u}{\partial x}$ is approximated by the backward-difference operator, then the resulting ordinary differential equation will be stable if and only if $\lambda > 0$ (i.e., the wave travels to the right). Conversely, if $\frac{\partial u}{\partial x}$ is approximated by the forward- difference operator, the resulting ordinary differential equation will be stable if and only if $\lambda < 0$.

Proceeding from the above considerations, the difference analogue of equation (3.24) should have the following form:

$$\begin{gathered}\frac{\delta u_i}{\Delta t} + \lambda^+ \frac{u_i - u_{i-1}}{\Delta x} + \lambda^- \frac{u_{i+1} - u_i}{\Delta x} = 0 \\ \lambda^+ = \frac{\lambda + |\lambda|}{2}, \quad \lambda^- = \frac{\lambda - |\lambda|}{2}\end{gathered} \tag{3.26}$$

so if $\lambda \geq 0$ the backward-difference operator is used in Eq. (3.26), and if $\lambda < 0$ the forward- difference operator is used.

We can use difference approximations described by Eq. (3.26) for all equations of the *uncoupled* system (3.22).

Using the above formulas, we split the diagonal matrix

$$\boldsymbol{\Lambda} = \boldsymbol{\Lambda}^+ + \boldsymbol{\Lambda}^- \tag{3.27}$$

where $\boldsymbol{\Lambda}^+$ and $\boldsymbol{\Lambda}^-$ have diagonal elements λ_l^+ and λ_l^-, respectively. Using these diagonal matrices Eq. (3.26) can be rewritten in the following vector form

$$\frac{\delta \widetilde{\mathbf{U}}_i}{\Delta t} + \boldsymbol{\Lambda}^+ \frac{\left(\widetilde{\mathbf{U}}_i - \widetilde{\mathbf{U}}_{i-1}\right)}{\Delta x} + \boldsymbol{\Lambda}^- \frac{\left(\widetilde{\mathbf{U}}_{i+1} - \widetilde{\mathbf{U}}_i\right)}{\Delta x} = 0 \tag{3.28}$$

By substituting Eq. (3.23) in Eq. (3.28) and multiplying it from the left by $\boldsymbol{S}^{-1}$, we obtain the following equation:

$$\frac{\delta \mathbf{U}_i}{\Delta t} + \boldsymbol{A}^+ \frac{\left(\mathbf{U}_i - \mathbf{U}_{i-1}\right)}{\Delta x} + \boldsymbol{A}^- \frac{\left(\mathbf{U}_{i+1} - \mathbf{U}_i\right)}{\Delta x} = 0 \tag{3.29}$$

where $\boldsymbol{A}^+ = \boldsymbol{S}^{-1}\boldsymbol{\Lambda}^+\boldsymbol{S}$, $\boldsymbol{A}^- = \boldsymbol{S}^{-1}\boldsymbol{\Lambda}^-\boldsymbol{S}$. (We remember that matrix $\boldsymbol{A} = \boldsymbol{S}^{-1}\boldsymbol{\Lambda}\boldsymbol{S}$ is “frozen”, i.e. constant).

Eq. (3.29) can be rewritten as

$$\frac{\delta \mathbf{U}_i}{\Delta t} + \frac{\left(\boldsymbol{A}^{+}\mathbf{U}_i + \boldsymbol{A}^{-}\mathbf{U}_{i+1}\right) - \left(\boldsymbol{A}^{+}\mathbf{U}_{i-1} + \boldsymbol{A}^{-}\mathbf{U}_i\right)}{\Delta x} = 0 \tag{3.30}$$

Comparing it with (3.18) we obtain formulas for convective flux vector **E** at the cell interfaces

$$\begin{aligned} \mathbf{E}_{i+1/2} &= \boldsymbol{A}^{+}\mathbf{U}_i + \boldsymbol{A}^{-}\mathbf{U}_{i+1} \\ \mathbf{E}_{i-1/2} &= \boldsymbol{A}^{+}\mathbf{U}_{i-1} + \boldsymbol{A}^{-}\mathbf{U}_i \end{aligned} \tag{3.31}$$

The obtained result can be interpreted by the scheme shown in Fig.3.2.

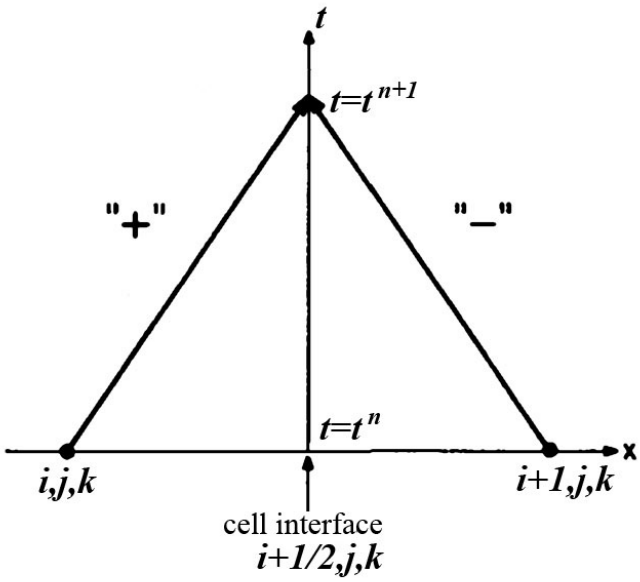

Fig.3.2. Direction of information travel in time to surface i + 1/2, $j.k$

At the moment $t = t^{n+1}$ a part of the convective flux defined by $\boldsymbol{A}^{+}\mathbf{U}_i$ comes to the cell interface (i+1/2) from the left; and a part of the flux defined by $\boldsymbol{A}^{-}\boldsymbol{U}_{i+1}$ comes from the right. If, for example, all eigenvalues of the matrix $\boldsymbol{A}$ are positive, then the matrix Λ^{-} and, respectively, the matrix $\boldsymbol{A}^{-}$ consists of only zero elements. In this case, the effect on the parameters of the interface (i+1/2) is exerted only by the nodes that are to the left of this interface.

The important formula (3.31) can be represented in a more general form. The split fluxes can be written in terms of $\mathbf{U}_L$ and $\mathbf{U}_R$ (Fig.3.3).

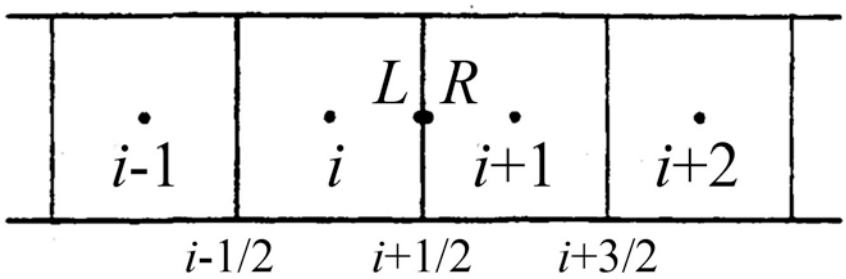

Fig.3.3. Split vector flux

1) The Steger-Warming split vector flux is

$$\mathbf{E}_{i+1/2} = \boldsymbol{A}_L^+ \mathbf{U}_L + \boldsymbol{A}_R^- \mathbf{U}_R \tag{3.32}$$

where the split Jacobians are evaluated also using the state vectors $\mathbf{U}_L$ and $\mathbf{U}_R$.

2) The Modified-Steger-Warming split vector flux is

$$\mathbf{E}_{i+1/2} = \bar{\boldsymbol{A}}_{i+1/2}^+ \mathbf{U}_L + \bar{\boldsymbol{A}}_{i+1/2}^- \mathbf{U}_R \tag{3.33}$$

where

$$\bar{\boldsymbol{A}}_{i+1/2} = \bar{\boldsymbol{A}}\left(\bar{\mathbf{U}}_{i+1/2}\right), \quad \bar{\mathbf{U}}_{i+1/2} = \frac{1}{2}\left(\mathbf{U}_L + \mathbf{U}_R\right) \tag{3.34}$$

3) The Roe split difference vector flux is

$$\mathbf{E}_{i+1/2} = 0.5\left(\mathbf{E}_L + \mathbf{E}_R\right) - 0.5\left|\hat{\mathbf{A}}_{i+1/2}\right|\left(\mathbf{U}_R - \mathbf{U}_L\right) \tag{3.35}$$

the Roe method uses a geometric averaging of the values $\mathbf{U}_L$ and $\mathbf{U}_R$ to form $\hat{\mathbf{A}}_{i+1/2}$:

$$\rho_{i+1/2} = \frac{\rho_R\sqrt{\rho_R} + \rho_L\sqrt{\rho_L}}{\sqrt{\rho_R} + \sqrt{\rho_L}} \tag{3.36}$$

$$u_{i+1/2} = \frac{u_R\sqrt{\rho_R} + u_L\sqrt{\rho_L}}{\sqrt{\rho_R} + \sqrt{\rho_L}} \tag{3.37}$$

$$v_{i+1/2} = \frac{v_R\sqrt{\rho_R} + v_L\sqrt{\rho_L}}{\sqrt{\rho_R} + \sqrt{\rho_L}} \tag{3.38}$$

$$w_{i+1/2} = \frac{w_R\sqrt{\rho_R} + w_L\sqrt{\rho_L}}{\sqrt{\rho_R} + \sqrt{\rho_L}} \tag{3.39}$$

$$H_{i+1/2} = \frac{H_R\sqrt{\rho_R} + H_L\sqrt{\rho_L}}{\sqrt{\rho_R} + \sqrt{\rho_L}} \tag{3.40}$$

where total enthalpy H is defined as

$$H = E + p/\rho \tag{3.41}$$

Three approximations for $\mathbf{U}_L$ and $\mathbf{U}_R$ follow [6].

1) First order upwind:

$$\mathbf{U}_L = \mathbf{U}_i, \quad \mathbf{U}_R = \mathbf{U}_{i+1} \tag{3.42}$$

2) Second order upwind:

$$\mathbf{U}_L = \frac{1}{2}\left(3\mathbf{U}_i - \mathbf{U}_{i-1}\right), \quad \mathbf{U}_R = \frac{1}{2}\left(3\mathbf{U}_{i+1} - \mathbf{U}_{i+2}\right) \tag{3.43}$$

3) Third order upwind biased:

$$\mathbf{U}_L = \frac{1}{8}\left(3\mathbf{U}_{i+1} + 6\mathbf{U}_i - \mathbf{U}_{i-1}\right), \quad \mathbf{U}_R = \frac{1}{8}\left(3\mathbf{U}_i + 6\mathbf{U}_{i+1} - \mathbf{U}_{i+2}\right) \tag{3.44}$$

3.5. Jacobian matrices, eigenvalues, eigenvectors

The Jacobian matrix $\boldsymbol{A} = \dfrac{\partial \mathbf{E}}{\partial \mathbf{U}}$ is easily computed for *calorically perfect gas* and found to be

$$\boldsymbol{A} = \frac{\partial \mathbf{E}}{\partial \mathbf{U}} = \begin{pmatrix} 0 & 1 & 0 & 0 & 0 \\ \alpha\beta - u^2 & u(2-\gamma) & -\beta v & -\beta w & \beta \\ -uv & v & u & 0 & 0 \\ -uw & w & 0 & u & 0 \\ u(\alpha\beta - H) & H - \beta u^2 & -\beta uv & -\beta uw & \gamma u \end{pmatrix} \tag{3.45}$$

where

$$\alpha = \frac{1}{2}\left(u^2 + v^2 + w^2\right), \quad \beta = \gamma - 1 \tag{3.46}$$

The following is true for calorically perfect gas:

$$\frac{p}{\rho} = \beta e \tag{3.47}$$

The eigenvalues of **A** are

$$\begin{aligned} &\lambda_1 = \lambda_3 = \lambda_4 = u, \\ &\lambda_2 = u + a, \quad \lambda_5 = u - a \end{aligned} \tag{3.48}$$

where a is a speed of sound.

These eigenvalues of matrix **A** have an important physical meaning. In fact, they characterize the *propagation of influence* in the flow of a compressible gas

in the direction of the x axis. Any point of the flow can propagate its influence on the surrounding space in the following way:

• with speed u due to the movement of the flow itself - downstream;

• with speed $u+a$ due to the movement of the flow itself and the propagation of sound oscillations - downstream;

• with speed u-a due to the propagation of sound vibrations; if the speed u exceeds the speed of sound a, this effect is pulled down and there is no upstream effect.

The matrices $\boldsymbol{S}$ and $\boldsymbol{S}^{-1}$, which are included in similarity transformation (3.20), are given by

$$\boldsymbol{S}_A = \begin{pmatrix} 1-\frac{\alpha\beta}{a^2} & \frac{\beta u}{a^2} & \frac{\beta v}{a^2} & \frac{\beta w}{a^2} & -\frac{\beta}{a^2} \\ \alpha\beta - ua & a-\beta u & -\beta v & -\beta w & \beta \\ -\frac{v}{\rho} & 0 & \frac{1}{\rho} & 0 & 0 \\ -\frac{w}{\rho} & 0 & 0 & \frac{1}{\rho} & 0 \\ \alpha\beta + ua & -a-\beta u & -\beta v & -\beta w & \beta \end{pmatrix} \tag{3.49}$$

and

$$\boldsymbol{S}^{-1} = \begin{pmatrix} 1 & \frac{1}{2a^2} & 0 & 0 & \frac{1}{2a^2} \\ u & \frac{u+a}{2a^2} & 0 & 0 & \frac{u-a}{2a^2} \\ v & \frac{v}{2a^2} & \rho & 0 & \frac{v}{2a^2} \\ w & \frac{w}{2a^2} & 0 & \rho & \frac{w}{2a^2} \\ \alpha & \frac{\alpha+ua}{2a^2}+\frac{1}{2\beta} & \rho v & \rho w & \frac{\alpha-ua}{2a^2}+\frac{1}{2\beta} \end{pmatrix} \tag{3.50}$$

We can use similar formulas for convective fluxes on all cell interfaces of the control volume:

$$\begin{aligned}
\mathbf{E}_{i+1/2,j,k} &= \boldsymbol{A}^{+}\mathbf{U}_{i,j,k} + \boldsymbol{A}^{-}\mathbf{U}_{i+1,j,k} \\
\mathbf{F}_{i,j+1/2,k} &= \boldsymbol{B}^{+}\mathbf{U}_{i,j,k} + \boldsymbol{B}^{-}\mathbf{U}_{i,j+1,k} \\
\mathbf{G}_{i,j,k+1/2} &= \boldsymbol{C}^{+}\mathbf{U}_{i,j,k} + \boldsymbol{C}^{-}\mathbf{U}_{i,j,k+1}
\end{aligned} \tag{3.51}$$

where

$$\boldsymbol{A} = \frac{\partial \mathbf{E}}{\partial \mathbf{U}}, \quad \boldsymbol{B} = \frac{\partial \mathbf{F}}{\partial \mathbf{U}}, \quad \boldsymbol{C} = \frac{\partial \mathbf{G}}{\partial \mathbf{U}} \tag{3.52}$$

3.6. Explicit and implicit Finite Volume Schemes

We can use explicit representation of fluxes in Eq. (3.16). In this case

$$\left(\frac{\partial \mathbf{U}}{\partial t}\right)_{i,j,k} + \frac{\mathbf{E}^{n}_{i+1/2,j,k} - \mathbf{E}^{n}_{i-1/2,j,k}}{\Delta x} + \frac{\mathbf{F}^{n}_{i,j+1/2,k} - \mathbf{F}^{n}_{i,j-1/2,k}}{\Delta y} + \frac{\mathbf{G}^{n}_{i,j,k+1/2} - \mathbf{G}^{n}_{i,j,k-1/2}}{\Delta z} = 0 \tag{3.53}$$

and the change in the solution at grid point *i,j,k* during the interval from time $n\Delta t$ to time $(n+1)\Delta t$ is determined as

$$\Delta \mathbf{U}^{n}_{i,j,k} = -\Delta t\left(\frac{\mathbf{E}^{n}_{i+1/2,j,k} - \mathbf{E}^{n}_{i-1/2,j,k}}{\Delta x} + \frac{\mathbf{F}^{n}_{i,j+1/2,k} - \mathbf{F}^{n}_{i,j-1/2,k}}{\Delta y} + \frac{\mathbf{G}^{n}_{i,j,k+1/2} - \mathbf{G}^{n}_{i,j,k-1/2}}{\Delta z}\right) \tag{3.54}$$

We use Eqs. (3.51) for inviscid fluxes and formulas similar to formulas (3.6), (3.7) - for viscous parts.

Eq. (3.54) is very easy to use but it is numerically stable only for Courant–Friedrichs–Lewy (CFL) numbers less than or equal to one. An estimate of the condition on Δt follows.

For one-dimensional case:

$$\Delta t \le \frac{1}{\dfrac{|u| + a}{\Delta x} + \dfrac{2\nu}{\Delta x^2}} \tag{3.55}$$

For two- dimensional case:

$$\Delta t \le \frac{1}{\dfrac{|u|}{\Delta x} + \dfrac{|v|}{\Delta y} + a\sqrt{\dfrac{1}{\Delta x^2} + \dfrac{1}{\Delta y^2}} + 2\nu\left(\dfrac{1}{\Delta x^2} + \dfrac{1}{\Delta y^2}\right)} \tag{3.56}$$

Here ν is connected with the kinematic viscosity or $\max(\mu, \lambda\mu/\Pr)/\rho$.

To remove the CFL restriction on Δt requires an implicit procedure.

For simplicity, we consider the two-dimensional case. And let us devide fluxes into inviscid and viscous parts:

$$\mathbf{E} = \underbrace{\mathbf{E}_C}_{\substack{\text{inviscid}\\ \text{part}}} + \underbrace{\mathbf{E}_V}_{\substack{\text{viscous}\\ \text{part}}} \tag{3.57}$$

If we focus on the inviscid problem for now, we can linearize the flux vector using

$$\begin{aligned} \mathbf{E}_C{}^{n+1} &\simeq \mathbf{E}_C{}^{n} + \left(\frac{\partial \mathbf{E}_C}{\partial \mathbf{U}}\right)^n \delta \boldsymbol{U}^{n+1} = \mathbf{E}_C{}^{n} + \boldsymbol{A}^n \delta \boldsymbol{U}^{n+1}, \\ \mathbf{F}_C{}^{n+1} &\simeq \mathbf{F}_C{}^{n} + \left(\frac{\partial \mathbf{F}_C}{\partial \mathbf{U}}\right)^n \delta \boldsymbol{U}^{n+1} = \mathbf{F}_C{}^{n} + \boldsymbol{B}^n \delta \boldsymbol{U}^{n+1}, \end{aligned} \tag{3.58}$$

Let us express inviscid fluxes in Eq. (3.16) as

$$\begin{aligned} \mathbf{E}_C &= (1-\alpha)\mathbf{E}_C{}^{n} + \alpha \mathbf{E}_C{}^{n+1} = \mathbf{E}_C{}^{n} + \alpha \boldsymbol{A}^n \delta \boldsymbol{U}^{n+1}, \\ \mathbf{F}_C &= (1-\alpha)\mathbf{F}_C{}^{n} + \alpha \mathbf{F}_C{}^{n+1} = \mathbf{F}_C{}^{n} + \alpha \boldsymbol{B}^n \delta \boldsymbol{U}^{n+1} \end{aligned} \tag{3.59}$$

The parameter α determines the order of accuracy of the time derivative. For $\alpha = 1/2$ the time derivative is centered, Crank-Nicholson like, and second order accurate, otherwise it is of first order. At $\alpha = 1$ the method is fully implicit and for $\alpha > 1$ it is over relaxed, but may have better convergence properties depending on the particular simulation.

We then split the fluxes according to the sign of the eigenvalues of the Jacobians according to Eqs. (3.31)-(3.34):

$$\mathbf{E}_{i+1/2} = \boldsymbol{A}^+ \mathbf{U}_i + \boldsymbol{A}^- \mathbf{U}_{i+1} \tag{3.60}$$

So the first of the Eqs. (3.59) can be rewritten as

$$(\mathbf{E}_C)_{i+1/2,j} = (\mathbf{E}_C)^n_{i+1/2,j} + \alpha\left[\left(\boldsymbol{A}^+\right)^n_{i+1/2,j} \delta \boldsymbol{U}^{n+1}_{i,j} + \left(\boldsymbol{A}^-\right)^n_{i+1/2,j} \delta \boldsymbol{U}^{n+1}_{i+1,j}\right], \tag{3.61}$$

where for explicit $(\mathbf{E}_C)^n_{i+1/2,j}$ we use one of the Eqs. (3.31)-(3.34).

Similar expressions are obtained for flux $\mathbf{F}_C$.

Upon substituting these equations in Eq. (3.16), for 2D case we obtain an implicit finite volume representation:

$$\mathbf{A}_{i,j}\delta\mathbf{U}^{n+1}_{i,j} + \mathbf{B}_{i,j}\delta\mathbf{U}^{n+1}_{i,j+1} + \mathbf{C}_{i,j}\delta\mathbf{U}^{n+1}_{i,j-1} + \mathbf{D}_{i,j}\delta\mathbf{U}^{n+1}_{i+1,j} + \mathbf{E}_{i,j}\delta\mathbf{U}^{n+1}_{i-1,j} = \Delta\mathbf{U}^n_{i,j} \tag{3.62}$$

where $\Delta\mathbf{U}^n_{i,j}$ is solution change, calculated explicitly by (3.54), and

$$\mathbf{A}_{i,j} = \mathbf{I} + \alpha \frac{\Delta t}{\Delta x}\left[\left(\boldsymbol{A}^{+}\right)^{n}_{i+1/2,j} - \left(\boldsymbol{A}^{-}\right)^{n}_{i-1/2,j}\right] + \alpha \frac{\Delta t}{\Delta y}\left[\left(\boldsymbol{B}^{+}\right)^{n}_{i,j+1/2} - \left(\boldsymbol{B}^{-}\right)^{n}_{i,j-1/2}\right]$$

$$\mathbf{B}_{i,j} = \alpha \frac{\Delta t}{\Delta y}\left(\boldsymbol{B}^{-}\right)^{n}_{i,j+1/2}, \quad \mathbf{C}_{i,j} = -\alpha \frac{\Delta t}{\Delta y}\left(\boldsymbol{B}^{+}\right)^{n}_{i,j-1/2} \tag{3.63}$$

$$\mathbf{D}_{i,j} = \alpha \frac{\Delta t}{\Delta x}\left(\boldsymbol{A}^{-}\right)^{n}_{i+1/2,j,k}, \quad \mathbf{E}_{i,j} = -\alpha \frac{\Delta t}{\Delta x}\left(\boldsymbol{A}^{+}\right)^{n}_{i-1/2,j,k}$$

I - identity martix.

3.7. Viscous fluxes

The vectors of viscous fluxes $\mathbf{E}_V, \mathbf{F}_V, \mathbf{G}_V$ considering formula (1.62) are as follows:

$$\mathbf{E}_V = \begin{bmatrix} 0 \\ -\tau_{xx} \\ -\tau_{yx} \\ -\tau_{zx} \\ -u\tau_{xx} - v\tau_{yx} - w\tau_{zx} + q_x \end{bmatrix}, \mathbf{F}_V = \begin{bmatrix} 0 \\ -\tau_{xy} \\ -\tau_{yy} \\ -\tau_{zy} \\ -u\tau_{xy} - v\tau_{yy} - w\tau_{zy} + q_y \end{bmatrix}, \mathbf{G}_V = \begin{bmatrix} 0 \\ -\tau_{xz} \\ -\tau_{yz} \\ -\tau_{zz} \\ -u\tau_{xz} - v\tau_{yz} - w\tau_{zz} + q_z \end{bmatrix} \tag{3.64}$$

Obviously, they are not basically the functions of vector **U** itself, but of its derivatives on spatial variables $\mathbf{U}_x \equiv \frac{\partial \mathbf{U}}{\partial x}, \mathbf{U}_y \equiv \frac{\partial \mathbf{U}}{\partial y}, \mathbf{U}_z \equiv \frac{\partial \mathbf{U}}{\partial z}$:

$$\mathbf{E}_V = \mathbf{E}_V\left(\mathbf{U}_x, \mathbf{U}_y, \mathbf{U}_z\right), \mathbf{F}_V = \mathbf{F}_V\left(\mathbf{U}_x, \mathbf{U}_y, \mathbf{U}_z\right), \mathbf{G}_V = \mathbf{G}_V\left(\mathbf{U}_x, \mathbf{U}_y, \mathbf{U}_z\right) \tag{3.65}$$

So we can linearize the viscous flux vector using

$$\mathbf{E}_V{}^{n+1} = \mathbf{E}_V{}^{n} + \left(\frac{\partial \mathbf{E}_V}{\partial \mathbf{U}_x}\right)^{n} \delta\left(\mathbf{U}_x\right)^{n+1} + \left(\frac{\partial \mathbf{E}_V}{\partial \mathbf{U}_y}\right)^{n} \delta\left(\mathbf{U}_y\right)^{n+1} + \left(\frac{\partial \mathbf{E}_V}{\partial \mathbf{U}_z}\right)^{n} \delta\left(\mathbf{U}_z\right)^{n+1} \tag{3.66}$$

where, for example, $\delta\left(\mathbf{U}_x\right)^{n+1} = \left(\mathbf{U}_x\right)^{n+1} - \left(\mathbf{U}_x\right)^{n}$

The papers [1,7] show that it is not necessary to consider all the members in implicit representation (3.66). Only those terms that sigficantly determine the flow and affect numerical stability need to be represented. In viscous fluxes the mixed derivatives play significantly a smaller role than other members.

Following the method of Tysinger and Caughey [7] we can linearize the viscous flux vectors, assuming that the transport coefficients are locally constant, to obtain

$$\begin{aligned}
\mathbf{E}_V{}^{n+1} &\simeq \mathbf{E}_V{}^{n} + \boldsymbol{L}^n \delta\left(\mathbf{U}_x\right)^{n+1} = \mathbf{E}_V{}^{n} + \frac{\partial}{\partial x}\left(\boldsymbol{L}^n \delta \mathbf{U}^{n+1}\right), \\
\mathbf{F}_V{}^{n+1} &\simeq \mathbf{F}_V{}^{n} + \boldsymbol{N}^n \delta\left(\mathbf{U}_y\right)^{n+1} = \mathbf{F}_V{}^{n} + \frac{\partial}{\partial y}\left(\boldsymbol{N}^n \delta \mathbf{U}^{n+1}\right), \\
\mathbf{G}_V{}^{n+1} &\simeq \mathbf{G}_V{}^{n} + \boldsymbol{K}^n \delta\left(\mathbf{U}_z\right)^{n+1} = \mathbf{G}_V{}^{n} + \frac{\partial}{\partial z}\left(\boldsymbol{K}^n \delta \mathbf{U}^{n+1}\right)
\end{aligned} \tag{3.67}$$

where $\boldsymbol{L} = \dfrac{\partial \mathbf{E}_V}{\partial \mathbf{U}_x}, \quad \boldsymbol{N} = \dfrac{\partial \mathbf{F}_V}{\partial \mathbf{U}_y}, \quad \boldsymbol{K} = \dfrac{\partial \mathbf{G}_V}{\partial \mathbf{U}_z}$.

Again for simplicity we will consider a two-dimensional case. We will present viscous streams in the main equation (3.16) in the same way as it is made in the formula (3.59). For example, on the verge $(i+1/2, j)$:

$$\left(\mathbf{E}_V\right)_{i+1/2,j} = \left(\mathbf{E}_V\right)^n_{i+1/2,j} + \alpha \frac{1}{\Delta x}\left(\boldsymbol{L}^n_{i+1,j}\delta \mathbf{U}^{n+1}_{i+1,j} - \boldsymbol{L}^n_{i,j}\delta \mathbf{U}^{n+1}_{i,j}\right) \tag{3.68}$$

Viscous fluxes on the other sides of control volume are written similarly. After substitution of these expressions in the main equation (3.16), we receive the same formula (3.62), except for the appearance of additional members connected with viscosity

$$\mathbf{A}_{i,j}\delta \mathbf{U}^{n+1}_{i,j} + \mathbf{B}_{i,j}\delta \mathbf{U}^{n+1}_{i,j+1} + \mathbf{C}_{i,j}\delta \mathbf{U}^{n+1}_{i,j-1} + \mathbf{D}_{i,j}\delta \mathbf{U}^{n+1}_{i+1,j} + \mathbf{E}_{i,j}\delta \mathbf{U}^{n+1}_{i-1,j} = \Delta \mathbf{U}^n_{i,j} \tag{3.69}$$

where

$$\begin{aligned}
\mathbf{A}_{i,j} &= \mathbf{I} + \alpha \frac{\Delta t}{\Delta x}\left[\left(\boldsymbol{A}^+\right)^n_{i+1/2,j} - \left(\boldsymbol{A}^-\right)^n_{i-1/2,j}\right] + \alpha \frac{\Delta t}{\Delta y}\left[\left(\boldsymbol{B}^+\right)^n_{i,j+1/2} - \left(\boldsymbol{B}^-\right)^n_{i,j-1/2}\right] \\
&\quad - 2\alpha \frac{\Delta t}{\Delta x^2}\boldsymbol{L}^n_{i,j} - 2\alpha \frac{\Delta t}{\Delta y^2}\boldsymbol{N}^n_{i,j} \\
\mathbf{B}_{i,j} &= \alpha \frac{\Delta t}{\Delta y}\left(\boldsymbol{B}^-\right)^n_{i,j+1/2} + \alpha \frac{\Delta t}{\Delta y^2}\boldsymbol{N}^n_{i,j+1}, \quad \mathbf{C}_{i,j} = -\alpha \frac{\Delta t}{\Delta y}\left(\boldsymbol{B}^+\right)^n_{i,j-1/2} + \alpha \frac{\Delta t}{\Delta y^2}\boldsymbol{N}^n_{i,j-1} \\
\mathbf{D}_{i,j} &= \alpha \frac{\Delta t}{\Delta x}\left(\boldsymbol{A}^-\right)^n_{i+1/2,j} + \alpha \frac{\Delta t}{\Delta x^2}\boldsymbol{L}^n_{i+1,j}, \quad \mathbf{E}_{i,j} = -\alpha \frac{\Delta t}{\Delta x}\left(\boldsymbol{A}^+\right)^n_{i-1/2,j} + \alpha \frac{\Delta t}{\Delta x^2}\boldsymbol{L}^n_{i-1,j}
\end{aligned} \tag{3.70}$$

3.8. Ways to improve the numerical method

When using the splitting of inviscid fluxes, the Modified-Steger-Warming method Eq. (3.33) gives the best results.

But this approach is not suitable in the vicinity of strong shock waves. Close to shock waves, the method needs to be switched to the original Steger-Warming scheme (Eq. (3.32)) which is more dissipative.

To solve this problem the following *pressure switch method* [15] can be used

$$\begin{aligned} &\mathbf{E}_{i+1/2} = \boldsymbol{A}^{+}\mathbf{U}_L + \boldsymbol{A}^{-}\mathbf{U}_R, \\ &\boldsymbol{A}^{+} = \boldsymbol{A}^{+}\left(\mathbf{U}_{+}\right), \quad \boldsymbol{A}^{-} = \boldsymbol{A}^{-}\left(\mathbf{U}_{-}\right) \end{aligned} \tag{3.71}$$

where

$$\begin{aligned} &\mathbf{U}_{+} = \left(1-z\right)\mathbf{U}_L + z\mathbf{U}_R, \\ &\mathbf{U}_{-} = z\mathbf{U}_L + \left(1-z\right)\mathbf{U}_R \end{aligned} \tag{3.72}$$

$$z = \frac{0.5}{\left(6\Gamma_{i+1/2}\right)^2 + 1} \tag{3.73}$$

The parameter Γ is determined by the normalized second differences of the pressure

$$\begin{aligned} &\Gamma_{i,j} = \max\left(\mathrm{e}_{i-1,j-1}, \mathrm{e}_{i-1,j}, \mathrm{e}_{i-1,j+1}, \mathrm{e}_{i,j-1}, \mathrm{e}_{i,j}, \mathrm{e}_{i,j+1}, \mathrm{e}_{i+1,j-1}, \mathrm{e}_{i+1,j}, \mathrm{e}_{i+1,j+1}\right) \\ &\mathrm{e}_{i,j} = \sqrt{\mathrm{e}_{Xi,j}{}^2 + \mathrm{e}_{Yi,j}{}^2} \\ &\mathrm{e}_{Xi,j} = \frac{\left|p_{i+1,j} - 2p_{i,j} + p_{i-1,j}\right|}{\left|p_{i+1,j} + 2p_{i,j} + p_{i-1,j}\right|}; \quad \mathrm{e}_{Yi,j} = \frac{\left|p_{i,j+1} - 2p_{i,j} + p_{i,j-1}\right|}{\left|p_{i,j+1} + 2p_{i,j} + p_{i,j-1}\right|} \end{aligned} \tag{3.74}$$

For small values of e parameter $z = 1 - z = 0.5$ and modified Steger-Warming is recovered from the Eq. (3.71). Close to shock waves the value of e is great, $z = 0$ and the method is switched to the original Steger-Warming scheme.

As already known there are three types of approximations for $\mathbf{U}_L$ and $\mathbf{U}_R$: first order (see Eq. (3.42)), second order (see Eq. (3.43)), third order (see Eq. (3.44)).

Using first-order approximation gives a very robust solution, however, with a significant error and «blur» of shocks. Using second and third orders provides more correct solution, but with bucking failure at great pressure gradient.

The simple extrapolation formulae assume a smooth variation of **U**; however, discontinuities in **U** are possible (i.e. shocks). There is a need for some mechanism to sense such discontinuities and limit the variation of **U** in these extrapolation formulas.

The following representation of fluxes is suggested:

$$\begin{aligned}\mathbf{U}_L &= \mathbf{U}_i + \Phi\left[\theta\cdot\frac{1}{2}\left(\mathbf{U}_i - \mathbf{U}_{i-1}\right) + \left(1-\theta\right)\cdot\frac{1}{8}\left(3\mathbf{U}_{i+1} - 2\mathbf{U}_i - \mathbf{U}_{i-1}\right)\right],\\ \mathbf{U}_R &= \mathbf{U}_{i+1} + \Phi\left[\theta\cdot\frac{1}{2}\left(\mathbf{U}_{i+1} - \mathbf{U}_{i+2}\right) + \left(1-\theta\right)\cdot\frac{1}{8}\left(3\mathbf{U}_i - 2\mathbf{U}_{i+1} - \mathbf{U}_{i+2}\right)\right]\end{aligned} \tag{3.75}$$

When $\Phi = 0$ we have first-order approximation; when $\Phi = 1$ we have second-order approximation ($\theta = 1$) or third-order approximation ($\theta = 0$).

The following formula is used for Φ:

$$\Phi = \max\left(0, r\right); \quad z = \frac{1}{\left(6\Gamma_{i+1/2}\right)^2 + 1} \tag{3.76}$$

In cases when pressure gradient is great a numerical dissipation is added to the scheme. The eigenvalues of the Jacobians $\boldsymbol{A}^+, \boldsymbol{A}^-, \boldsymbol{B}^+, \boldsymbol{B}^+$ are calculated by

$$\lambda^{\pm} = \frac{1}{2}\left(\lambda \pm \sqrt{\lambda^2 + e^2}\right) \tag{3.77}$$

where e is supposed to be a small number used only to correct the sonic glitch problem.

In the current work the parameter e is calculated by

$$e_A = k_1\Gamma\left(|u| + a\right), \quad e_B = k_2\Gamma\left(|v| + a\right) \tag{3.78}$$

The constants k_1, k_2 are set within the range from 0.5 to 2.5 .

Problems

1. Define the Jacobian matrix $\boldsymbol{B} = \dfrac{\partial \mathbf{F}}{\partial \mathbf{U}}$ for *calorically perfect gas* .

2. Define the matrices $\boldsymbol{S}_B^{-1}, \boldsymbol{\Lambda}_B, \boldsymbol{S}_B$ included in the representation

$$\boldsymbol{B} = \boldsymbol{S}_B^{-1}\boldsymbol{\Lambda}_B\boldsymbol{S}_B \tag{3.79}$$

4. SOLUTION OF SYSTEMS OF LINEAR EQUATIONS WITH BLOCK COEFFICIENTS

4.1. Finite approximating difference/volume equation

A finite difference/volume equation, approximating the Eq. (3.16), is given by Eq. (3.69)

$$\mathbf{A}_{i,j}\delta\mathbf{U}_{i,j}^{n+1}+\mathbf{B}_{i,j}\delta\mathbf{U}_{i,j+1}^{n+1}+\mathbf{C}_{i,j}\delta\mathbf{U}_{i,j-1}^{n+1}+\mathbf{D}_{i,j}\delta\mathbf{U}_{i+1,j}^{n+1}+\mathbf{E}_{i,j}\delta\mathbf{U}_{i-1,j}^{n+1}=\Delta\mathbf{U}_{i,j}^{n}$$

where $\mathbf{A}_{i,j},\mathbf{B}_{i,j},\mathbf{C}_{i,j},\mathbf{D}_{i,j},\mathbf{E}_{i,j}$ are block matrix elements and $\Delta\mathbf{U}_{i,j}^{n}$ is given by Eq. (3.54). This system contains 5 unknown vectors and is described by a pentadiagonal matrix of block coefficients.

The system contains seven unknown variables in a three-dimensional case.

Eq. (3.69) can also be expressed in full matrix form

$$\mathbf{M}\cdot[\delta\mathbf{U}]=[\Delta\mathbf{U}] \tag{4.1}$$

where

$$\mathbf{M}=\begin{pmatrix}
x & x & . & . & x & . & . & . & . & . & . & . & . \\
x & x & x & . & . & x & . & . & . & . & . & . & . \\
. & x & x & x & . & . & x & . & . & . & . & . & . \\
. & . & x & x & x & . & . & x & . & . & . & . & . \\
x & . & . & x & x & x & . & . & x & . & . & . & . \\
. & x & . & . & x & x & x & . & . & x & . & . & . \\
. & . & \mathbf{D} & . & . & \mathbf{B} & \mathbf{A} & \mathbf{C} & . & . & \mathbf{E} & . & . \\
. & . & . & x & . & . & x & x & x & . & . & x & . \\
. & . & . & . & x & . & . & x & x & x & . & . & x \\
. & . & . & . & . & x & . & . & x & x & x & . & . \\
. & . & . & . & . & . & x & . & . & x & x & x & . \\
. & . & . & . & . & . & . & x & . & . & x & x & x \\
. & . & . & . & . & . & . & . & x & . & . & x & x
\end{pmatrix} \tag{4.2}$$

And the solution change vectors $\Delta\mathbf{U}$, calculated explicitly, and $\delta\mathbf{U}$, calculated implicitly, are given by

$$[\delta\mathbf{U}] = \begin{pmatrix} . \\ . \\ \delta\mathbf{U}_{i+1,j} \\ . \\ . \\ \delta\mathbf{U}_{i,j+1} \\ \delta\mathbf{U}_{i,j} \\ \delta\mathbf{U}_{i,j-1} \\ . \\ . \\ \delta\mathbf{U}_{i-1,j} \\ . \\ . \end{pmatrix}, \quad [\Delta\mathbf{U}] = \begin{pmatrix} . \\ . \\ . \\ . \\ . \\ . \\ \Delta\mathbf{U}_{i,j} \\ . \\ . \\ . \\ . \\ . \\ . \end{pmatrix} \tag{4.3}$$

If a grid has dimension $N_X \times N_Y$, then vectors $[\delta\mathbf{U}]$ and $[\Delta\mathbf{U}]$ have the order of $N_X \times N_Y$, and order of matrix $\mathbf{M}$ equals $(N_X \times N_Y)\times(N_X \times N_Y)$

Each element of a matrix $\mathbf{M}$ itself is a matrix of size 4×4; each element of vectors $[\delta\mathbf{U}]$ и $[\Delta\mathbf{U}]$ is also a vector consisting of 4 components.

The matrix is $\mathbf{M}$ sparse but it would be very expensive (computationally) to solve the algebraic system. For instance, for a reasonable two-dimensional calculation of transonic flow past an airfoil we could use approximately 400 points in the *x* direction and 200 points in the *y* direction. The resulting algebraic system is a 320,000 x 320,000 matrix problem to be solved and although we could take advantage of its banded sparse structure it would still be very costly in terms of both CPU time and storage.

Unlike a one-dimensional problem, which is described by a block tridiagonal matrix of coefficients and which is effectively solved by a Thomas algorithm (TDMA) (see the paragraph 2.11), there are no such effective methods for two-dimensional or three-dimensional matrices.

Therefore, most methods of the solution of a system with a pentadiagonal matrix or a septa-diagonal matrix are bases on reducing these systems to block tridiagonal inversions which can be performed in an efficient way through the Thomas algorithm.

In the following paragraphs these methods will be described:

- Gauss-Seidel iteration with alternating sweeps
- Approximate Factorization method
- Modified Approximate Factorization method

All these methods are approximate and require several iterations.

4.2. Gauss-Seidel iteration method

Eq. (3.69) can be rewritten as

$$\mathbf{A}\delta\mathbf{U}_{i,j} + \mathbf{B}\delta\mathbf{U}_{i,j+1} + \mathbf{C}\delta\mathbf{U}_{i,j-1} + \mathbf{D}\delta\mathbf{U}_{i+1,j} + \mathbf{E}\delta\mathbf{U}_{i-1,j} = \Delta\mathbf{U}^{n}_{i,j} \tag{4.4}$$

where for convenience we have deleted the superscript $n+1$ on the $\delta\mathbf{U}$'s and the subscripts on the block 4 x 4 matrices.

Eq. (4.4) can be solved (see Fig. 4.1.) by line Gauss-Seidel iteration with alternating sweeps in the backward and forward x-directions.

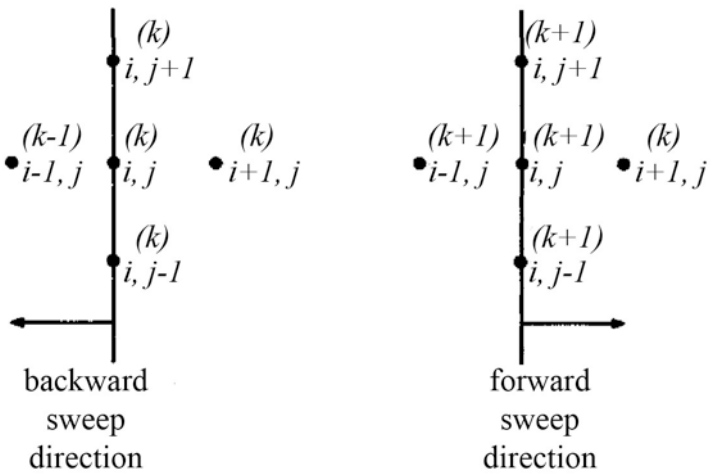

Figure 4.1. Sweep directions for line Gauss-Seidel iteration

For k = 1, 3, ...

Backward Sweep:

$$\mathbf{A}\delta\mathbf{U}^{(k)}_{i,j} + \mathbf{B}\delta\mathbf{U}^{(k)}_{i,j+1} + \mathbf{C}\delta\mathbf{U}^{(k)}_{i,j-1} = \Delta\mathbf{U}^{n}_{i,j} - \mathbf{D}\delta\mathbf{U}^{(k)}_{i+1,j} - \mathbf{E}\delta\mathbf{U}^{(k-1)}_{i-1,j} \tag{4.5}$$

and

Forward Sweep:

$$\mathbf{A}\delta\mathbf{U}_{i,j}^{(k+1)}+\mathbf{B}\delta\mathbf{U}_{i,j+1}^{(k+1)}+\mathbf{C}\delta\mathbf{U}_{i,j-1}^{(k+1)}=\Delta\mathbf{U}_{i,j}^{n}-\mathbf{D}\delta\mathbf{U}_{i+1,j}^{(k)}-\mathbf{E}\delta\mathbf{U}_{i-1,j}^{(k+1)} \tag{4.6}$$

To initiate the sweeps set $\delta\mathbf{U}_{i,j}^{(0)}=\mathbf{0}$. For the most applications only two sweeps, one backward and one forward, per step, can be used.

The right parts of the equations (4.5) and (4.6) are taken from the previous iteration and boundary conditions. Each of the matrixes in these equations is three-diagonal and is solved by a TDMA (see paragraph 4.5)

4.3. Approximate Factorization (AF)

The matrix **M** in Eq. (4.1) is factored by

$$\mathbf{M}\simeq\mathbf{M}_x\cdot\mathbf{M}_y \tag{4.7}$$

where

$$\mathbf{M}_x=\begin{pmatrix} x & . & x & . & . & . & . \\ . & x & . & x & . & . & . \\ x & . & x & . & x & . & . \\ . & \mathbf{D} & . & \mathbf{A}_x & . & \mathbf{E} & . \\ . & . & x & . & x & . & x \\ . & . & . & x & . & x & . \\ . & . & . & . & x & . & x \end{pmatrix},\ \mathbf{M}_y=\begin{pmatrix} x & x & . & . & . & . & . \\ x & x & x & . & . & . & . \\ . & x & x & x & . & . & . \\ . & . & \mathbf{B} & \mathbf{A}_y & \mathbf{C} & . & . \\ . & . & . & x & x & x & . \\ . & . & . & . & x & x & x \\ . & . & . & . & . & x & x \end{pmatrix} \tag{4.8}$$

The matrix elements $\mathbf{B}_{i,j},\mathbf{C}_{i,j},\mathbf{D}_{i,j}$ and $\mathbf{E}_{i,j}$ are defined as before in Eq. (3.70), and

$$\begin{aligned}(\mathbf{A}_x)_{i,j}&=\mathbf{I}+\alpha\frac{\Delta t}{\Delta x}\left[\left(\boldsymbol{A}^{+}\right)_{i+1/2,j}^{n}-\left(\boldsymbol{A}^{-}\right)_{i-1/2,j}^{n}\right]-2\alpha\frac{\Delta t}{\Delta x^2}\boldsymbol{L}_{i,j}^{n}\\ (\mathbf{A}_y)_{i,j}&=\mathbf{I}+\alpha\frac{\Delta t}{\Delta y}\left[\left(\boldsymbol{B}^{+}\right)_{i,j+1/2}^{n}-\left(\boldsymbol{B}^{-}\right)_{i,j-1/2}^{n}\right]-2\alpha\frac{\Delta t}{\Delta y^2}\boldsymbol{N}_{i,j}^{n}\end{aligned} \tag{4.9}$$

Each factor represents a block tridiagonal matrix.

Let us introduce the following notation

$$\mathbf{M}_y\cdot[\delta\mathbf{U}]=[\delta\mathbf{W}] \tag{4.10}$$

Then from (4.7) we obtain:

$$\mathbf{M}_x\cdot[\delta\mathbf{W}]=[\Delta\mathbf{U}] \tag{4.11}$$

This equation is as follows:

$$\left(\mathbf{A}_x\right)_{i,j}\delta\mathbf{W}_{i,j}^{n+1}+\mathbf{D}_{i,j}\delta\mathbf{W}_{i+1,j}^{n+1}+\mathbf{E}_{i,j}\delta\mathbf{W}_{i-1,j}^{n+1}=\Delta\mathbf{U}_{i,j}^{n} \tag{4.12}$$

Now we can solve Eq. (4.10):

$$\left(\mathbf{A}_y\right)_{i,j}\delta\mathbf{U}_{i,j}^{n+1}+\mathbf{B}_{i,j}\delta\mathbf{U}_{i,j+1}^{n+1}+\mathbf{C}_{i,j}\delta\mathbf{U}_{i,j-1}^{n+1}=\delta\mathbf{W}_{i,j}^{n+1} \tag{4.13}$$

which is solved by a TDMA method too.

Upon matrix multiplication of the two factors in Eq. (4.7), none of the original matrix elements are returned exactly and some *zero* elements of **M** become significantly *nonzero*. This factorization error reduces accuracy and slows algorithm convergence.

4.4. Modified Approximate Factorization (MAF)

The approximate factorization procedure can be modified to significantly reduce the adverse effects of decomposition error. The modified procedure has the property of Stone's Strongly Implicit Method (SIP) [8] for matrix decomposition of returning exactly the original nonzero elements of the matrix **M** upon factor multiplication, although some originally zero elements become nonzero. This modification was used by Bardina and Lombard [9] in 1987, which they called their Diagonally Dominant Alternating Direction Implicit (DDADI) procedure. When applied to the matrix M

$$\mathbf{M}\simeq\mathbf{M}'_x\cdot\left[\mathbf{D}\right]^{-1}\mathbf{M}'_y \tag{4.14}$$

where

$$\mathbf{M}'_x = \begin{pmatrix} x & . & x & . & . & . & . \\ . & x & . & x & . & . & . \\ x & . & x & . & x & . & . \\ . & \mathbf{D} & . & \mathbf{A} & . & \mathbf{E} & . \\ . & . & x & . & x & . & x \\ . & . & . & x & . & x & . \\ . & . & . & . & x & . & x \end{pmatrix} \tag{4.15}$$

$$\mathbf{M}'_y = \begin{pmatrix} x & x & . & . & . & . & . \\ x & x & x & . & . & . & . \\ . & x & x & x & . & . & . \\ . & . & \mathbf{B} & \mathbf{A} & \mathbf{C} & . & . \\ . & . & . & x & x & x & . \\ . & . & . & . & x & x & x \\ . & . & . & . & . & x & x \end{pmatrix} \tag{4.16}$$

and diagonal matrix

$$\mathbf{D} = \begin{pmatrix} x & . & . & . & . & . & . \\ . & x & . & . & . & . & . \\ . & . & x & . & . & . & . \\ . & . & . & \mathbf{A} & . & . & . \\ . & . & . & . & x & . & . \\ . & . & . & . & . & x & . \\ . & . & . & . & . & . & x \end{pmatrix} \tag{4.17}$$

The block matrix elements appearing above are defined by Eq. (3.70).

Although the original nonzero elements of matrix **M** are returned exactly by the above MAF decomposition procedure, other formerly zero elements are disturbed and can contribute to both error and reduced convergence speed. The following section describes an iterative procedure for eliminating or further reducing this remaining decomposition error.

Removal of Decomposition Error

Eq. (4.14) can be expanded as follows.

$$\mathbf{M} \simeq \mathbf{M}'_x \cdot [\mathbf{D}]^{-1} \mathbf{M}'_y = \mathbf{M} + \mathbf{P} \tag{4.18}$$

The equation actually solved, instead of Eq.(3.69) or (4.1), is

$$\mathbf{M}\cdot[\delta\mathbf{U}]+\mathbf{P}\cdot[\delta\mathbf{U}]=[\Delta\mathbf{U}] \tag{4.19}$$

The difference between Eq. (4.1) and Eq. (4.19) is the decomposition error term $\mathbf{P}\cdot[\delta\mathbf{U}]$. We now present an iterative procedure for removing this decomposition error.

The decomposition error term is fed back into the matrix equation on the right hand side for self cancellation. A *k*-step iterative modified approximate factorization algorithm, MAFk (*MAFk Algorithm*), is defined as follows.

$$\mathbf{M}\cdot\left[\delta\mathbf{U}^{(k)}\right]+\mathbf{P}\cdot\left[\delta\mathbf{U}^{(k)}\right]=[\Delta\mathbf{U}]+\mathbf{P}\cdot\left[\delta\mathbf{U}^{(k-1)}\right] \tag{4.20}$$

where $\left[\delta\mathbf{U}^{(0)}\right]=[\mathbf{0}]$ $\quad k=1,2,3,...$

MAF1 is the same as Eq. (4.19) above. For this iterative procedure to work, each MAF iteration must be numerically stable and the sequence must converge. For it to be efficient, the number of iterations must be kept small, ideally at two. A simplified stability analysis and examples showed the optimum value for the maximum number of *k* sub-iterations per time step was shown to be two for flows going to steady states.

4.5. Block TriDiagonal-Matrix Algorithm

The majority of the numerical methods described above resolve the solution of difficult problems into repeated solutions of an equation system with a block tri-diagonal matrix

$$\boldsymbol{a}_i\Phi_i=\boldsymbol{b}_i\Phi_{i+1}+\boldsymbol{c}_i\Phi_{i-1}+\boldsymbol{d}_i \tag{4.21}$$

where $i=1,2,...,N-1,N$

Here an unknown value of Φ and coefficient $\boldsymbol{d}$ are vectors which order is equal 5 (for a 3-dimensional task) or 4 (for a two-dimensional task). Coefficients $\boldsymbol{a}_m,\boldsymbol{b}_m,\boldsymbol{c}_m$ are (5x5) or (4x4) olrder matrixes respectively.

For the solution of a system it is possible to use an algorithm similar to Thomas algorithm, described in paragraph 2.11. The only essential difference is

that a multiplication by an inverse matrix is used instead of division into number.

The algorithm of the solution of system (4.21) is as follows

1. Calculate $\boldsymbol{P}_1, \boldsymbol{Q}_1$

$$\boldsymbol{P}_1 = \boldsymbol{a}_1^{-1}\boldsymbol{b}_1, \quad \boldsymbol{Q}_1 = \boldsymbol{a}_1^{-1}\boldsymbol{d}_1 \tag{4.22}$$

2. Use the recurrence relations

$$\begin{aligned} \boldsymbol{P}_i &= \left(\boldsymbol{a}_i - \boldsymbol{c}_i\boldsymbol{P}_{i-1}\right)^{-1}\boldsymbol{b}_i, \\ \boldsymbol{Q}_i &= \left(\boldsymbol{a}_i - \boldsymbol{c}_i\boldsymbol{P}_{i-1}\right)^{-1}\left(\boldsymbol{c}_i\boldsymbol{Q}_{i-1} + \boldsymbol{d}_i\right) \end{aligned} \tag{4.23}$$

to obtain $\boldsymbol{P}_i, \boldsymbol{Q}_i$ for $i = 2,3,...,N$

3. Set $\boldsymbol{Q}_N = \boldsymbol{\Phi}_N$

4. Use

$$\boldsymbol{\Phi}_i = \boldsymbol{P}_i\boldsymbol{\Phi}_{i+1} + \boldsymbol{Q}_i \tag{4.24}$$

for $i = N-1, N-2,...,3,2,1$, to obtain $\Phi_{N-1}, \Phi_{N-2},...,\Phi_3, \Phi_2, \Phi_1$

5. BOUNDARY CONDITIONS

Setting boundary conditions for Navier-Stokes's equations is not a trivial task. From a theoretical point of view it is the most difficult part of the problem considered in this book.

At first sight, it seems that from the point of view of space variables we deal with a typical ***boundary value problem***, and for its decision it is necessary to set *all* gasdynamic parameters on *all the boundary* of an estimated area.

Actually, it is not so.

Let’s consider, as an example, a compressed gas flow along an axis *x* with speed *u* from left to right.

As mentioned above any point of the flow can propagate its influence on the surrounding space as follows:

- with speed u due to movement of the flow - down the flow;
- with speed $u+a$ due to movement of the flow and propagation of sound vibrations - down the flow;
- with speed u-a due to propagation of sound vibrations; if speed u exceeds the speed of sound a, there is no upwind influence.

Thus, in case of a supersonic flow from left to right, the right boundary of an estimated area can't influence up the flow in any way; and setting boundary conditions on it contradicts any physical sense.

If speed at the exit from an estimated area is subsonic, then extension of influence up the flow is possible owing to propagation of sound vibrations, and it is required to set boundary conditions on this boundary.

What boundary conditions are needed to be set on various types of boundary of an estimated area?

The answer to this question is connected with ‘so-called’ *characteristics*.

5.1. Characteristics. Riemann's invariants.

It is supposed that on the boundaries of a computational domain it is possible to neglect the influence of viscosity. (This assumption is fair for many types of boundaries, except for cases when a boundary is a wall or a plane (line) of symmetry.)

The Euler equations are a set of quasilinear hyperbolic equations governing adiabatic and inviscid flow

Consider the following unsteady homogeneous hyperbolic equation

$$\frac{\partial u}{\partial t} + a(u)\frac{\partial u}{\partial x} = 0, \quad u(0,x) = \phi(x), \quad -\infty < x < \infty \tag{5.1}$$

Characteristics are the curves in *x*-*t* plane determined by the equation

$$\frac{dx(t)}{dt} = a\big(u(t, x(t))\big) \tag{5.2}$$

If the solution $u(t,x)$ is differentiable, then it remains constant along the characteristic $x(t)$. Really

$$\frac{du(t,x(t))}{dt} = \frac{\partial u}{\partial t} + \frac{\partial u}{\partial x}\frac{dx(t)}{dt} = \frac{\partial u}{\partial t} + a(u)\frac{\partial u}{\partial x} = 0 \tag{5.3}$$

Now let's consider a one-dimensional non-stationary problem of a compressed inviscid gas flow along an axis *x*.

The main equations in this case are as follows:

$$\begin{aligned} &\frac{\partial \rho}{\partial t} + \frac{\partial}{\partial x}(\rho u) = 0 \\ &\frac{\partial}{\partial t}(\rho u) + \frac{\partial}{\partial x}\left(\rho u^2 + p\right) = 0 \\ &\frac{\partial}{\partial t}(\rho E) + \frac{\partial}{\partial x}(\rho u E + up) = 0 \end{aligned} \tag{5.4}$$

It is a 'so-called' conservative form of the equations. The other form is obtained by subtracting the continuity equation from the second and third equations of the system and multiplied by *u* и *E* respectively:

$$\begin{aligned} &\frac{\partial \rho}{\partial t} + u\frac{\partial \rho}{\partial x} + \rho\frac{\partial u}{\partial x} = 0 \\ &\rho\frac{\partial u}{\partial t} + \rho u\frac{\partial u}{\partial x} + \frac{\partial p}{\partial x} = 0 \\ &\rho\frac{\partial E}{\partial t} + \rho u\frac{\partial E}{\partial x} + \frac{\partial}{\partial x}(up) = 0 \end{aligned} \tag{5.5}$$

If the gas is calorically perfect the total energy E can be expressed through pressure and speed

$$E = e + \frac{1}{2}u^2 = \frac{p}{\beta\rho} + \frac{1}{2}u^2, \tag{5.6}$$

where $\beta = \gamma - 1$

Hence:

$$dE = \frac{dp}{\beta\rho} - \frac{pd\rho}{\beta\rho^2} + udu \tag{5.7}$$

Substituting Eq. (5.7) in the 3rd equation of (5.5), we obtain:

$$\frac{1}{\beta}\frac{\partial p}{\partial t} + \frac{u}{\beta}\frac{\partial p}{\partial x} - \frac{p}{\beta\rho}\left(\frac{\partial \rho}{\partial t} + u\frac{\partial \rho}{\partial x}\right) + u\left(\rho\frac{\partial u}{\partial t} + \rho u\frac{\partial u}{\partial x} + \frac{\partial p}{\partial x}\right) + p\frac{\partial u}{\partial x} = 0 \tag{5.8}$$

From here, considering the continuity and momentum equations, we receive the energy equation through pressure:

$$\frac{\partial p}{\partial t} + \gamma p\frac{\partial u}{\partial x} + u\frac{\partial p}{\partial x} = 0 \tag{5.9}$$

Thus, we solve the considered equation in unknown vector

$$\mathbf{W} = \begin{pmatrix} \rho \\ u \\ p \end{pmatrix} \tag{5.10}$$

The system of equations in a vector form is as follows

$$\frac{\partial \mathbf{W}}{\partial t} + \boldsymbol{A}\frac{\partial \mathbf{W}}{\partial x} = 0, \tag{5.11}$$

where

$$\boldsymbol{A} = \begin{pmatrix} u & \rho & 0 \\ 0 & u & 1/\rho \\ 0 & \gamma p & u \end{pmatrix} \tag{5.12}$$

The eigenvalues of this matrix are equal to $\lambda_1 = u, \lambda_2 = u - a, \lambda_3 = u + a$

The corresponding eigenvectors are

$$\begin{pmatrix} 1 \\ 0 \\ 0 \end{pmatrix}, \begin{pmatrix} -\rho / a \\ 1 \\ -\rho a \end{pmatrix}, \begin{pmatrix} \rho / a \\ 1 \\ \rho a \end{pmatrix} \tag{5.13}$$

Thus, in similarity transformation

$$\boldsymbol{A} = \boldsymbol{S}^{-1}\boldsymbol{\Lambda}\boldsymbol{S} \tag{5.14}$$

matrices are equal to

$$\boldsymbol{S}^{-1} = \begin{pmatrix} 1 & -\rho/a & \rho/a \\ 0 & 1 & 1 \\ 0 & -\rho a & \rho a \end{pmatrix}, \quad \boldsymbol{S} = \begin{pmatrix} 1 & 0 & -1/a^2 \\ 0 & 1/2 & -1/(2\rho a) \\ 0 & 1/2 & 1/(2\rho a) \end{pmatrix} \tag{5.15}$$

(matrix $\boldsymbol{S}^{-1}$ is composed of eigenvectors, and $\boldsymbol{S}$ is found as the inverse for it)

Considering Eq. (5.14) the vector equation (5.11) is transformed to so-called *characteristic form*

$$\boldsymbol{S}\frac{\partial \mathbf{W}}{\partial t} + \boldsymbol{\Lambda}\boldsymbol{S}\frac{\partial \mathbf{W}}{\partial x} = 0 \tag{5.16}$$

The *characteristic variables* $\boldsymbol{\xi} = (\xi_1, \xi_2, \xi_3)^T$ are defined as follows (note the differential form)

$$d\boldsymbol{\xi} = \boldsymbol{S}d\mathbf{W} \tag{5.17}$$

Substituting the definition of the characteristic variables in the characteristic form of the governing equations (5.16) leads to

$$\frac{\partial \boldsymbol{\xi}}{\partial t} + \boldsymbol{\Lambda}\frac{\partial \boldsymbol{\xi}}{\partial x} = 0 \tag{5.18}$$

which is also called the *characteristic form* of the governing equations and has the advantage of decoupling the characteristic variables.

Each characteristic equation within Eq. (5.18) can be written as

$$\frac{\partial \xi_i}{\partial t} + \lambda_i \frac{\partial \xi_i}{\partial x} = 0 \tag{5.19}$$

As

$$d\boldsymbol{\xi} \equiv \boldsymbol{S}d\mathbf{W} = \begin{pmatrix} 1 & 0 & -1/a^2 \\ 0 & 1/2 & -1/(2\rho a) \\ 0 & 1/2 & 1/(2\rho a) \end{pmatrix} \begin{pmatrix} d\rho \\ du \\ dp \end{pmatrix} = \begin{pmatrix} d\rho - dp/a^2 \\ du/2 - dp/(2\rho a) \\ du/2 + dp/(2\rho a) \end{pmatrix}, \tag{5.20}$$

then for the considered problem the characteristic variables are (up to a numerical constant):

$$\begin{aligned} d\xi_1 &\equiv d\xi_0 = d\rho - dp/a^2 = ds, \\ d\xi_2 &\equiv d\xi_- = du - dp/(\rho a) \\ d\xi_3 &\equiv d\xi_+ = du + dp/(\rho a) \end{aligned} \tag{5.21}$$

where s is an entropy, a is a speed of sound.

Notice that characteristic variables are strictly conserved during their propagation along the characteristic; that is the quantity ξ_i, satisfying Eq. (5.19) remains constant along the characteristic C_i, defined by

$$\frac{dx_i(t)}{dt} = \lambda_i \tag{5.22}$$

since along C_i

$$\frac{d\xi_i}{dt} = \frac{\partial \xi_i}{\partial t} + \frac{\partial \xi_i}{\partial x}\frac{dx}{\partial t} = \frac{\partial \xi_i}{\partial t} + \lambda_i \frac{\partial \xi_i}{\partial x} = 0 \tag{5.23}$$

The variables ξ_i are also called *Riemann variables* and *Riemann invariants* when they remain constant. The system of equations in characteristic form can also, be written as follows

$$\begin{aligned} &d^{(0)}\rho - \frac{1}{a^2} d^{(0)} p = 0, && d^{(0)} = \partial_t + u\partial_x \\ &d^{(+)}u + \frac{1}{\rho a} d^{(+)} p = 0, && d^{(+)} = \partial_t + (u+a)\partial_x \\ &d^{(-)}u - \frac{1}{\rho a} d^{(-)} p = 0, && d^{(-)} = \partial_t + (u-a)\partial_x \end{aligned} \tag{5.24}$$

with the definitions of the three characteristics

$$
\begin{aligned}
&on\, C_0: \quad \frac{dx}{dt} = u \\
&on\, C_+: \quad \frac{dx}{dt} = u + a \\
&on\, C_-: \quad \frac{dx}{dt} = u - a
\end{aligned}
\tag{5.25}
$$

Note that these lines are not rectilinear since λ_i are variable.

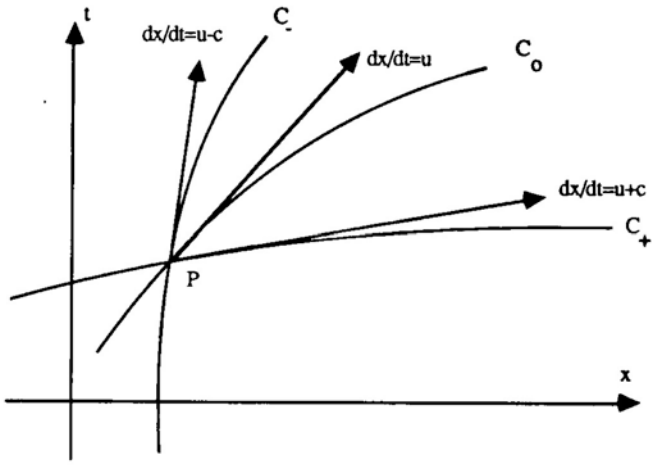

Figure 5.1. Characteristic lines for a one-dimensional flow

It is of interest also to notice that the first characteristic equation expresses the constant transport of entropy *s* along the path line *dx/dt =u*. As we know the following is true for isentropic process

$$p = k\rho^{\gamma} \tag{5.26}$$

where *k* is a constant.

So

$$dp = k\gamma\rho^{\gamma-1}d\rho = \frac{\gamma p}{\rho}d\rho = a^2 d\rho \tag{5.27}$$

where *a* is speed of sound($a^2 = \gamma\frac{p}{\rho}$).

Hence the first equation of (5.24) is equivalent to the condition

$$d^{(0)}s = 0 \quad \text{along } \frac{dx}{dt} = u \tag{5.28}$$

Thus the entropy propagates along the path line and is conserved along this characteristic, as long as discontinuities do not appear.

For isentropic flows, the Riemann or characteristic variables can be integrated as follows, for either C_+ or C_-.;. For instance, on C_+,

$$\xi_+ = u + \int \frac{dp}{\rho a} = u + \int a(\rho)\frac{d\rho}{\rho} \tag{5.29}$$

where the isentropic relations

$$p = k\rho^\gamma, \quad a^2 = k\gamma\rho^{\gamma-1} \tag{5.30}$$

can be introduced, k being a constant. This gives

$$\xi_+ = u + \frac{2}{\gamma - 1}a \tag{5.31}$$

and similarly

$$\xi_- = u - \frac{2}{\gamma - 1}a \tag{5.32}$$

for the two Riemann variables on the characteristics C_+ and C_-.

In the literature, another notation for invariants is often used:

$$\begin{aligned} R_0 &\equiv \xi_0 = s \\ R_+ &\equiv \xi_+ = u + \frac{2}{\gamma - 1}a \\ R_- &\equiv \xi_- = u - \frac{2}{\gamma - 1}a \end{aligned} \tag{5.33}$$

One can interpret the physical state at a given point in a one-dimensional isentropic inviscid flow as resulting from the quantities transported along the characteristics.

At a given point P(x, t) (Figure 5.2), the physical flow condition will be determined by the entropy transported along C_0 at speed u, that is along the

streamline. The velocity u and the pressure or the density are determined from the quantities $[u \pm 2a/(\gamma - 1)]$ transported at velocity $(u \pm a)$ along $C_{\pm}$. Hence,

$$\left(u + \frac{2}{\gamma - 1}a\right)_P = \left(u + \frac{2}{\gamma - 1}a\right)_{P_+} \tag{5.34}$$

$$\left(u - \frac{2}{\gamma - 1}a\right)_P = \left(u - \frac{2}{\gamma - 1}a\right)_{P_-} \tag{5.35}$$

$$s_P = s_{P_0} \tag{5.36}$$

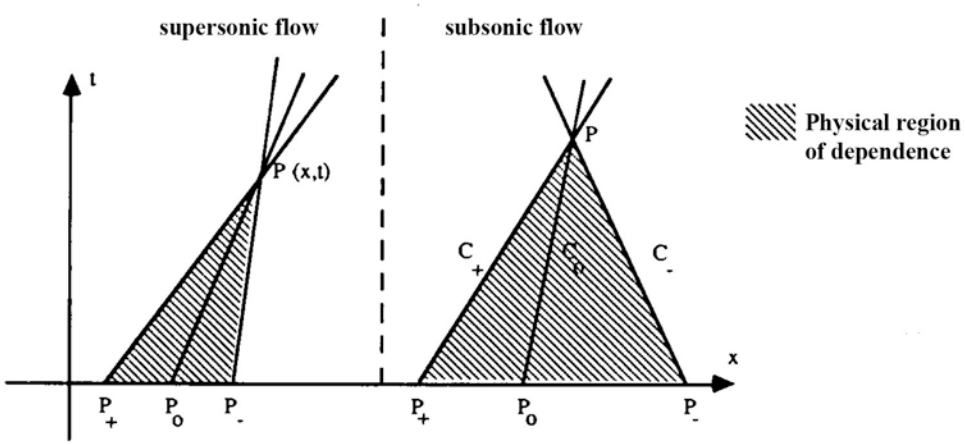

Figure 5.2. Propagation of flow quantities in a one-dimensional inviscid flow

The left side of Figure 5.2 is drawn for the case of a supersonic flow, while for a subsonic flow, the C_- characteristic has a negative slope and one has the situation shown on the right side of the figure.

Each point P in the (x, t) plane is reached by one characteristic of each type and therefore the flow situation at a given position x, at the time t, is solely dependent on the domain between P_+ and P_. This is the *domain of dependence* of P. Inversely, referring to Figure 5.1, the region included between the characteristics issuing from P forms the *domain of influence* of P.

The considered problem is easily generalized to a three-dimensional case. It is easy to show that in this case there appear two more characteristics determined by the equation

$$\frac{dx(t)}{dt} = u\,, \tag{5.37}$$

and the corresponding Riemann's invariants are

$$R_4 = v, \quad R_5 = w \tag{5.38}$$

5.2. Types of boundary conditions

As a rule, boundary conditions are divided into 5 types.

1) INLET – boundary on which the velocity vector is directed *inside* an estimated area
2) OUTLET – boundary on which the velocity vector is directed *outside from* an estimated area
3) FREE STREAM BOUNDARY – boundary between an estimated area and an external flow or quiescent space; the direction of a speed vector is unknown here in advance
4) WALL – an impenetrable surface
5) The PLANE (LINE) of SYMMETRY – boundary relative to which all parameters of a flow are symmetric.

The considerations from previous paragraph have a direct bearing on the number of boundary conditions to be imposed in a one-dimensional inviscid flow problem. Consider an inlet plane $x = x_0$, an outlet plane $x = x_1$ and points P_0 and P_1 at a given time on these boundaries. The number of boundary conditions to be imposed will depend on the way the information transported along the characteristics interacts with the boundaries (Figure 5.3).

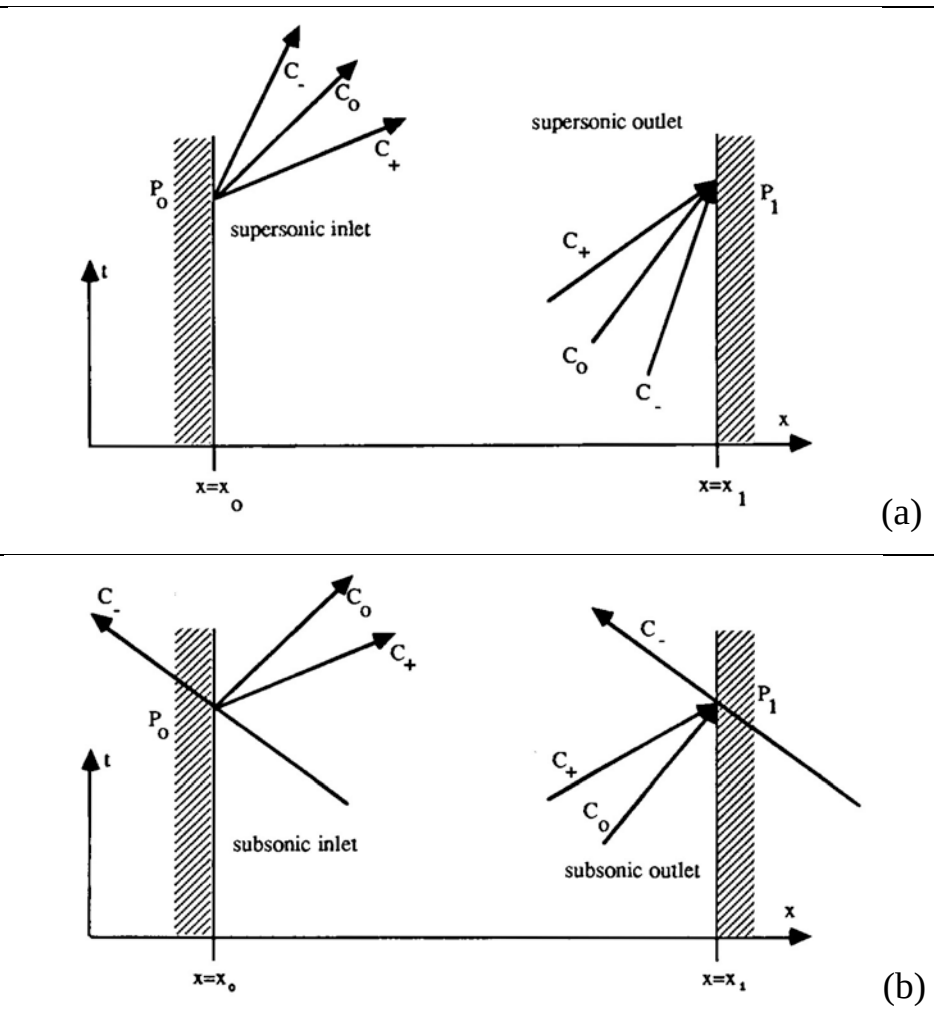

Figure 5.3. Boundary conditions for one-dimensional inviscid flows
(a) - supersonic flow, (b)) - subsonic flow

At an inlet point P_0, the characteristics C_+ and C_0 have speeds u and $a + u$, which are always positive, for a flow in the positive x direction. Therefore, they will always carry information from the boundaries towards the inside of the domain. This requires the values of the transported quantities to be known at P_0.

The third characteristic C_- has a slope whose sign depends on the inlet Mach number. For supersonic inlet flow conditions, C_- will have a positive slope, but a negative slope at subsonic inlet conditions.

In the first case, the information from the inlet surface enters the domain and a corresponding boundary condition has to be imposed. On the other hand, at subsonic inlet conditions, information from inside the domain reaches the

boundary along C_- and no boundary condition associated with C_- is allowed to be fixed arbitrarily.

Similar considerations can be made at the outlet. Two characteristics, C_+ and C_0 , always reach the outlet from inside the domain and therefore they determine two of the three independent characteristic variables in the outlet plane from the behaviour of the interior flow.

The third condition is dependent on the outlet flow Mach number. For supersonic outlet velocities no boundary condition is to be imposed, while at subsonic outlet velocities one boundary condition is to be fixed at the outlet section.

We will consider these cases in more detail

5.2.1. INLET

We assume that this boundary is located perpendicular to an axis *x*, i.e. is on a plane $0yz$.

There are two possible options.

If a velocity component *u* is more than the speed of sound, all eigenvalues of the matrix determining convective transport through the boundary $\lambda_1 = u, \lambda_2 = u + a, \lambda_3 = u, \lambda_4 = u, \lambda_5 = u - a$ have a positive sign. That means that all five characteristics are directed *inside* an estimated area, and propagation of influence is directed only from the boundary inside.

In this case, the boundary is called a SUPERSONIC INLET, and it is necessary to set all 5 parameters of a flow on it. Most often, they are 3 components of speed, temperature and pressure (or density).

In case of a supersonic inlet, usually there are no problems with setting boundary conditions.

The option when $u < a$ is more difficult. In this case, only 4 characteristics are directed *inside* an estimated area, and the one – from the internal part of an estimated area to the boundary.

Such border is called a SUBSONIC INLET, and 4 parameters of a flow are set on it. The fifth parameter is defined by extrapolation from the internal part of an estimated area.

Here are various possible options depending on a specific problem.

For example, for the solution of a problem of a flow in a pipe or problems of expiration a flow from a subsonic nozzle, 3 components of speed and temperature are most often set at an inlet.

The pressure at an inlet is determined from a condition of constancy of the invariant connected with the eigenvalue $\lambda = u - a$, i.e. from a condition:

$$du - dp / (\rho a) = 0 \tag{5.39}$$

For this purpose we take an internal point which is next to a considered boundary point, determine speed and pressure received during calculation in it, and then, as a result of the solution of a differential analog of the equation (5.39) we obtain the pressure in the boundary point.

In more detail this process is like that. We assume that on the *n*-th step by time all parameters of the flow are known. It is required to determine pressure on the boundary on the *(n*+1*)* - th step by time. We designate parameters on the boundary with index b, and parameters of the next internal point – with index i. From the equation (5.39) we obtain:

$$p_b^{n+1} = p_i^n + (\rho a)\left(u_b^{n+1} - u_i^n\right) \tag{5.40}$$

The coefficient (ρa) is taken as an average between two points and can be found iteratively (2 iterations enough).

Let’s see another example: a flow in the combustion chamber of a rocket engine. As a rule, pressure and temperature are known at the inlet of the chamber.

In this case, speed at an inlet is easily found from a condition of constancy of Riemann’s invariant of $R = u - \frac{2a}{(\gamma - 1)}$:

$$R_b = R_i \tag{5.41}$$

The value R_i is known on n-th step by time, the sound speed is determined by pressure and temperature. From here we obtain u_b.

It is possible to consider other variants of setting parameters on a subsonic inlet. All of them are easily solved with the use of Riemann’s invariant.

5.2.2. OUTLET

In this case, it is also necessary to consider 2 options: SUPERSONIC OUTLET and SUBSONIC OUTLET.

In case of a supersonic outlet, all 5 characteristics leave an estimated area. Boundary conditions are not set, and the values of parameters on the boundary are found from extrapolation from next points inside the estimated area. In this case, it isn't even required to use Riemann’s invariants.

In case of a subsonic outlet, it is necessary to set one parameter of a flow on the boundary - that is pressure, as a rule.

For jet flows, for flow past bodies with a gas flow and for a flow in a pipe this pressure is supposed to be equal to the pressure of a surrounding area.

If we consider the right boundary of an estimated area, which is located perpendicular to an axis *x*, the influence up the flow is determined by the characteristic $\lambda = u - a$ и and the corresponding Riemann’s invariant.

The other parameters of a flow are determined using Riemann's invariants.

As before, we will designate parameters on the boundary with index b, and parameters of the next internal point – with index i.

From the condition of constancy of Riemann's invariants relating to the characteristics directed down a flow, we obtain:

$$\begin{aligned} &\left(\rho_b^{n+1} - \rho_i^n\right) - \left(p_b^{n+1} - p_i^n\right) / a^2 = 0 \\ &\left(u_b^{n+1} - u_i^n\right) + \left(p_b^{n+1} - p_i^n\right) / (\rho a) = 0 \end{aligned} \tag{5.42}$$

From here:

$$\begin{aligned} \rho_b^{n+1} &= \rho_i^n + \frac{\left(p_b^{n+1} - p_i^n\right)}{a^2} \\ u_b^{n+1} &= u_i^n - \frac{\left(p_b^{n+1} - p_i^n\right)}{\rho a} \end{aligned} \tag{5.43}$$

As in the previous paragraph, on n-th step by time the values ρ_i^n, p_i^n, u_i^n are known in the internal part of an estimated area; p_b^{n+1} is set.

Further by formulas (5.43) we determine the values of parameters ρ_b^{n+1}, u_b^{n+1} on the boundary on $(n+1)$ - th step by time.

For the other speed components from (5.38) it appears:

$$\begin{aligned} v_b^{n+1} &= v_i^n \\ w_b^{n+1} &= w_i^n \end{aligned} \tag{5.44}$$

5.2.3. FREE STREAM BOUNDARY

On this boundary, a speed component directed by normal to the boundary is always subsonic. As it was already said, the direction of this speed can be any. Therefore, the characteristics can be also directed inside or outside the estimated area.

As a rule, such boundary separates an estimated area from an external stream or quiescent space. It would seem that in this case it is possible to set the boundary conditions coinciding with the parameters of an external stream.

In some cases it is acceptable, but it is more correct to use characteristic variables.

As an example, we will consider the boundary which is above the estimated area perpendicular to an axis *y*.

As always, we have 5 characteristics which in this case correspond to eigenvalues $\lambda_1 = v, \lambda_2 = v + a, \lambda_3 = v, \lambda_4 = v, \lambda_5 = v - a$

Obviously, the second characteristic comes to the boundary from within an estimated area, and the fifth one - from the external area. We will designate parameters of the external area with index *e* (from the English word external). We consider that the influence of an external stream is also caused by other characteristics.

From the point of view of characteristic variables it means that there is a relation between an external flow and the boundary:

$$\begin{aligned} &d\rho - dp / a^2 = 0, \\ &dv - dp / (\rho a) = 0, \\ &du = 0, \\ &dw = 0 \end{aligned} \tag{5.45}$$

and between the internal area and the boundary–

$$dv + dp / (\rho a) = 0 \tag{5.46}$$

The differential form of these equations is as follows:

$$
\begin{aligned}
&\left(\rho_b^{\,n+1}-\rho_e^{\,n}\right)-\left(p_b^{\,n+1}-p_e^{\,n}\right)/a^2=0,\\
&\left(v_b^{\,n+1}-v_e^{\,n}\right)-\left(p_b^{\,n+1}-p_e^{\,n}\right)/\left(\rho a\right)=0,\\
&\left(u_b^{\,n+1}-u_e^{\,n}\right)=0,\\
&\left(w_b^{\,n+1}-w_e^{\,n}\right)=0,\\
&\left(v_b^{\,n+1}-v_i^{\,n}\right)+\left(p_b^{\,n+1}-p_i^{\,n}\right)/\left(\rho a\right)=0
\end{aligned}
\tag{5.47}
$$

The solution to this system:

$$
\begin{aligned}
&u_b^{\,n+1}=u_e^{\,n}\\
&w_b^{\,n+1}=w_e^{\,n}\\
&v_b^{\,n+1}=\frac{1}{2}\left(v_e^{\,n}+v_i^{\,n}\right)+\frac{p_i^{\,n}-p_e^{\,n}}{2\rho a}\\
&p_b^{\,n+1}=\frac{1}{2}\left(p_i^{\,n}+p_e^{\,n}\right)+\frac{1}{2}\left(\rho a\right)\left(v_i^{\,n}-v_e^{\,n}\right)\\
&\rho_b^{\,n+1}=\rho_e^{\,n}+\frac{1}{a^2}\left[\frac{1}{2}\left(p_i^{\,n}-p_e^{\,n}\right)+\frac{1}{2}\left(\rho a\right)\left(v_i^{\,n}-v_e^{\,n}\right)\right]
\end{aligned}
\tag{5.48}
$$

The analysis of these formulas shows that even if an external stream is quiescent, i.e. $u_e=v_e=w_e=0$, when a positive indignation of pressure approaches the boundary, there appears a positive normal component of speed v_b. Also, the pressure on the boundary will change. Thus, parameters on the boundary will differ from parameters of an external stream.

It is possible to set the boundary conditions coinciding with parameters of an external stream only in case when it is known in advance that no indignations happening in an internal part of the estimated area will reach the boundary.

All equations obtained for the boundaries located parallel to the coordinate planes are easily applied to randomly located boundaries. Only instead of speeds *u*,*v*,*w* it is necessary to use speed components which are normal and tangential to the boundary.

For example, for the considered case instead of v we use u_n - a speed component normal to border; and instead of u, w we use a tangential components of speed.

5.2.4. WALL

Walls can be with *free slip*. Then a normal component of speed on the boundary is equal to zero, and for tangential components:

$$\frac{\partial u_t}{\partial n} = 0 \tag{5.49}$$

where $\frac{\partial}{\partial n}$ - normal derivative to a surface.

If there is *no slip* on a wall, then all speed components on the boundary are equal to zero.

In both cases we assume for pressure:

$$\frac{\partial p}{\partial n} = 0 \tag{5.50}$$

The temperature on the wall can be set

$$T_b = T_W, \tag{5.51}$$

or a wall can be adiabatic, then

$$\frac{\partial T}{\partial n} = 0 \tag{5.52}$$

Using characteristic variables near a wall is difficult, since a strong impact is exerted by viscosity here.

Conditions (5.49), (5.50), (5.52) should be set implicitly. For this purpose, it is very convenient to use so-called *"ghost" cells*, which will be considered in the following section in detail.

5.2.5. PLANE (LINE) of SYMMETRY

From the mathematics point of view, this type of boundary is a special case of a WALL when there is free slip and a wall is adiabatic.

5.3. Ghost cells

In this section for simplicity of description we will consider boundaries in two-dimensional problems, however all obtained results are easily applied to three-dimensional problems.

First of all, we will note that the control volumes located in close proximity to the boundary of an estimated area can be designed in various ways.

Let's consider this using an example of a lower boundary of a two-dimensional grid.

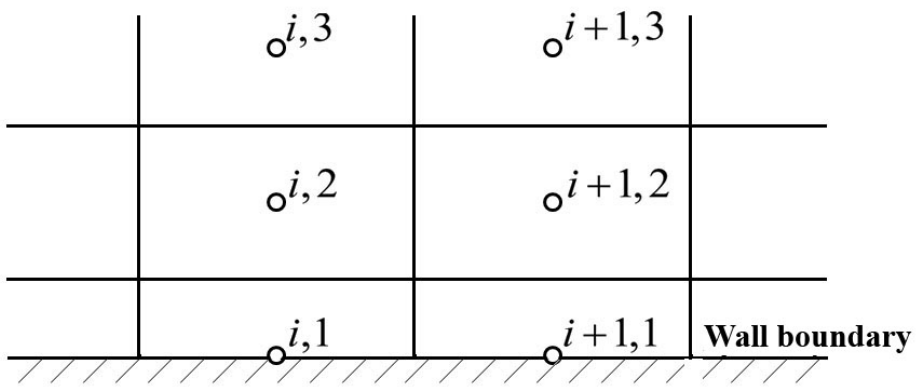

Fig.5.4. Wall boundary, method *I*

Fig. 5.4. shows method *I*, when the boundary of an estimated area passes through grid points. The near-boundary control volumes are twice less than next volumes there. Such method is convenient when values of all flow parameters are known, or they are directly set by boundary conditions, or determined using characteristics. In this case, there is no need to write down the equations of balances for near-boundary control volumes, since the values of parameters in grid points of these cells are already known. In this example they are grid points $(i,1), \quad i=1,2,...,N_X$.

The values of flow parameters in these grid point are used to determine fluxes through the sides of next cells: $(i,2), \quad i=1,2,...,N_X$ ..

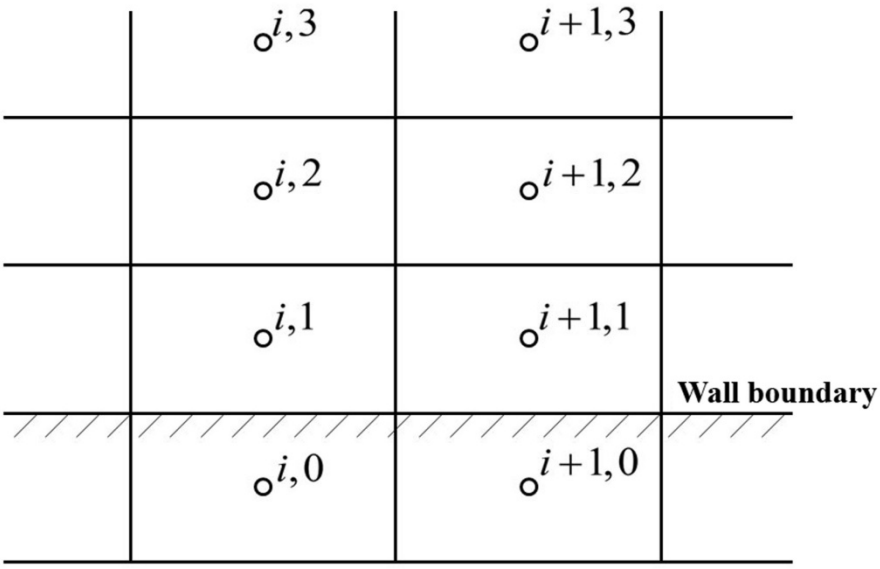

Fig.5.5 Wall boundary, method *II*

Method *II* presented in fig. 5.5 is based on the fact that the boundary of an estimated area passes through the lower sides of near-boundary control volumes. In that case, the values of flow parameters in near-boundary grid points are unknown in advance, and the same balance equations are written for them as well as for the other cells.

If flow parameters on the boundary are known, then by making up balances the fluxes are easily determined by the lower sides of near-boundary cells.

The situation is worse for boundaries like WALL or SYMMETRY, on which it is not parameters that are set but their derivatives. In order to use such boundary conditions, it is necessary to enter relations between parameters in several layers of near-boundary cells in implicit form.

The implementation of boundary conditions can be performed using “ghost” cells. Ghost cells are not created by the grid generator. Instead, they are logically created by the numerical code and are associated with a boundary face.

The values of its properties are set so that the flux calculation on the boundary face yields the correct flux. For instance, for a wall boundary face, the correct inviscid flux calculations should yield zero mass and energy fluxes and a

momentum flux equal to the pressure. The viscous flux for the wall boundary face should yield a prescribed diffusion flux, viscous forces and heat fluxes. Only one set of properties is not enough to satisfy all the constraints. In this work, the properties of the ghost cell change according to the flux calculation being performed. When the inviscid fluxes are being calculated, the ghost cells hold properties such that the inviscid fluxes are correct at the boundaries. The same happens at the viscous flux calculation.

5.3.1. Boundary conditions for inviscid fluxes

WALL and SYMMETRY

The inviscid flux for a symmetry face and a wall are the same. No mass and energy fluxes and momentum flux given by the pressure only. That is accomplished by setting the normal velocity to the wall to zero. This is easier to achieve by working in the face coordinate frame.

For example, for the lower boundary (fig. 5.5) this condition is provided by the fact that the normal component of velocity in a ghost cell is taken with the opposite sign in relation to a near-boundary cell:

$$v_{i,0} = -v_{i,1} \tag{5.53}$$

In this case, on the boundary:

$$v_{i,0+1/2} = \frac{1}{2}\left(v_{i,0} + v_{i,1}\right) = 0$$

This condition is written in a vector form:

$$\boldsymbol{U}_{i,0} = \boldsymbol{W}\boldsymbol{U}_{i,1}, \quad i = 1, 2, \ldots, N_X \tag{5.54}$$

where

$$\boldsymbol{W} = \begin{pmatrix} 1 & 0 & 0 & 0 \\ 0 & 1 & 0 & 0 \\ 0 & 0 & -1 & 0 \\ 0 & 0 & 0 & 1 \end{pmatrix} \tag{5.55}$$

If a boundary is located to the left of an estimated area, then for it we assume in a ghost cell

$$u_{0,j} = -u_{1,j}, \quad j = 1, 2, ... N_Y, \tag{5.56}$$

and matrix $\boldsymbol{W}$ contains a negative unit on the second position.

Implicit Boundary Conditions

The global differential equation (3.69) for a two-dimensional problem is as follows:

$$\mathbf{A}_{i,j}\delta\mathbf{U}_{i,j}^{n+1} + \mathbf{B}_{i,j}\delta\mathbf{U}_{i,j+1}^{n+1} + \mathbf{C}_{i,j}\delta\mathbf{U}_{i,j-1}^{n+1} + \mathbf{D}_{i,j}\delta\mathbf{U}_{i+1,j}^{n+1} + \mathbf{E}_{i,j}\delta\mathbf{U}_{i-1,j}^{n+1} = \Delta\mathbf{U}_{i,j}^{n} \tag{5.57}$$

For increments $\delta\mathbf{U}$ on a wall, there are the same relation as for the main vector $\mathbf{U}$.

For example, for the lower wall boundary

$$\delta\boldsymbol{U}_{i,0}^{n+1} = \boldsymbol{W}\,\delta\boldsymbol{U}_{i,1}^{n+1}, \quad i = 1, 2, ..., N_X, \tag{5.58}$$

from here we obtain that at $j = 1$ inviscid fluxes through the lower side are calculated by the following formula

$$\begin{aligned} (\mathbf{G}_C)_{i,j+1/2} &= (\mathbf{G}_C)_{i,j+1/2}^{n} + \alpha\left[(\boldsymbol{B}_+)_{i,j+1/2}^{n}\,\delta\mathbf{U}_{i,j}^{n+1} + (\boldsymbol{B}_-)_{i,j+1/2}^{n}\,\delta\mathbf{U}_{i,j+1}^{n+1}\right], \\ (\mathbf{G}_C)_{i,j-1/2} &= (\mathbf{G}_C)_{i,j-1/2}^{n} + \alpha\left[(\boldsymbol{B}_+)_{i,j-1/2}^{n}\,\boldsymbol{W} + (\boldsymbol{B}_-)_{i,j-1/2}^{n}\right]\delta\mathbf{U}_{i,j}^{n+1} \end{aligned} \tag{5.59}$$

$$(\mathbf{G}_C)_{i,j-1/2}^{n} = (\boldsymbol{B}_+)_{i,j-1/2}^{n}\,\mathbf{U}_L + (\boldsymbol{B}_-)_{i,j-1/2}^{n}\,\mathbf{U}_R = \left((\boldsymbol{B}_+)_{i,j-1/2}^{n}\,\boldsymbol{W} + (\boldsymbol{B}_-)_{i,j-1/2}^{n}\right)v_R \tag{5.60}$$

Eq. (5.57) for $j = 1$ is as follows

$$\mathbf{A}_{i,j}\delta \boldsymbol{U}_{i,j}^{n+1}+\mathbf{D}_{i,j}\delta \boldsymbol{U}_{i+1,j}^{n}+\mathbf{E}_{i,j,k}\delta \boldsymbol{U}_{i-1,j}^{n}+\mathbf{B}_{i,j,k}\delta \boldsymbol{U}_{i,j+1}^{n}=\Delta \boldsymbol{U}_{i,j}^{n}\,, \tag{5.61}$$

here coefficients $\mathbf{D}_{i,j},\mathbf{E}_{i,j},\mathbf{B}_{i,j}$ are calculated by the same formulas as for not near-boundary grid points, and the contribution of convection $\mathbf{G}_C$ to coefficient $\mathbf{A}_{i,j}$ is determined by a formula

$$\mathbf{A}_{i,j}\to\mathbf{A}_{i,j}+\frac{\alpha\Delta t}{\Delta y}\left[\left(\boldsymbol{B}_{+}\right)_{i,j+1/2}^{n}-\left(\boldsymbol{B}_{-}\right)_{i,j-1/2}^{n}-\left(\boldsymbol{B}_{+}\right)_{i,j-1/2}^{n}\boldsymbol{W}\right] \tag{5.62}$$

instead of

$$\mathbf{A}_{i,j}\to\mathbf{A}_{i,j}+\frac{\alpha\Delta t}{\Delta y}\left[\left(\boldsymbol{B}_{+}\right)_{i,j+1/2}^{n}-\left(\boldsymbol{B}_{-}\right)_{i,j-1/2}^{n}\right]$$

SUPERSONIC OUTPUT

For a boundary of this kind it is convenient to use ghost cells too. For example, if an output is located on the right, then

$$\boldsymbol{U}_{Nx+1,j}=\boldsymbol{U}_{Nx,j},\quad j=1,2,...N_Y \tag{5.63}$$

Implicit Boundary Conditions

For implicit form of boundary conditions at $i=N_X$ we obtain :

$$\begin{aligned}\left(\mathbf{F}_C\right)_{i+1/2,j,k}&=\left(\mathbf{F}_C\right)_{i+1/2,j,k}^{n}+\alpha\left[\left(\boldsymbol{A}_{+}\right)_{i+1/2,j,k}^{n}+\left(\boldsymbol{A}_{-}\right)_{i+1/2,j,k}^{n}\right]\delta\mathbf{U}_{i,j,k}^{n+1},\\ \left(\mathbf{F}_C\right)_{i-1/2,j,k}&=\left(\mathbf{F}_C\right)_{i-1/2,j,k}^{n}+\alpha\left[\left(\boldsymbol{A}_{+}\right)_{i-1/2,j,k}^{n}\delta\mathbf{U}_{i-1,j,k}^{n+1}+\left(\boldsymbol{A}_{-}\right)_{i-1/2,j,k}^{n}\delta\mathbf{U}_{i,j,k}^{n+1}\right],\end{aligned} \tag{5.64}$$

The differential equation:

$$\mathbf{A}_{i,j}\delta\mathbf{U}_{i,j}^{n+1}+\mathbf{E}_{i,j}\delta\mathbf{U}_{i-1,j}^{n}+\mathbf{B}_{i,j}\delta\mathbf{U}_{i,j+1}^{n}+\mathbf{C}_{i,j}\delta\mathbf{U}_{i,j-1}^{n}=\Delta\mathbf{U}_{i,j}^{n} \tag{5.65}$$

And the contribution of convection F_C to coefficient $\mathbf{A}_{i,j}$ is determined by a formula

$$\mathbf{A}_{i,j}\to\mathbf{A}_{i,j}+\frac{\alpha\Delta t}{\Delta x}\left[\left(\boldsymbol{A}_{+}\right)_{i+1/2,j,k}^{n}-\left(\boldsymbol{A}_{-}\right)_{i-1/2,j,k}^{n}+\left(\boldsymbol{A}_{-}\right)_{i+1/2,j,k}^{n}\right] \tag{5.66}$$

Instead of

$$\mathbf{A}_{i,j} \to \mathbf{A}_{i,j} + \frac{\alpha \Delta t}{\Delta x}\left[\left(\boldsymbol{A}_{+} \right)^{n}_{i+1/2,j,k} - \left(\boldsymbol{A}_{-} \right)^{n}_{i-1/2,j,k} \right]$$

FREE STREAM BOUNDARY

Here it is also convenient to use ghost cells. In this case, the parameters in these cells are assumed equal to the parameters of an external stream.

Ghost cells can be also used in other types of borders: INLET, SUBSONIC OUTLET. But this method doesn't give great advantages in comparison with the method of setting fluxes directly on the boundary.

5.3.2. Viscous Boundary Condition

WALL

There is no point in considering a wall with free slip as there is no viscosity there.

On a wall without slip the following parameters are set:

$$\begin{aligned} u_W &= v_W = w_W = 0 \\ p_W &= p_{in} \end{aligned} \tag{5.67}$$

Here, parameters on a wall are designated by index W, and parameters in the closest internal grid point of an estimated area are designated by the index in.

For an equation of energy there are different possible options of boundary conditions:

1) Temperature can be set on a wall - T_W
2) A wall can be adiabatic, then

$$T_W = T_{in} \tag{5.68}$$

3) We also can use a non-catalytic wall in radiative equilibrium. That is accomplished by setting the radiative flux equal to the convective heating crossing the wall. The balance of heat is as follows

$$\varepsilon\sigma_0 T_W{}^4 = \lambda_W \frac{T_{in} - T_W}{\Delta n}, \tag{5.69}$$

where Δn - a distance from grid point of a near-boundary cell to a wall by normal, ε - wall emissivity, σ_0 - Stefan-Boltsman's constant, λ_W - heat conductivity coefficient of gas at a wall.

The equation in unknown T_W (5.69) is solved iteratively at each moment of time in each near-boundary cell.

Knowing the values of all parameters on a wall, we can determine them also in the grid points of ghost cells. For example, for the lower boundary (see fig. 5.5) these values are determined by a formula

$$f_{i,0} = 2 f_W - f_{i,1}, \quad i = 1, 2, ..., N_X, \tag{5.70}$$

where $f = (u, v, w, p, T)$ - any parameter of a flow.

Implicit boundary conditions

To obtain an implicit form of boundary conditions on the lower wall we do the following.

Viscous fluxes on the upper and lower edge of a near-boundary cell *j=1* are determined by a formula

$$\begin{aligned} (\mathbf{G}_V)_{i,j+1/2} &= (\mathbf{G}_V)^n_{i,j+1/2} + \alpha \boldsymbol{N}^n_{i,j+1/2} \frac{1}{\Delta y}\left(\delta \mathbf{U}^n_{i,j+1} - \delta \mathbf{U}^n_{i,j}\right), \\ (\mathbf{G}_V)_{i,j-1/2} &= (\mathbf{G}_V)^n_{i,j-1/2} + \alpha \boldsymbol{N}^n_{i,j-1/2} \frac{1}{\Delta y}\left(\delta \mathbf{U}^n_{i,j} - \delta \mathbf{U}^n_{i,j-1}\right) \end{aligned} \tag{5.71}$$

where $\delta \mathbf{U}^n_{i,j-1}$ - an increment in a ghost cell.

It is necessary to express it somehow through increments in the main cells.

For this purpose, we introduce a vector

$$\mathbf{V} = \left[\rho, u, v, e\right]^T \tag{5.72}$$

Let

$$\delta\mathbf{V}_{i,j-1} = \mathbf{\Omega}\delta\mathbf{V}_{i,j} \tag{5.73}$$

Then

$$\delta\mathbf{U}_{i,j-1} = \frac{\partial\mathbf{U}}{\partial\mathbf{V}}\delta\mathbf{V}_{i,j-1} = \frac{\partial\mathbf{U}}{\partial\mathbf{V}}\mathbf{\Omega}\delta\mathbf{V}_{i,j} \tag{5.74}$$

Note that considering that

$$\mathbf{G}_V = \boldsymbol{M}_V \frac{\partial\mathbf{V}}{\partial y} = \boldsymbol{M}_V \frac{\partial\mathbf{V}}{\partial\mathbf{U}}\frac{\partial\mathbf{U}}{\partial y} \tag{5.75}$$

Using this, it is possible to approximate a viscous flux on the boundary as

$$\mathbf{G}_V = \boldsymbol{M}_V \frac{\mathbf{V}_{i,j} - \mathbf{V}_{i,j-1}}{\Delta y} \tag{5.76}$$

From here, considering (5.73)

$$\left(\boldsymbol{G}_V\right)_{i,j-1/2} = \left(\boldsymbol{G}_V\right)^n_{i,j-1/2} + \alpha\frac{\boldsymbol{M}_V}{\Delta y}\left(\boldsymbol{I} - \mathbf{\Omega}\right)\delta V^{n+1}_{i,j} \tag{5.77}$$

Finally we obtain:

$$\left(\boldsymbol{G}_V\right)_{i,j-1/2} = \left(\boldsymbol{G}_V\right)^n_{i,j-1/2} + \alpha\frac{1}{\Delta y}\widetilde{\boldsymbol{N}}^n_{i,j-1/2}\delta\boldsymbol{U}^{n+1}_{i,j} \tag{5.78}$$

where

$$\widetilde{\boldsymbol{N}}^n_{i,j-1/2} = \boldsymbol{M}_V\left(\boldsymbol{I} - \mathbf{\Omega}\right)\frac{\partial\boldsymbol{V}}{\partial\boldsymbol{U}} \tag{5.79}$$

Thus, the differential equation for grid point $j = 1$ is as follows

$$\mathbf{A}_{i,j}\delta\boldsymbol{U}^{n+1}_{i,j} + \mathbf{D}_{i,j}\delta\boldsymbol{U}^n_{i+1,j} + \mathbf{E}_{i,j,k}\delta\boldsymbol{U}^n_{i-1,j} + \mathbf{B}_{i,j,k}\delta\boldsymbol{U}^n_{i,j+1} = \Delta\boldsymbol{U}^n_{i,j} \tag{5.80}$$

And the contribution of a viscous flux $\mathbf{G}_V$ to coefficient $\mathbf{A}_{i,j}$ is determined by a formula

$$\mathbf{A}_{i,j} \to \mathbf{A}_{i,j} - \frac{\alpha \Delta t}{\Delta y^2}\left(\boldsymbol{N}^n_{i,j+1/2} + \widetilde{\boldsymbol{N}}^n_{i,j-1/2} \right) \tag{5.81}$$

instead of

$$\mathbf{A}_{i,j} \to \mathbf{A}_{i,j} - \frac{\alpha \Delta t}{\Delta y^2}\left(\boldsymbol{N}^n_{i,j+1/2,k} + \boldsymbol{N}^n_{i,j-1/2,k} \right)$$

There is still an open issue of determining matrix $\mathbf{\Omega}$, included in a formula (5.73). It is created with the use of relations (5.70) and depends on boundary conditions for the energy equation.

1) Temperature set on a wall - T_W

$$\mathbf{\Omega} = \begin{pmatrix} 1 & 0 & 0 & 0 \\ 0 & -1 & 0 & 0 \\ 0 & 0 & -1 & 0 \\ 0 & 0 & 0 & -1 \end{pmatrix} \tag{5.82}$$

2) Adiabatic wall

$$\mathbf{\Omega} = \begin{pmatrix} 1 & 0 & 0 & 0 \\ 0 & -1 & 0 & 0 \\ 0 & 0 & -1 & 0 \\ 0 & 0 & 0 & 1 \end{pmatrix} \tag{5.83}$$

3) An option with a radiation by a formula (5.69). After differentiating this formula, we obtain

$$4\varepsilon\sigma_0 T_W{}^3 \delta T_W - \lambda_W \frac{\delta T_{in} - \delta T_W}{\Delta n} = 0 \tag{5.84}$$

It can be shown that at small values of Δn the first member in this equation is significantly smaller than the second one and so can be neglected. Therefore:

$$\delta T_W = \delta T_{in} = \delta T_{i,j} \tag{5.85}$$

Considering a formula (5.70) we obtain

$$\delta T_{i,0} = 2\delta T_W - \delta T_{i,1} = \delta T_{i,j} \tag{5.86}$$

Therefore, the formula for Ω coincides with (5.83)

6. COMPUTATIONAL RESULTS

This chapter presents some calculation results obtained using the computer program UNIVERSE-CFD, developed in the Moscow Aviation Institute [15]. This program used the Modified Approximate Factorization (MAF) (see Section 4.4) method with the additions described in Section 3.8 "Ways to improve the numerical method".

6.1. Supersonic jet at high exit static pressure ratio

The first test aimed at checking the capabilities of the proposed numerical method. For this purpose, simulation was performed for an air jet with the following parameters:

$M_a = 4; \quad T_a = 2000[K]; \quad p_a / p_e = 10^5; \quad M_e = 12; \quad T_e = 288[K]$

This flow is characterized by regions with very high pressure gradients and high Mach numbers. The numerical computation of this variant is very complicated when using shock-capturing method without grid adaptation.

Figure 6.1 presents the predicted Mach number field. For comparison we used the results of Averenkova et al. [16], where the method of characteristics was applied to the simulation of ideal gas jet structure. The 800x120 grid was used.

Figure 6.2 presents centerline pressure and density profiles. The results are compared when using the 1-st approximation order of convective fluxes (dashed lines) and the 2-st approximation order with limiter functions (solid lines). The results of Ref. 16 are also presented.

After analyzing the results we can see that the use of the shock-capturing numerical method allowed for obtaining quite a true picture of parameter distribution in a supersonic jet with strong shocks. Using first approximation order for convective fluxes results in a big «blur» of the solution in the vicinity of strong shock waves if compared with second approximation order with limiter function (see Eq. (3.75)).

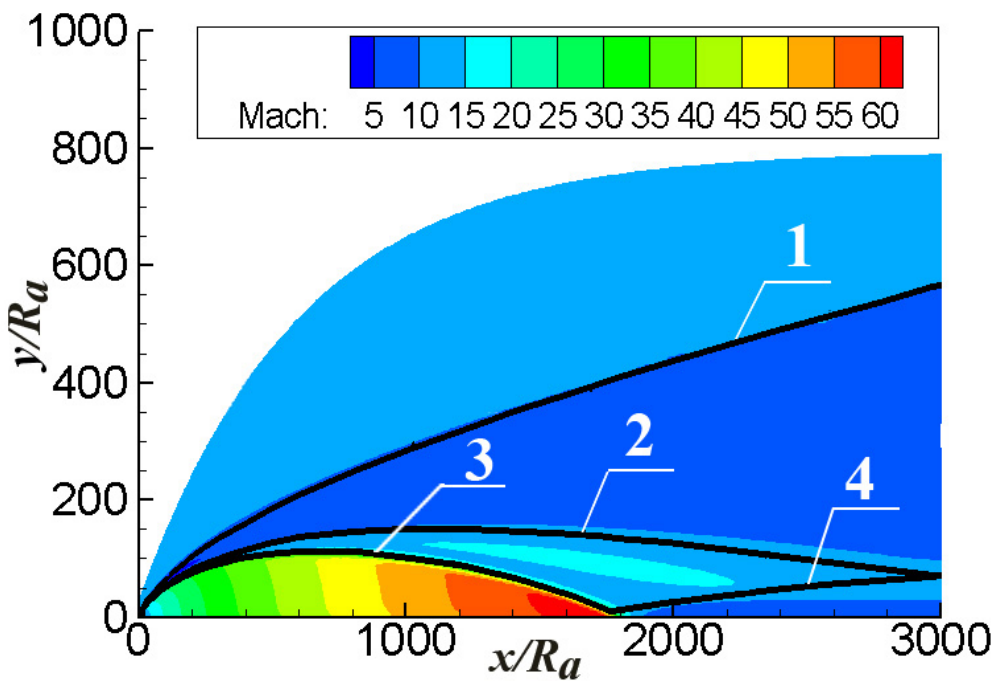

Figure 6.1. Mach number magnitude field and jet structure. 1 – attached shock, 2 – jet boundary, 3 – intercepting (barrel) shock, 4 – reflected shock.

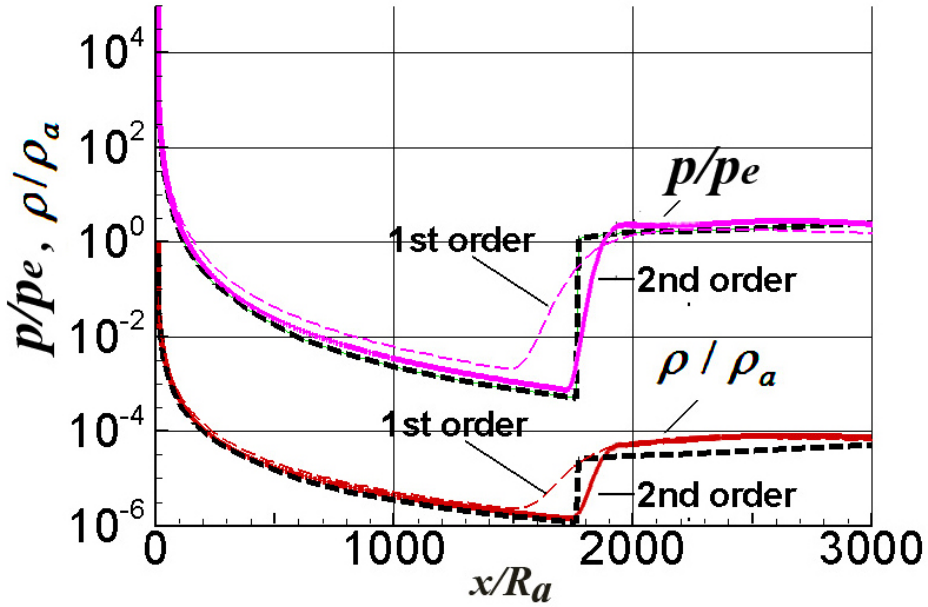

Figure 6.2. Centerline pressure and density profiles. Calculation results using first and second order approximation of convective fluxes, compared to simulation data of Averenkova et al. [16] (dashed lines).

When using the second approximation order of inviscid fluxes without limiter function Φ the numerical solution is always unstable for this simulation.

6.2. Supersonic oxygen jet in high-temperature ambient.

This test aimed at investigating the effect of high ambient temperature field on the supersonic oxygen jet behavior. This kind of a flow has great gradients of density and temperature.

For this purpose, simulation was performed for a jet with the following parameters: $u_a = 451\, m/s$; $T_a = 190K$; $p_a = 10^5 Pa$, jet fluid – O_2. Nozzle exit radius: $R_a = 9.2mm$

Three variants of ambient parameters were considered:

$T_e\,[K]$	$\%O_2$	$\%N_2$	$\%CO_2$

285	54	46	0
772	85	9	6
1002	88	3	9

The simulation results were compared with the experimental data of Sumi et al. [17]. Supersonic oxygen jet behavior in a high-temperature field was investigated by measuring the velocity, O_2 concentration and temperature of the oxygen jet in a heated furnace.

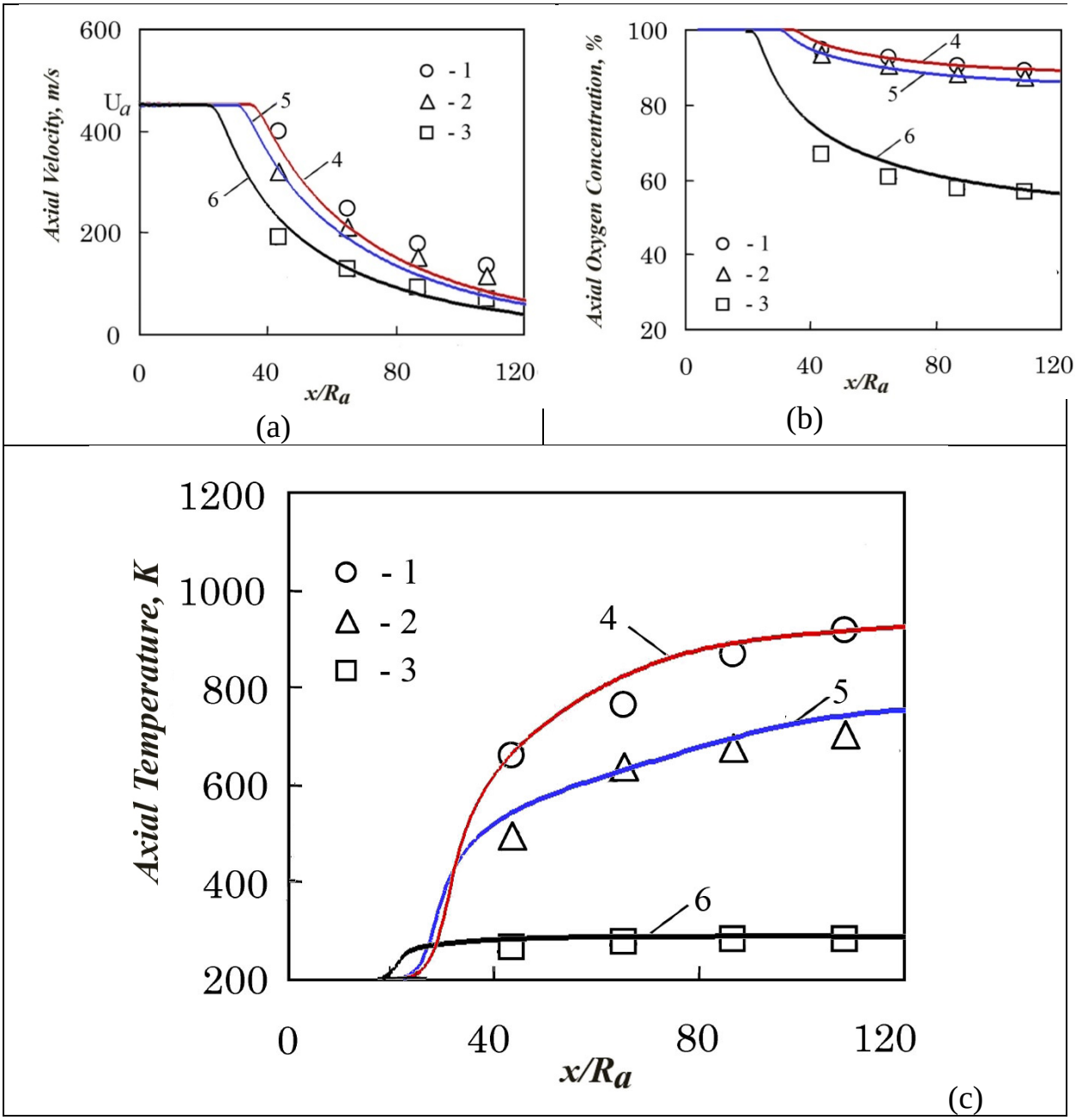

Figure 6.3. Centerline (a) velocity, (b) oxygen concentration and (c) temperature profiles.
1,2,3 – Sumi et al. [17] experiment: 1 - $T_e = 1002\ K$, 2 - $T_e = 772\ K$, 3 - $T_e = 285\ K$;
4,5,6 – simulations: 4 - $T_e = 1002\ K$, 5 - $T_e = 772\ K$, 6 - $T_e = 285\ K$

Figures 6.3 present the distribution of velocity, the concentration of oxygen and temperature on the jet axis at different ambient temperatures. The comparison of the simulation results using the presented method with the experimental data of Sumi et al. [17] shows a good agreement and also demonstrates the fact that the attenuation of the jet is restrained as the ambient temperature increases.

6.3. Cold under-expanded and over-expanded air jets

The simulation was performed for air jets having total temperature $T_0 = 300K$ and nozzle exit Mach number $M_a = 3.3$. The simulation results were compared with the experimental data of Safronov and Khotulev [18].

Figures 6.4 present the simulation results and the experimental data for an under-expanded jet with static pressure ratio $p_a / p_e = 1.5$, diameter of the profiled nozzle $D_a = 53.7mm$ and nozzle exit half cone angle $\theta_a = 10°$.

The simulation was performed using a 400x100 trapezoidal grid. Various turbulence models were used:

1) standard *K*-*ε* model;

2) *K*-*ε* turbulence model with compressibility correction [22]

Using standard $K\text{-}\varepsilon$ turbulence model considerably under-predicts the jet length if compared with the experimental data, and also reduces a number of shock diamonds; all shock waves are having significantly lower amplitude than measured.

Using the turbulence model with compressibility correction gave results, which are in a good agreement with the experimental data of Safronov, Khotulev [18].

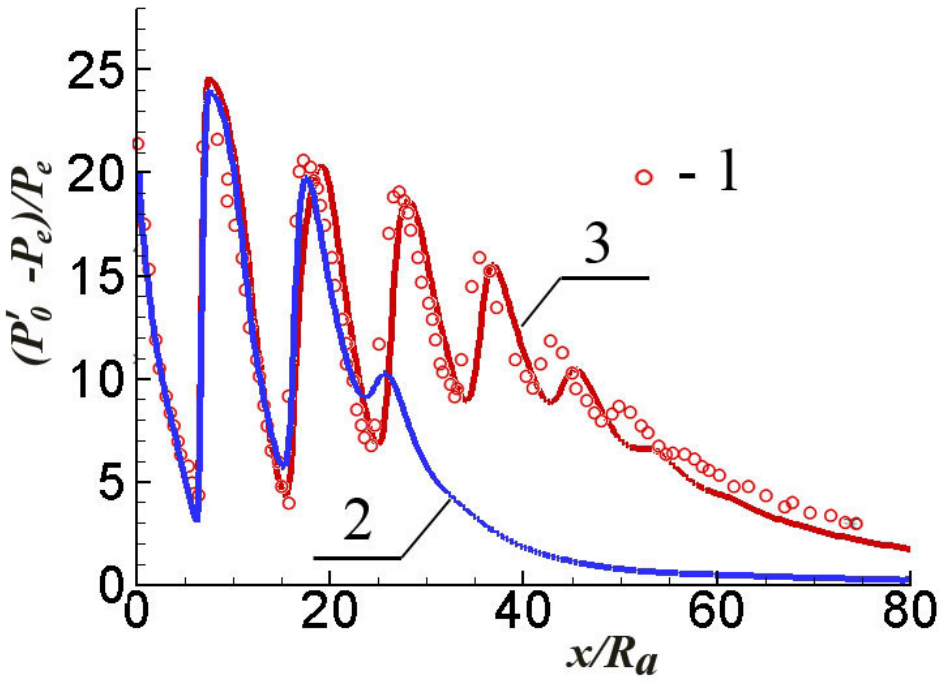
25
20
15
10
5
0
0
20
40
60
80
$(P_0' - P_e)/P_e$
x/R_a
- 1
3
2

(a)

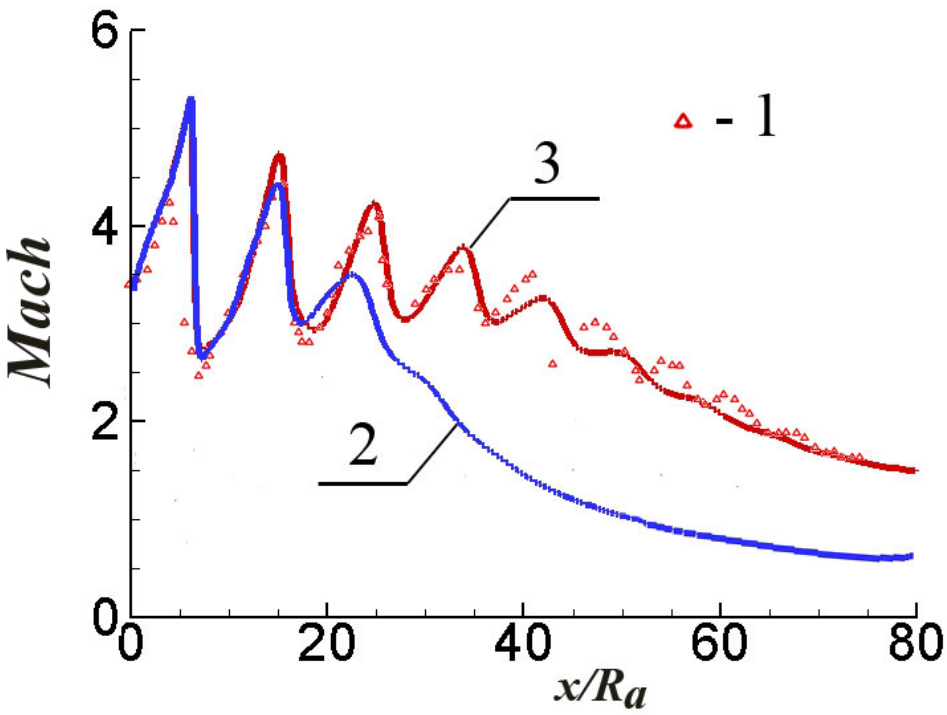
6
4
2
0
0
20
40
60
80
Mach
x/R_a
- 1
3
2

(b)

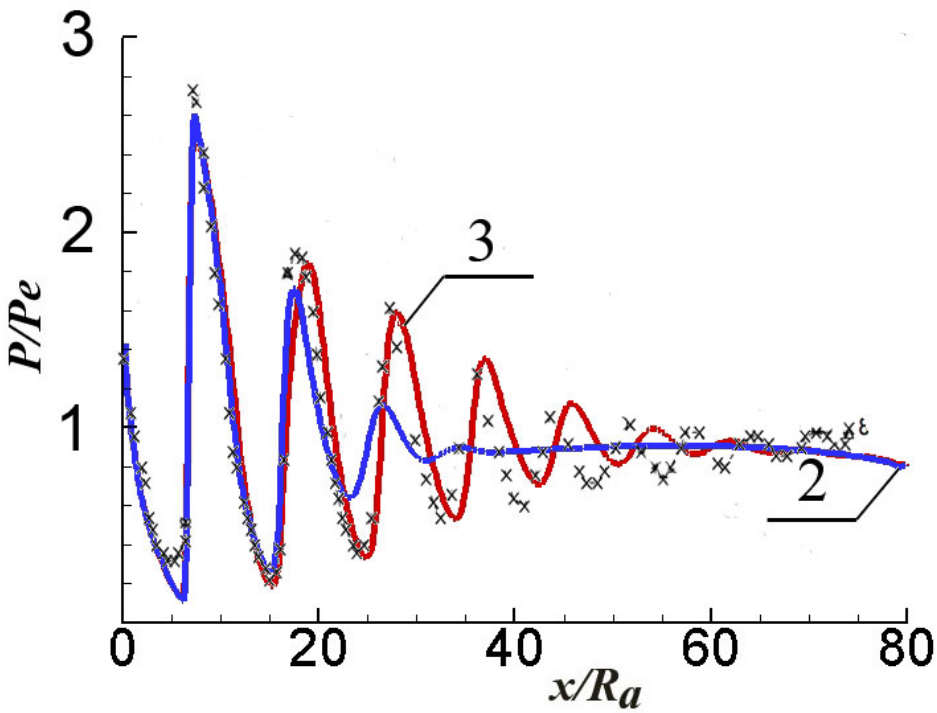

(c)

Figure 6.4. Centerline distribution of (a) normalized relative pitot pressure, (b) Mach number and (c) static pressure in jet with

$T_0 = 300K, M_a = 3.3, p_a / p_e = 1.5, \theta_a = 10°$.

Calculations using various turbulence models, compared to experiment.
1 – experiment; 2 – simulation with standard K-ε model; 3 – K-ε turbulence model with compressibility correction [22]

This test also investigates the influence of the grid resolution and the spatial order of numerical scheme on the results of simulations.

Figures 6.5 show the influence of the grid resolution at various spatial orders of numerical scheme. A 400x200 grid and a relatively coarse 200x60 grid were compared. When using second and third approximation order the simulation results were very similar for the both grids. Using a coarse 200x60 grid with first order resulted in too large restraining of the waves and rapid amplitude decay.

This result goes to show that using higher order approximation for convective fluxes allowed for obtaining quite precise results even with relatively coarse grids, which saves computer resources in terms of both CPU time and storage. For example, with laptop (Intel® Core™ i5, 2.27 Ghz, 4GB) the simulation of this variant only takes 40 sec with a 200x60 grid, and 230 sec with a 400x200 grid.

Figure 6.6. presents the comparison of the results obtained with a 200x60 grid for various spatial approximation orders of numerical scheme. The results with second and third approximation orders are very similar.

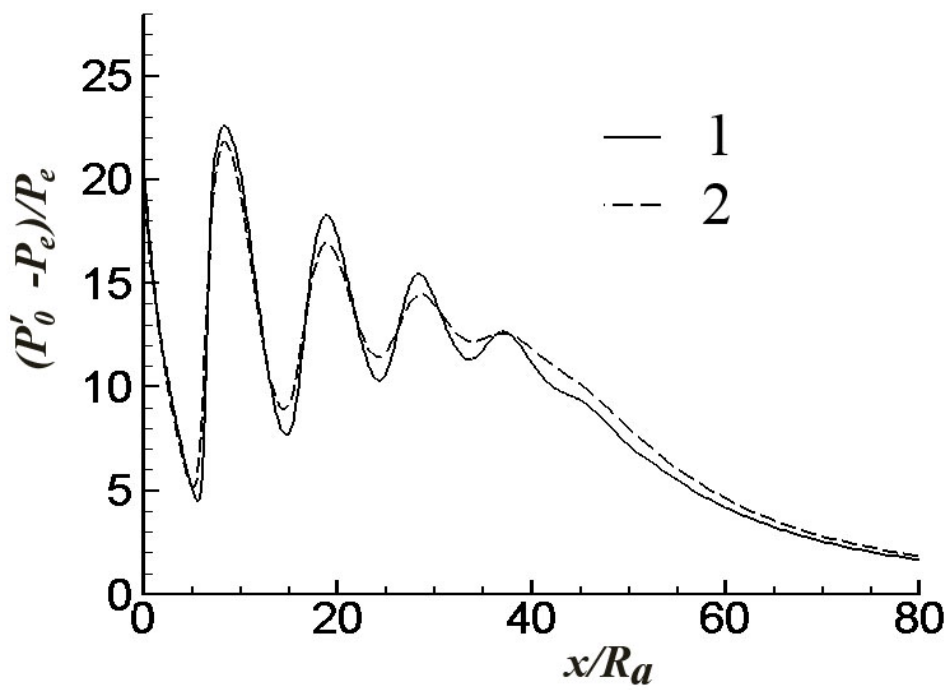

(a)

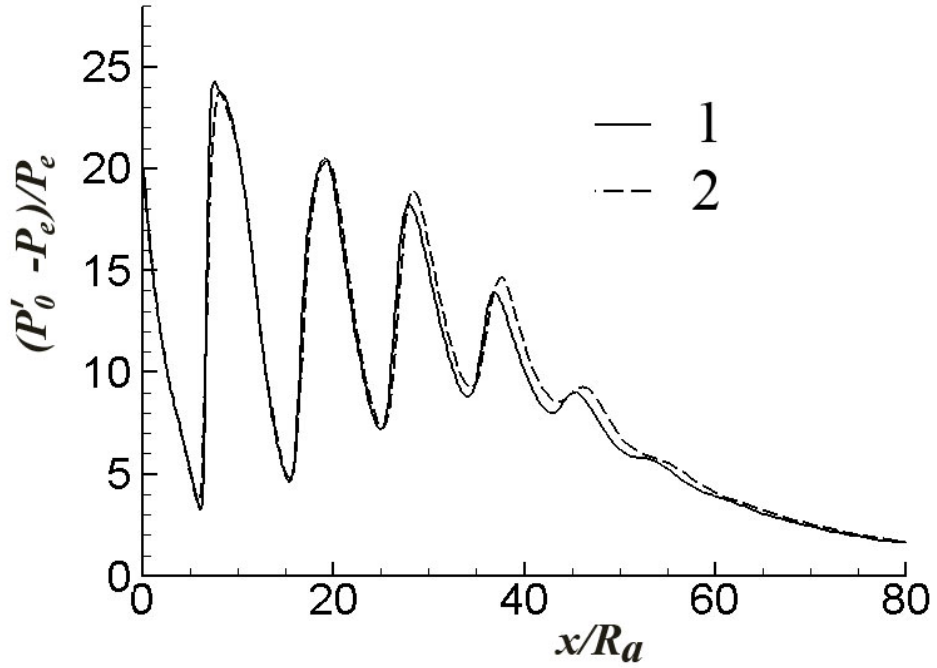

(b)

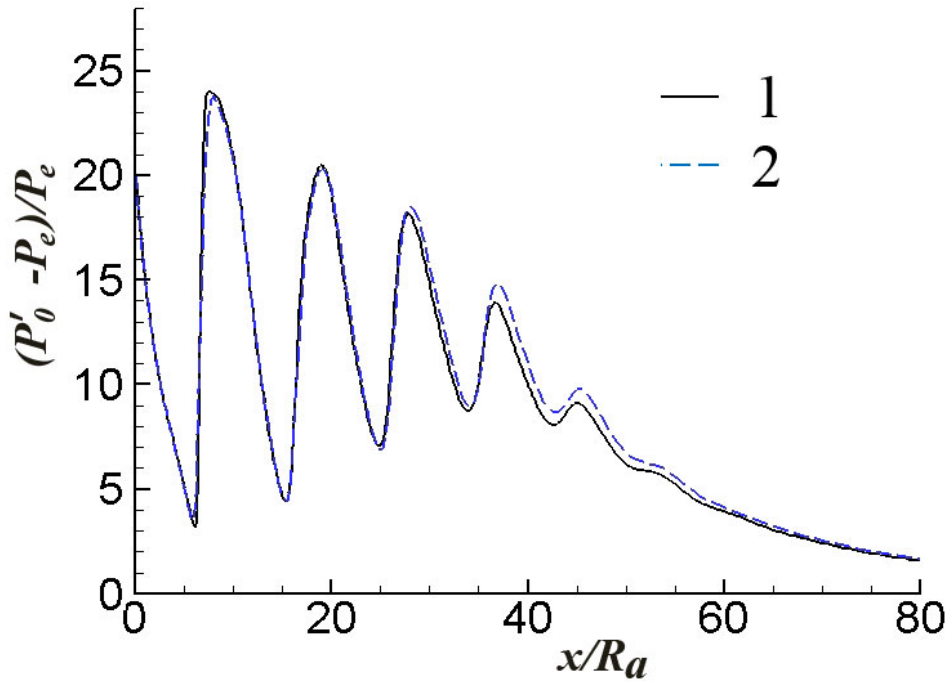

(c)

Figure 6.5. Centerline distribution of normalized relative pitot pressure in jet with $T_0 = 300K$, $M_a = 3.3$, $p_a / p_e = 1.5$, $\theta_a = 10°$. Calculation results for various grids, using various spatial orders of numerical scheme:
(a) - first order, (b) – second order, (c) – third order.

1 – 400x100 grid, 2 – 200x60 grid.

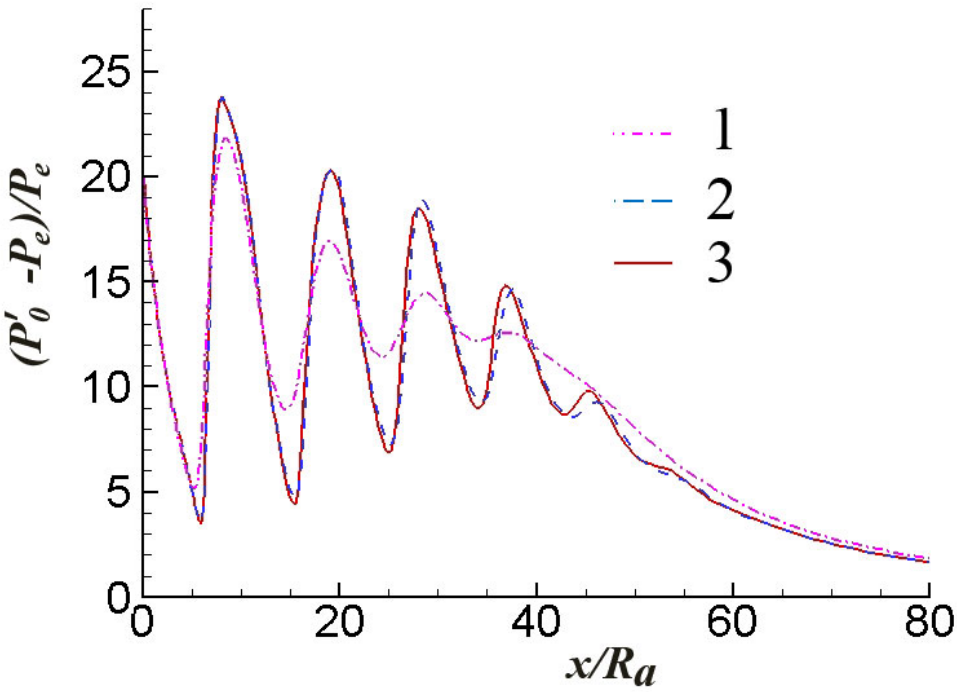

Figire 10. Test 4. Centerline distribution of normalized relative pitot pressure in jet with $T_0 = 300K, M_a = 3.3, p_a / p_e = 1.5, \theta_a = 10°$.
Calculation results for various spatial orders of numerical scheme, using 200x60 grid: 1 - first order, 2 – second order, 3 – third order.

6.4. Highly Under-Expanded Chemically Reacting Jets

This test aims at the jets of combustion products exhausting from model engines through sonic throats. The main features of these jets are high pressure ratio and generation of a big normal shock wave (Mach disk).

The simulation results were compared with the experimenting data of two model engines: kerosene-air (Chauveau et.al. [19]) and hydrogen -air (Klavhun et al. [20])

In the first test case the combustion chamber is fed with air and liquid kerosene at normal temperature. The pressure and temperature in the combusting chamber are $p_0 \approx 27 \cdot 10^5 Pa$; $T_0 \approx 1950K$ respectively.

The contour of the sonic throat is smooth, as it is shown in Figure 6.7, providing a uniform velocity profile at the jet origin.

PIV (Particles Image Velocimetry) was a technique to measure the velocity field in a fluid flow. To apply PIV, the flow must be seeded with fine particles that are supposed to follow precisely the fluid motion within the measurement zone.

The following parameters at the nozzle exit are used in the simulation:

$$u_a = 792\text{m/s}; T_a = 1720\text{K}; p_a = 14.77 \cdot 10^5 Pa;$$
$$Y_{O_2} = 0.05535; Y_{H_2O} = 0.06001; Y_{CO} = 0.00007; Y_{CO_2} = 0.15116; Y_{N_2} = 0.73341$$

The ambient is air at normal conditions.

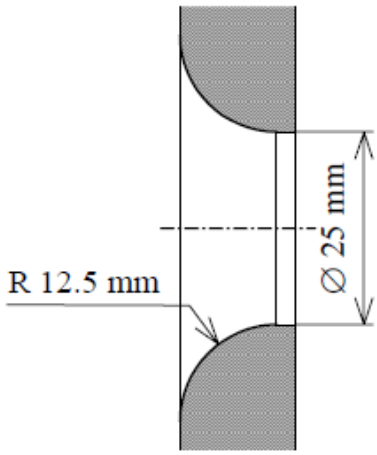

Figire 6.7. Geometry of the sonic throat of kerosene-air engine.

Figure 6.8 presents the predicted and the experimental structure of the jet. Direct processing of instantaneous PIV images allows for measuring the Mach disk and other shocks geometry. The similar results were obtained through the

simulation based on the picture of velocity field. The comparison shows a good agreement of the simulation results with the experimental data.

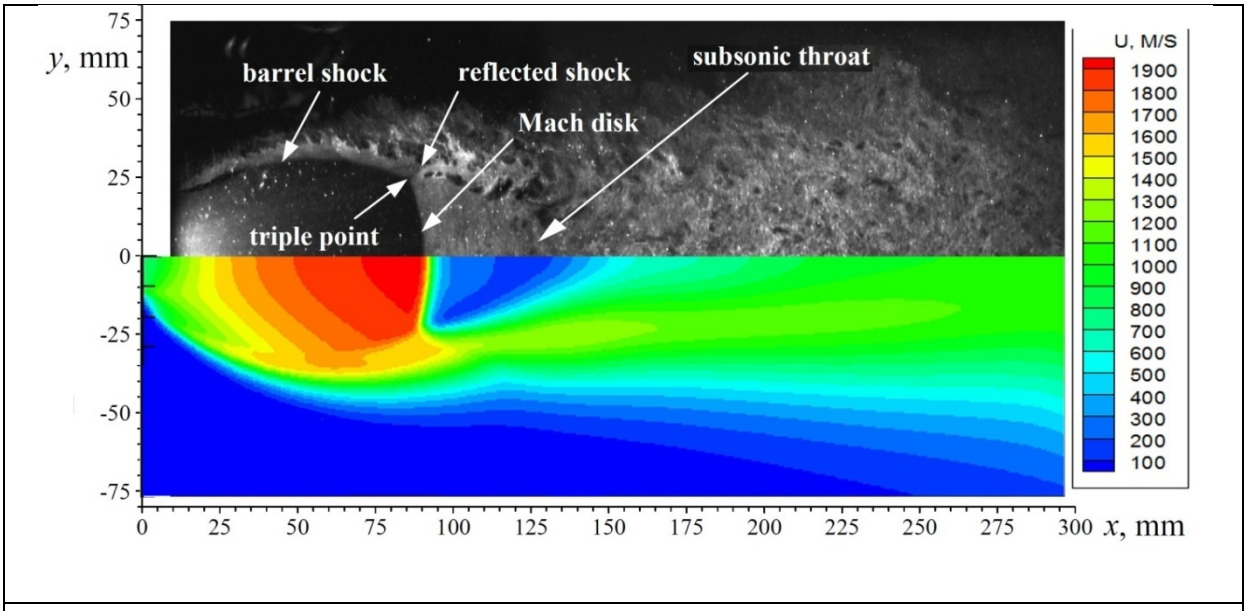

Figure 6.8. Jet structure obtained from an instantaneous PIV image (upper half) [19] and velocity magnitude fields predicted by the simulation (lower half)

Figures 6.9, 6.10 show the axial distributions and radial profiles of velocity obtained though simulation and compared with the experimental data.

The comparison showed a good agreement of simulation results with the experimental data in all the areas of the flow except for Mach disk region. The authors of the experiment explain that the observed discrepancies should be attributed to the flow tracking problems and limited capabilities of the PIV system.

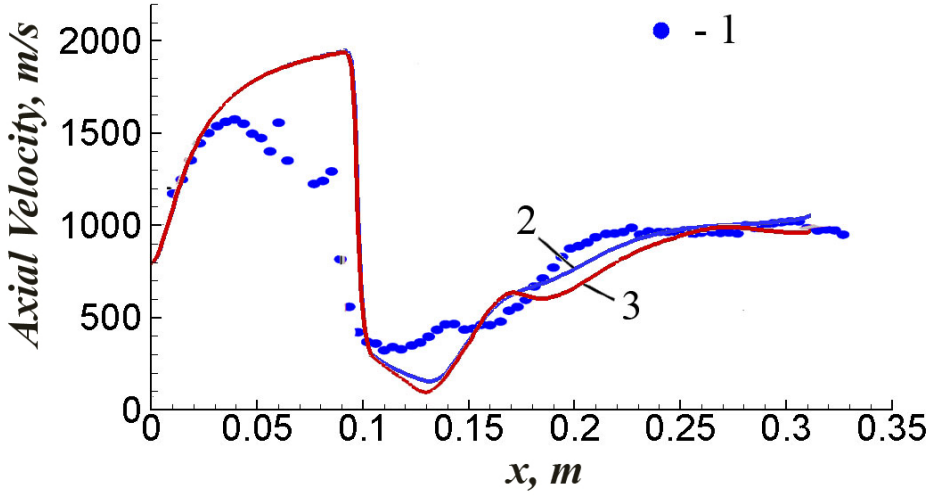

Figire 6.9. Centerline velocity vs. distance from nozzle exit x in jet exhausting from kerosene-air engine. $u_a = 792\text{m/s}; T_a = 1720\text{K}; p_a / p_e = 14.77$

1 – Chauveau et al. [19] experiment; 2 – simulation with standard K-ε model; 3 – simulation with K-ε turbulence model with compressibility correction [22]

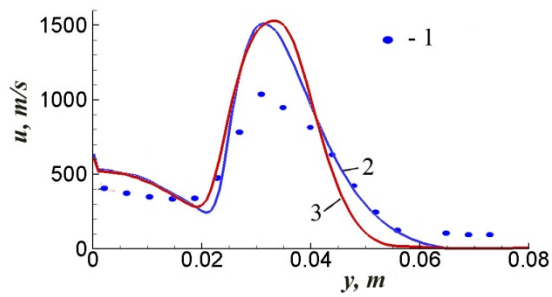

(a)

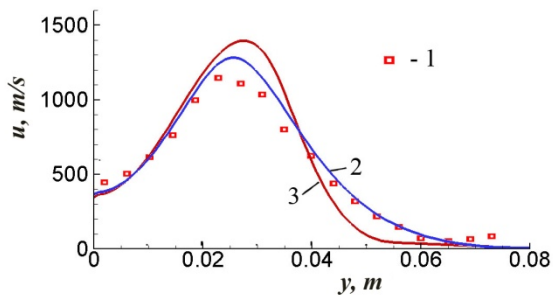

(b)

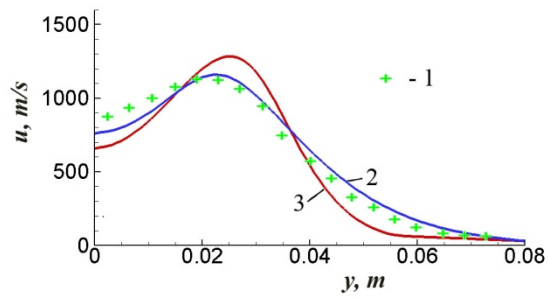

(c)

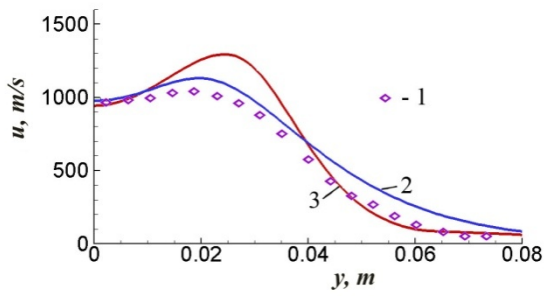

(d)

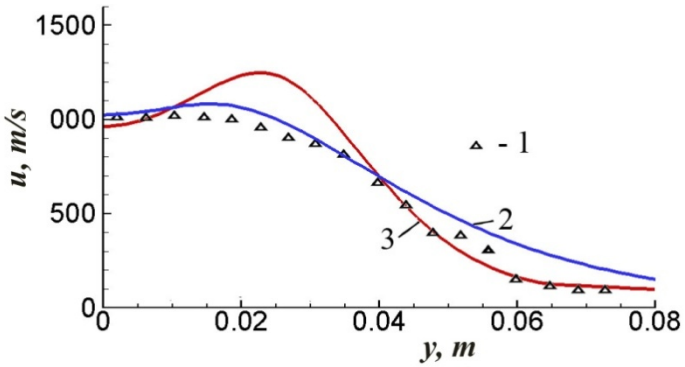

(e)

Figure 6.10. Radial profiles of velocity magnitude in jet exhausting from kerosene-air engine. $u_a = 792\text{m/s}; T_a = 1720\text{K}; p_a / p_e = 14.77$
(a) - $x = 0.1\,m$; (b) - $x = 0.15\,m$; (c) - $x = 0.2\,m$; (d) - $x = 0.25\,m$; (e) - $x = 0.3\,m$.
Calculation results (lines) are compared to the experimental data (points).
1 – Chauveau et al.[29] experiment; 2 – simulation with standard K-ε model; 3 – simulation with K-ε turbulence model with compressibility correction [22]

The second experiment used in this test was to show how well the presented method describes the flow in Mach disk region.

The comparison was made using the experimental data of Klavhun et al. [20], which involves the investigation of a sonic under-expanded jet exhausting from a model engine. The jet facility consists of a small ceramic-lined combustion chamber that contains a stoichiometric hydrogen-air flame, the products of which are accelerated through a 3.15-mm-i.d. alumina tube into a low-pressure chamber to form a reacting under-expanded jet. The pressure in the combusting chamber is $p_0 = 1.6 \cdot 10^5 Pa$, the temperature in the combusting chamber is $T_0 = 2000K$. The low- pressure chamber has $p_e = 0.11 \cdot 10^5 Pa$. It is assumed that the jet reacts chemically with the air present in this chamber.

A high-resolution OH laser-induced fluorescence (LIF) velocity measurement technique was used in this experiment [20]. The approach for measuring velocity is based on detection of the laser-induced fluorescence from a Doppler-shifted OH absorption line.

The following parameters at the nozzle exit were used:

$u_a = 871\text{m/s}; T_a = 1765\text{K}; p_a = 0.7 \cdot 10^5 Pa;$
$Y_H = 0.00023; Y_O = 0.00006; Y_{OH} = 0.00205; Y_{H_2} = 0.00509$
$Y_{O_2} = 0.00167; Y_{H_2O} = 0.33903; Y_{N_2} = 0.65187$

Figure 6.11 presents centerline velocity distribution. The simulation results are provided at constant and variable values of Pr_T, Sc_T. As it can be seen, those are very similar, i.e. considering the variability of these criteria does not impact much on the dynamic characteristics of the flow.

The comparison shows a good agreement of simulation results with the experimental data in all flow regions including Mach disk region.

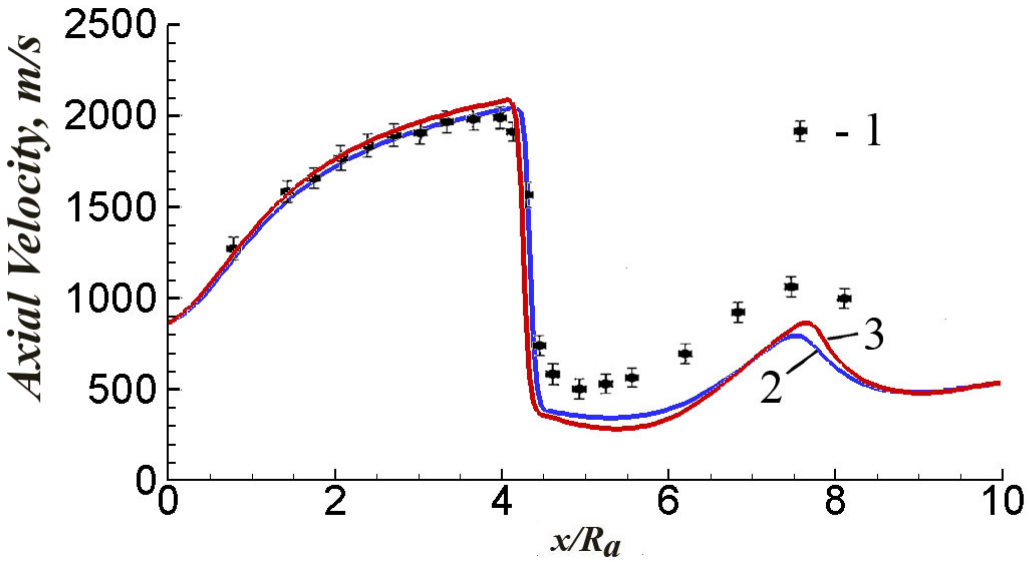

Figure 6.11 Centerline velocity vs. distance from nozzle exit in jet exhausting from hydrogen-air engine. $u_a = 871\text{m/s}; T_a = 1765\text{K}; p_a / p_e = 6.36$
Calculation results for various Pr_T, Sc_T models (constant and variable),
1 – Klavhun et al. [20] experiment; 2 – simulation using constant $Pr_T = Sc_T = 0.7$;
3 – simulation using variable Pr_T, Sc_T model

6.5. Afterburning of exhaust plume.

This test aimed at validating the presented method for investigating of supersonic non-isobaric jets which contain unburned combustible species: H_2, CO. These species chemically react with the oxygen contained in air; their afterburning causes a considerable increase of temperature.

This test included the simulation of jets exhausting from hot-gas generator, described in Safronov and Khotulev[18, 21]. Pitot pressure and total temperature were measured.

The numerical investigation for two gas generator operational modes was performed using the same fuel.

Figure 6.12 presents centerline distribution of normalized relative pitot pressure in over-expanded jet with the following parameters:

$$T_0 = 2860K\,,\ M_a = 4.0\,,\ p_a / p_e = 0.65$$

Mass fractions of afterburning species are: $Y_{H_2} = 0.01;\quad Y_{CO} = 0.29$

The simulation was carried out with the use of different turbulence models. The simulation results with the presented turbulence model are in a good agreement with the experimental data; using standard $K\text{-}\varepsilon$ model considerably under predicts the jet length; $K\text{-}\varepsilon$ turbulent model with compressibility correction of Sarkar et al. [23] slightly over predicts the jet length.

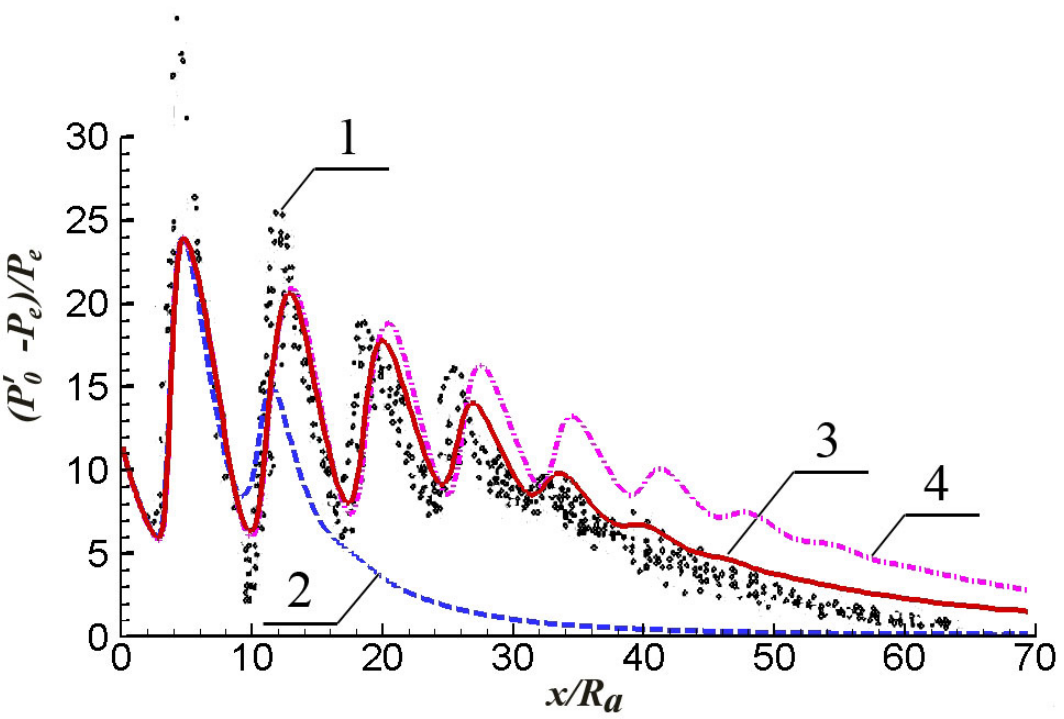

Figure 6.12. Centerline distribution of normalized relative pitot pressure in overexpanded jet with $T_0 = 2860K,\quad M_a = 4.0,\quad p_a / p_e = 0.65$.

Calculations using various turbulence models, compared to experiment.
1 – Safronov experiment;
2 – simulation using standard K-ε model without compressibility correction;
3 – 3 – simulation with K-ε turbulence model with compressibility correction [22];
4 – simulation with K-ε model with Sarkar et al.[23] compressibility correction

REFERENCES

1. MacCormack, R.W. Current Status of Numerical Solutions of the Navier-Stokes Equations //AIAA-85-0032. - 1985. 14p.

2. MacCormack, R.W., The Effect of Viscosity in Hypervelocity Impact Cratering // AIAA Paper No. 69-354. - 1969. 7p.

3. Patankar, S.V. Numerical Heat Transfer and Fluid Flow // Hemisphere Publishing Corporation. - 1980. 197 pages.

4. Godunov S.K., Ryabenkii V.S. Difference Schemes: An Introduction to the Underlying Theory // Elsevier, 1987 - Pages 488.

5. Tannehill J. C., Anderson D. A., Pletcher R. H. Computational Fluid Mechanics and Heat Transfer. Taylor & Francis, 1997. 792 pp. ISBN 1 56032 045X.

6. *MacCormack, R.W., and Pulliam, T.* Assessment of A New Numerical Procedure For Fluid Dynamics //AIAA Paper 98-2821. -1998. 9p.

7. Tysinger, T., and Caughey, D., “Implicit Multigrid Algorithm for the Navier–Stokes Equations,” AIAA Paper 91-0242, 1991, pp.1-16.

8. Stone, H.L., “Iterative Solution of Implicit Approximations of Multidimensional Partial Differential Equations,” Siam J. Numer. Anal., Vol. 5, No. 3, Sept., 1968, pp. 530-558.

9. Bardina, J. and C.K. Lombard, “Three Dimensional Hyper sonic Flow Simulations with the CSCM Implicit Upwind Navier-Stokes Method,” AIAA Paper No. 87-11Ц, 1987.

10. Versteeg H. K. and Malalasekera W. An introduction to computational fluid dynamics. The finite volume method // Pearson Education, Limited, 2011 - Finite volume method - 552 pages

11. Wangda Zuo. Introduction of Computational Fluid Dynamics // FAU Erlangen-Nürnberg, JASS 05, St. Petersburg, 205, 8 pages

12. Scalabrin L.C. Numerical Simulation of Weakly Ionized Hypersonic Flow over Reentry Capsules //A dissertation submitted in partial fulfillment of the requirements for the degree of Doctor of Philosophy (Aerospace Engineering) in The University of Michigan. -2007. -182p.

13. Steger, J. and Warming, R. F. "Flux Vector Splitting of the Inviscid Gasdynamics Equations with Application to Finite Difference Methods," NASA TM-78605, 1979.

14. MacCormack, R. W,, "A Numerical Method for Solving the Equations of Compressible Viscous Flow," AIAA Paper No. 81-0110.

15. Molchanov A.M. Numerical Simulation of Supersonic Chemically Reacting Turbulent Jets. 2011. AIAA Paper 2011-3211, 37p.

16. Averenkova, G.P., Ashratov, E.A., Volkonskaya, T.G., et al. Supersonic Jets of the Ideal Gas. In 2 parts. [in Russian] Moscow: Publishing House of Moscow State University, 1970-1971. Part 1. 1970, 279p., Part 2, 1971, 170 p.

17. Sumi, I., Kishimoto, Y., Kikichi, Y. and Igarashi, H.,"Effect of high temperature field on supersonic oxygen jet behavior," ISIJ International, Vol. 46, 2006, pp. 1312-1317.

18. Safronov A., Khotulev V. Results of experimenal researches of the supersonic cold and hot jet // Physical-Chemical Kinetics in Gas Dynamics. 2008. V.6. http://chemphys.edu.ru/issues/2008-6/articles/280/

19. Chauveau, C., Davidenko, D. M., Sarh, B., Gökalp, I., Avrashkov, V., Fabre, C., “PIV Measurements in an Underexpanded Hot Free Jet,” 13th Int Symp on Applications of Laser Techniques to Fluid Mechanics, Paper No.1161, 2006, pp.1-12.

20. Klavhun,K.G., Gauba, G., McDanial,J. C., "OH Laser-Induced Fluorescence Velocimetry Technique for Steady, High-Speed, Reacting Flows," Journal of Propulsion and Power, Vol. 10, No. 6, 1994, pp.787-797.

21. Safronov A. The method of calculation of the jets of combustion products at the rocket launch//Physical-Chemical Kinetics in Gas Dynamics. 2006. V.4. http://chemphys.edu.ru/issues/2006-4/articles/100/

22. Molchanov, A.M., "A calculation of supersonic non-isobaric jets with compressibility corrections in a turbulence model," Vestnik MAI, No.1, Vol.16, 2009, pp.38-48.

23. Sarkar, S., Erlebacher, G., Hussaini, M.Y. and Kreiss, H.O., "The analysis and modeling of dilatational terms in compressible turbulence," *Journal of Fluid Mechanics*, Vol. 227, 1991, pp.473–493.